Perspectives in Contemporary Mathematics

Editors

Dr. Rupjyoti Borah

Dr. Bijoy Patir

Dr. Jyoti Saikia

AkiNik Publications ®
New Delhi

Published By: AkiNik Publications

AkiNik Publications
169, C-11, Sector - 3,
Rohini, Delhi-110085, India
Toll Free (India) – 18001234070
Phone No.: 9711224068, 9911215212
Website: www.akinik.com
Email: akinikbooks@gmail.com

Editors: *Dr. Rupjyoti Borah, Dr. Bijoy Patir and Dr. Jyoti Saikia*

Publication Year: 2025

Edition: 1st

Pages: 158

Paperback ISBN: 978-93-7150-517-8

E-Book ISBN: 978-93-7150-849-0

Book DOI: https://doi.org/10.22271/ed.book.3573

Price: ₹ 680 /-

Registration Details

- Printing Press License No.: F.1 (A-4) press 2016
- Trade Mark Registered Under
  - Class 16 (Regd. No.: 5070429)
  - Class 35 (Regd. No.: 5070426)
  - Class 41 (Regd. No.: 5070427)
  - Class 42 (Regd. No.: 507042

Editor's Column

It gives us immense pleasure to present the edited book "*Perspectives in Contemporary Mathematics"*, published by the Department of Mathematics, Tingkhong College. This book is a sincere academic effort to showcase contemporary research trends and diverse perspectives in mathematics, reflecting both its theoretical depth and practical relevance.

The present volume (Vol-1) is a collection of twelve research articles contributed by scholars from different institutions. These papers span a wide spectrum of mathematical disciplines, covering significant topics from both pure and applied mathematics. The diversity of themes addressed in this book highlights the dynamic and evolving nature of mathematics as a subject that continuously responds to new scientific challenges while strengthening its foundational theories.

The primary objective of this edited book is to provide a common platform for researchers to share original ideas, recent findings, and innovative methodologies. It is hoped that this volume will serve as a valuable reference for researchers, academicians, and postgraduate students, and will encourage further research and collaboration across institutions.

We sincerely thank all the contributors for their scholarly inputs and for trusting this volume as a medium to disseminate their work. We are also grateful to the reviewers for their constructive suggestions, which have helped in maintaining the academic quality of the book. Our heartfelt thanks go to the faculties of Tingkhong College, whose consistent support and encouragement played a vital role in bringing out this publication. The editors gratefully acknowledge the officials of Akinik Publication for their valuable support and encouragement in the publication of this work.

We believe that *Perspectives in Contemporary Mathematics* will be a meaningful addition to the existing mathematical literature and will inspire readers to explore new directions in research.

Editors:

Dr. Rupjyoti Borah

Dr. Bijoy Patir

Dr. Jyoti Saikia

Dedication

This volume is lovingly dedicated to the cherished memory of **Late Dr. Bijoy Patir**, one of the editors of this book. A distinguished mathematician, devoted teacher, and inspiring academician, Dr. Patir's commitment to mathematical research and higher education continues to guide and motivate us. His scholarly vision, intellectual integrity, and humane approach left an indelible mark on colleagues and students alike. Though he is no longer with us, his ideas, values, and academic legacy live on through this work. This book stands as a humble tribute to his enduring contribution to the discipline of mathematics and to the academic community he served with dedication and grace.

Contents

Chapter - 1
Application of Linear Algebra in Machine Learning

Authors

Bikash Chutia
Department of Mathematics, Dibrugarh University,
Dibrugarh, Assam, India

Chapter - 1

Application of Linear Algebra in Machine Learning

Bikash Chutia

Abstract

In this chapter, it is intended to discuss few examples of machine learning that may be familiar with that use, require and are really best understood using linear algebra. Linear algebra structures are used in data science such as tabular data sets and images. Linear algebra concepts working with data preparation to reduce one hot encoding and dimensional. This research highlights the essential ideas and real-world applications of linear algebra as it examines the substantial influence of the subject on machine learning applications. Additionally, this chapter illustrates the vital importance of linear algebra by examining certain machine learning applications such as Word/Vector Embedding, Image Compression and Movie Recommendation systems. The ingrained use of linear algebra notation and methods in sub-fields such as deep learning/neural networks, natural language processing, robotics, image processing etc. The study contributes to current initiatives aimed at enhancing machine learning applications effectiveness and efficiency.

Keywords: Linear Algebra, Machine Learning, Matrix, Data Representation

Introduction

Linear algebra is a branch of mathematics concerned with vectors, matrices, linear equations, and linear transformations. In other words, linear algebra is the study of linear functions in vector spaces. It is one of the most central topics of all areas of mathematics. Most modern geometrical concepts and functional analysis are based on linear algebra. Linear algebra facilitates the modeling of many natural phenomena and efficiently computing with such models and hence, is an integral part of physics, engineering, natural sciences, computer animation, and social science (particularly in economics). The importance of linear algebra has increased recently, particularly because of its critical role in comprehending and refining machine learning algorithms. In machine learning, a branch of artificial intelligence, use data to provide insights that help them make predictions or judgments that are well-informed.

Linear algebra offers the mathematical foundation that is required for data representation, manipulation and modeling. This makes it easier to solve complicated machine learning problems. In machine learning, matrices and vectors are frequently used to represent data allowing for manipulation through a variety of linear algebraic operations. These operations, which compute eigenvalues, matrix multiplications and inner products, are the building blocks of machine learning algorithms. Machine learning techniques develop because linear algebra makes tasks easier like dimensionality reduction, model optimization and data transformations. For nonlinear systems, which cannot be modeled with linear algebra, linear algebra is often used as a first-order approximation. It is a key foundation to the field of machine learning from notations used to describe the operations of algorithms to the implementation of algorithms in code. Despite the fact that linear algebra is essential to machine learning, the close like between the two is frequently left unclear or discussed in terms of abstract ideas like vector spaces or certain matrix operations, from the implementation of algorithms and techniques in the code (such as Regularization, Deep learning, one hot encoding, Principal Component Analysis, Single value Decomposition (SVD) etc.) to the notations that are used to describe the operations of the machine learning algorithm.

Organization of the paper: In section 1, contains preliminaries of linear algebra which will be used in the sections to follow. Section 2 discussing some real-life examples of Linear Algebra in Machine Learning and section 3 include conclusion of the whole work.

1. Preliminaries

Vectors: A vector is just an element of a vector space. It is a phenomenon that possesses two separate properties: magnitude and direction, such as force, weight, acceleration, and magnetic field etc.

Matrix: A matrix is a rectangular array of numbers or functions. Usually, the numbers are real or complex. Matrices consisting of only one column or row are called vectors; while higher-dimensional, example three-dimensional, arrays of numbers are called tensors. Matrix multiplication may be done according to a rule that relates to the composition of linear transformations, and entry-wise addition and subtraction is also possible. These operations satisfy the usual identities, except that matrix multiplication is not commutative: the identity $AB = BA$ can fail.

Linear Equation: An algebraic equation that has every term as either a constant or the product of constant and the first power of a single variable is called a linear equation. Linear equation can have one or more variables. A

finite set of linear equations in a finite set of variables, for example: $x_1, x_2, x_3, \ldots x_n$ or x, y, z is called system of linear equations, forms a fundamental part of linear algebra. Linear algebra through vector spaces and matrices, many problems may be interpreted in terms of linear systems.

Machine Learning: Machine learning is a sub-field of artificial intelligence (AI) that uses algorithms trained on data sets to create self-learning models that are capable of predicting outcomes and classifying information without human intervention. Now a days, machine learning is applied to a broad range of commercial purposes such as translating text from one language to another, predicting stock market fluctuations, and making product recommendations to customers based on their previous purchases. The phrases "machine learning" and "artificial intelligence" are frequently used synonymously because machine learning is so widely employed in the modern world for AI objectives. In supervised machine learning, algorithms are trained using labeled data sets, where each example is paired with a corresponding label or result, allowing the algorithm to learn the mapping between inputs and outputs. Supervised machine learning is often used to create machine learning models used for prediction and classification purposes. While unsupervised machine learning uses dimensionality reduction and clustering approaches to find latent patterns of structures within unlabeled data, Semi-supervised machine learning uses both labeled and unlabeled data to improve model performance. Reinforcement machine learning uses trial and error to trains algorithms and builds models. During the training process, algorithms operate in certain Environments and after each result, they get feedback.

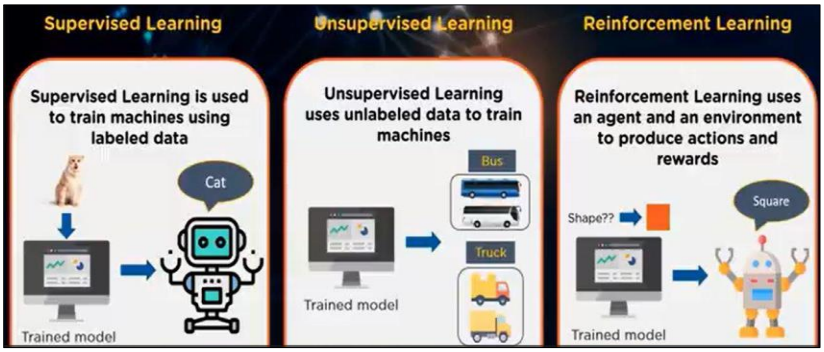

Fig 1: Types of machine learning

The key steps in the machine learning pipeline include data collection, preprocessing, feature engineering, model selection, training, assessment, and

deployment. Each of these steps is essential to guaranteeing the model's efficiency and quality. Various components of the process are improved by ongoing investigation of innovative techniques including data augmentation, transfer learning and strong assessment metrics. Applications of machine learning may be found in many different fields, such as natural language processing, medical image analysis, fraud detection, and stock market forecasting in the finance and healthcare sectors, as well as chat-bot development and sentiment analysis in natural language processing.

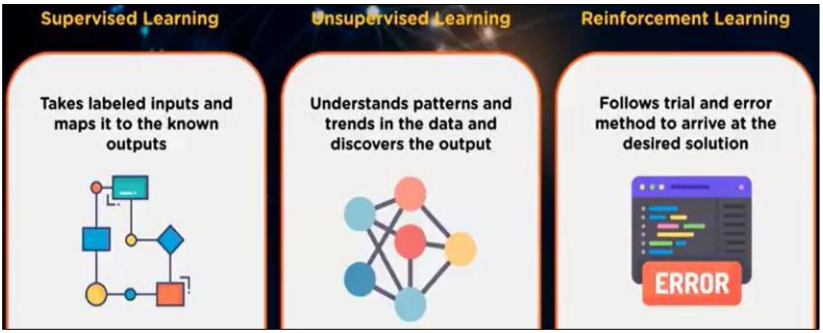

Fig 2: Machine Learning Approach

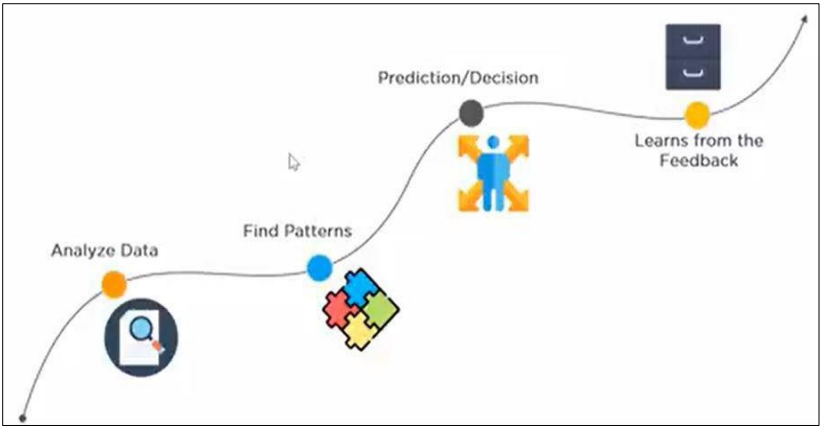

Fig 3: Machine Learning Process

Linear Algebra Representation: In the field of machine learning, data is transformed into vectors to enable computational processing. The terms like "feature vector" and "feature space" are commonly used in this field. A feature vector is a representation of an object's attributes, with each component of the vector corresponding to a specific feature. On the other hand, a feature space encompasses these feature vectors. An example of this idea is given below

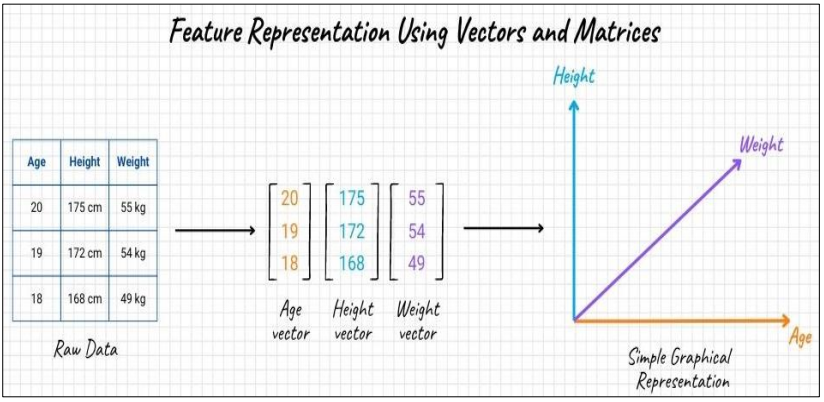

Fig 4: Using of matrices and vectors for features

Images can be shown in a matrix format. In a black and white image, pixels are represented by 0s and 1s, as demonstrated in the example image below.

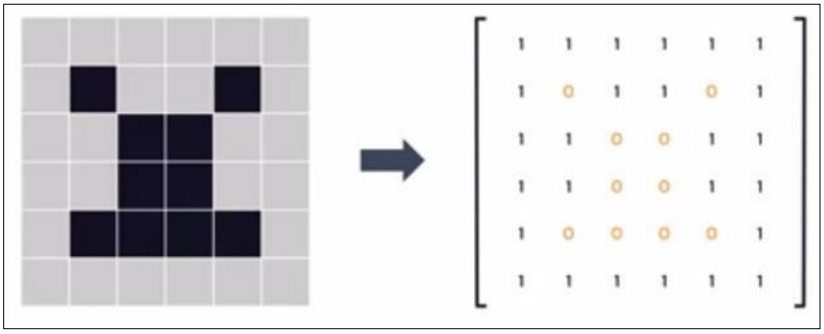

Fig 5: Diagram of an Image Using Matrices

For ratings of yes or no, each movie can be associated with a feature vector, whose dimensions correspond to various qualities. Mathematical processes like similarity measurements and customized suggestions based on user preferences and movie attributes are made possible by these vectors. This user feedback system is a useful tool for sharing preferences and thoughts about movies or items. When expressed as vectors, ratings are more useful in data analysis and recommendation systems. The relationship between the viewer, movie title, and its vector representation is illustrated.

Fig 6: Vector Diagram of Movie to User Synergy

Linear Algebra in Machine Learning

Since Machine Learning serves as the interface between Statistics and Computer Science, Linear Algebra facilitates the integration of science, technology, finance & accounting, and business. Here we discuss ten existing examples of linear algebra in machine learning, which are as follows

1.1 Dataset and Data Files

In linear algebra, a data is a matrix or a key data structure. A data set contains the table-like set of numbers where each row represents an observation and each column represents a feature of the observation. Each row has the same length i.e., the same number of columns, therefore we can say that the data is vectorised when rows can be provided to a model one at a time or in a batch and the model can be preconfigured to expect rows of fixed width.

1.2 Images and Photographs

As computer vision applications we are more used to working with images or photographs. All images are tabular in structure. Each picture we

deal with has a width, a height and either one- or three-pixel values in each cell depending on whether it is a black and white or colour image. Another illustration of a matrix from linear algebra is a picture. The notation and operations of linear algebra are all used to express actions on the picture, such as cropping, scaling, shearing and other similar techniques.

1.3 One-Hot Encoding

Categorical data are variables that contain label values rather than numeric values. The number of possible values is often limited to a fixed set. Categorical variables are often called nominal. Categorical variables are frequently encoded to make them simpler to use and understand via certain ways. The one hot encoding is a common method for encoding categorical values. In a one-hot encoding, a table is made to represent the variables, with a row for each case in the dataset and a column for each category. The column that corresponds to the category value for a particular row receives a check, or one value, while all other columns receive a zero value.

1.4 Linear Regression

A technique for simulating the connection between one or more independent variables and a dependent variable is linear regression. An established statistical technique for explaining the connection between variables is linear regression. In machine learning, it is frequently used to forecast numerical values in less complex regression issues. Finding a collection of coefficients that, when multiplied by each of the input variable, is how the issue of linear regression is often defined and solved. The most popular approach of solving linear regression if we have employed a machine learning tool or library is via a least squares optimization i.e., resolved using matrix factorization techniques from linear regression, such as a LU decomposition or a singular-value decomposition, or SVD.

Even the typical method of rewriting the linear regression equation does so using linear algebra notation: $= A \cdot b$, where y is the output variable, A is the dataset or matrix and b are the model coefficients.

1.5 Regularization

In applied machine learning, we frequently look for the most straightforward models that solve our problem with the highest skill. Simpler models are frequently more effective at extrapolating from particular examples to new data. Simpler models are frequently described by models that have fewer coefficient values in various approaches that include coefficients, such as regression methods and artificial neural networks.

Regularization is a method that is frequently used to urge a model to decrease the size of its coefficients when it is being fitted to data. Regularization techniques like L1 and L2 are often used. Both of these regularization techniques, known as the vector norm, are taken straight from linear algebra and quantify the magnitude or length of the coefficients as a vector.

1.6 Principal Component Analysis

Principal Component Analysis (PCA) is a vital machine learning technique for dimensionality reduction. It is a technique that calculates a projection of the original data into the same number of dimensions or less using straightforward matrix operations from linear algebra and statistics. When working with high-dimensional data for visualization and model operations, principal component analysis is suitable. We frequently eliminate the duplicate columns when we discover unnecessary data. PCA therefore serves as remedy. A linear algebraic matrix factorization technique is the basis of the PCA approach. The singular-value decomposition, or SVD can be used in place of the eigen decomposition for more reliable implementations.

1.7 Singular-Value Decomposition

Singular-Value Decomposition (SVD) is a matrix decomposition method for reducing a matrix to its constituent parts in order to make certain subsequent matrix calculations simpler. It has several applications in linear algebra and is immediately applicable to many different tasks, including feature selection, visualization, noise reduction, and more.

1.8 Latent Semantic Analysis

Natural language processing is a sub field of machine learning for handling text input, frequently represents documents as large matrices of word occurrences.

For example, the rows and columns of the matrix might represent sentences, paragraphs, pages and other text-based documents, with the cells in the matrix denoting the count or frequency of how frequently each word appeared.

The text is shown here as a sparse matrix. This spare matrix may be factorised using techniques like the singular-value decomposition (SVD), which reduce the representation to its most essential components. This method of processing documents makes it much simpler to compare, query, and build supervised machine learning models on top of them. Latent Semantic Analysis (LSA) and Latent Semantic Indexing (LSI) are two names for this type of data preparation.

1.9 Recommender Systems

Recommender system is a branch of machine learning that are used to solve predictive modelling issues involving product recommendations. Examples include suggesting books based on past purchases and purchases made by customers similar to you on Flipkart, and suggesting movies and TV episodes to watch based on our viewing history and the viewing histories of members similar to you on Netflix. The main focus of recommender system is development on linear algebra techniques. The computation of the similarity of sparse customer behaviour vectors using distance metrics like Euclidean distance or dot products is a straightforward example. In recommender systems, matrix factorization techniques like the singular-value decomposition (SVD) are frequently used to reduce item and user data to its essential components for querying, searching, and comparison.

1.10 Deep Learning

Predictive modelling is the only one of the many issues that artificial neural networks have successfully solved. These nonlinear machine learning techniques are inspired by aspects of the information processing in the brain. Deep learning is the current renaissance in the usage of artificial neural networks with better techniques and faster technology that enable the building and training of larger and deeper (more layers) networks on very large datasets. On a variety of complex issues, including speech recognition, photo captioning, and machine translation, deep learning techniques consistently produce state-of-the-art results. Neural networks operate primarily by multiplying and averaging data structures from linear algebra. Deep learning techniques operate with vectors, matrices and even tensors of inputs and coefficients- a tensor is a matrix with more than two dimensions- when scaled up to many dimensions.

2. Conclusion

Linear algebra basically is the study of the planes and lines, mapping and vector spaces, which are needed for linear transformations. Therefore, it is necessary to know what are the application of linear algebra. In the above we have explained those applications. Linear algebra has broader use in machine learning from notation to the implementation of algorithms in datasets and images. With the help of machine learning, linear algebra has got a larger impact in real life applications such as search-engine analysis, facial recognition, predictions, computer graphics etc.

References

1. https://www.educba.com/linear-algebra-in-machine-learning/
2. https://machinelearningmastery.com/examples-of-linear-algebra-in-machine-learning/
3. Audu, K. J., Oluwole, O. O., Yahaya, Y. A., and Egwu, S. D. (2024). Tha application of linear algebra in machine learning. 4th school of physical sciences biennial international conference futminna 2024.
4. Brownlee, J. (2018). Basics of Linear Algebra for Machine Learning: Discover the Mathematical Language of Data in Python. Machine Learning Mastery, 24-Jan-2018.
5. Bau III, David, Trefethen, Lloyd N. (1995). Numerical linear algebra, Philadelphia, PA: Society for Industrial and Applied Mathematics. ISBN 978-0-89871-361-9, 1995. Introduction to Linear Algebra -Fifth edition- Gilbert Strang.
6. Patait, S.N., & Sasane, P.G. (2021). A Study on the Linear Algebra and Matrix in Mathematics. International Research Journal of Humanities and Interdisciplinary Studies. Volume 2, Issue 4 April 2021. DOI Link:: http://doi-ds.org/doilink/04.2021-45438843/IRJHIS2104006
7. Velusamy, N., Sowmiya, J., Maheshwaran, R., & Ranjani, S. (2021). Real Life Applications of Linear Algebra Under Matrix Multiplications. Bulletin Monumental - ISSN / e-ISSN 0007-473X . Volume 22 : Issue 3 - 2021. http://bulletinmonumental.com/

Chapter - 2
Application of Fuzzy Theory for Intelligent Traffic Management in Urban Road Networks

Author

Dr. Md Nazir Hussain
Assistant Professor, Bilasipara College, Bilasipara,
Dhubri, Assam, India

Chapter - 2

Application of Fuzzy Theory for Intelligent Traffic Management in Urban Road Networks

Dr. Md Nazir Hussain

Abstract

Globally, urban road networks are congested, with unpredictable driving behaviour and diverse traffic mixtures that affect mobility, safety, and air quality. Traditional fixed-time and many actuated traffic control techniques rely on precise inputs and fail to respond adequately to the uncertainty inherent in real-world traffic. This work offers a fuzzy logic-based **Intelligent Traffic Management System (ITMS)** that models uncertain traffic parameters (e.g., "high density", "long queue", "moderate delay") with linguistic variables and membership functions to create adaptive signal timing and intersection control. The study will create a Mamdani-type **Fuzzy Inference System (FIS)** with inputs like traffic density, queue length, and waiting time, and outputs like green-time extension and phase-priority modifications. The system will be conceived, built, and tested using microscopic traffic simulation, **Simulation of Urban Mobility (SUMO)** and algorithmic simulation in Python/MATLAB. Performance will be compared to fixed-time and actuated controllers based on measures such as average delay, queue length, throughput, and environmental indicators (fuel consumption/CO_2 estimates). Expected benefits include a demonstrated reduction in average waiting time and line length during peak and off-peak periods, as well as a strong control strategy appropriate for mixed-traffic scenarios common in many growing cities. This study tries to bridge the gap between theoretical fuzzy-control approaches and real, deployable traffic management solutions that work with existing intersection infrastructure.

Keywords: Fuzzy logic, MATLAB, Traffic management

Introduction

Traffic congestion is a fast developing issue in major cities around the world. With growing populations, economic development, and an increase in vehicle traffic, metropolitan road networks are frequently pushed beyond their

original capacity. Many cities' traditional traffic light systems operate on predefined timings that do not adjust to real-time route circumstances. These systems rely on consistent and exact inputs, which rarely represent actual traffic behaviour.

Fuzzy theory provides an adaptive method for reasoning with uncertain, imprecise, or missing data. Rather than using binary true/false logic, fuzzy logic permits variables to belong to many categories to varied degrees. This function mimics human reasoning and decision-making processes, making it ideal for handling complex traffic situations.

This paper introduces the overall motivation for the research, the need for a smarter traffic management strategy, and an overview of fuzzy logic in **intelligent transportation systems** (ITS). This study examines research in traffic control, fuzzy logic applications, and intelligent transportation systems. Traditional systems are investigated, including fixed-time controls, actuated signals, and adaptive techniques such as **Split Cycle Offset Optimization Technique (SCOOT)** and the **Sydney Coordinated Adaptive Traffic System (SCATS)**. While useful to some extent, these technologies frequently rely on exact sensor data and necessitate lengthy calibration.

Fuzzy logic has been extensively researched for traffic control due to its ability to handle uncertainty. Several studies have demonstrated that fuzzy-based techniques increase delay reduction, queue management, and intersection throughput. Hybrid models that combine fuzzy logic with neural networks, evolutionary algorithms, and reinforcement learning have also been investigated for improving system flexibility and performance. Despite significant advances, there are still gaps in real-time deployment, scalability for rising metropolitan regions, and dealing with the diverse traffic situations found in developing countries.

This study's methodology is systematic, with steps such as data collecting, fuzzy system design, rule creation, membership function development, and simulation. Traffic statistics, such as vehicle count, queue length, and waiting time, were gathered at urban crossings. These inputs were divided into fuzzy categories like low, medium, and high.
A Mamdani-type fuzzy inference system was chosen for its interpretability and broad applicability. Membership functions were defined with triangular and trapezoidal shapes. Based on expert knowledge and research, 27 fuzzy rules were developed.

Simulations were carried out using Python's scikit-fuzzy module and MATLAB's Fuzzy Logic Toolbox. Waiting time, line length, and vehicle throughput were all used to evaluate performance.

The fuzzy logic model consists of three major components: fuzzification, fuzzy inference, and defuzzification. The input variables are traffic density (vehicles per minute), queue length (meters), and waiting time (seconds). Each variable was separated into linguistic groups and assigned membership functions.

Fuzzy inference examines rule conditions, such as: If traffic density is high, queue length is long, and waiting time is high, the green time extension is long. The centroid approach is used in the defuzzification process to transform fuzzy outputs into precise green-time adjustments. The simulation environment was designed to emulate real-world intersection situations. The baseline performance was measured using a fixed-time controller, followed by the execution of the fuzzy logic controller. The key parameters compared are average waiting time, queue length, and throughput.
The results show that employing the fuzzy model reduces average waiting time by up to 35% and queue length by 20-40%. These findings support the effectiveness of fuzzy theory in real-time traffic control.

A comparison of fixed-time, actuated, and fuzzy logic controllers demonstrates that fuzzy logic outperforms the other two under a variety of traffic circumstances. Fixed-time systems cannot react to real-time fluctuations, whereas actuated controllers rely significantly on exact sensor data. The fuzzy system's capacity to accept imprecise inputs and apply human-like reasoning makes it especially useful in unexpected traffic patterns.
This research demonstrates that fuzzy logic is an effective framework for intelligent traffic management. The proposed methodology effectively decreases congestion and improves signal responsiveness in dynamic settings.

Future research may look into integration with **the integration of Internet of Things** (IoT)-based sensors, hybrid deep learning-fuzzy systems, and city-wide adaptive traffic coordination. In conclusion, the goal of this research is to demonstrate the feasibility and usefulness of using fuzzy logic to urban traffic control, as well as to contribute to scalable smart city solutions that support sustainable transportation systems. Successful implementation may open the way for the real-world deployment of intelligent, adaptive, and context-aware traffic management systems in emerging and developed cities.

References

1. Chiu, S. L. (1992). Adaptive traffic signal control using fuzzy logic. Transportation Research Part C: Emerging Technologies, *1*(2), 119-133.
2. Hoogendoorn, S., & Bovy, P. (2001). State-of-the-art of vehicular traffic flow modelling. Proceedings of the Institution of Mechanical Engineers, Part I: Journal of Systems and Control Engineering, 215(4), 283-303.

3. Kachroudi, S., Said, A. M., & Alimi, A. M. (2014). Intelligent control of urban traffic using adaptive fuzzy systems. *Journal of Advanced Transportation, 48*(3), 274-289.

4. Kosko, B. (1992). *Neural networks and fuzzy systems*. Prentice Hall.

5. Li, X., Yang, Q., & Wang, Y. (2018). Real-time traffic signal optimization using fuzzy inference mechanisms. *International Journal of Transportation Science and Technology, 7*(2), 134-142.

6. Pandey, R., & Ghosh, S. (2020). Review of fuzzy logic applications in modern intelligent transportation systems. *IEEE Transactions on Intelligent Transportation Systems, 21*(7), 2984-2999.

7. Yager, R. R., & Zadeh, L. A. (Eds.). (1992). *An introduction to fuzzy logic applications in intelligent systems*. Springer.

8. Zadeh, L. A. (1965). Fuzzy sets. *Information and Control, 8*(3), 338-353.

Chapter - 3
Flow and Heat Transmission of Fenugreek Paste in Porous Medium across a Non-isothermal Stretching Sheet

Author

Dr. Ruhul Kuddus Ahmed
Assistant Professor, Department of Mathematics,
Bilasipara College, Bilasipara, Dhubri, Assam, India

Chapter - 3

Flow and Heat Transmission of Fenugreek Paste in Porous Medium across a Non-isothermal Stretching Sheet

Dr. Ruhul Kuddus Ahmed

Abstract

Fenugreek paste exhibiting shear-thinning nature of flow at different temperature is considered in this study. The flow and heat transmission of fenugreek paste in porous medium across a non-isothermal stretching sheet employing Power-law fluid model is investigated. The varying thermal conductivity is taken as a linear function of temperature. The resultant coupled nonlinear governing equations and the relevant boundary conditions of the fenugreek paste flow are reduced to self-similar form using suitable similarity transformation. MATLAB's "bvp4c" solver is utilised to perform the numerical computations. The numerically obtained results of velocity and temperature are represented graphically for different values of involved flow feature parameters and conclusions are drawn from physical point of view.

Keywords: Fenugreek paste, Power-Law fluid, Flow index, stretching sheet, non-isothermal

1. Introduction

Fenugreek (Trigonella Foenum-graecum) is widely grown in Mediterranean region, Indian, and China. It contains protein, amino acid, 4-hydroxyisoleucine, fatty acid, carbohydrates, fiber. The fenugreek seed also contains flavonoids, coumarins, saponins, calcium, phosphorous, iron, zinc, and manganese. It can lower blood sugar levels in diabetes, useful for atherosclerosis, constipation, diabetes, high cholesterol and hypertriglyceridemia, a substitute for cod liver oil in scrofula, rickets, anemia debility following infectious diseases as presented by Schryver (2002).

The mathematical analysis of rheological parameters is essential to the design of flow operations, quality assurance, storage and processing stability measures, texture prediction, and the understanding of molecular and structural changes in food ingredients. The rheological characterization of food items offers crucial information for food scientists, techniques for

choosing ingredients that will help them design, develop, and optimize their goods and production processes and create packaging and storage plans as discussed by Ofoli (1990). Mathematical analysis of reliable and accurate steady rheological data is necessary to design continuous-flow processes, select and size pumps and other fluid-moving machinery and to evaluate heating rates during engineering operations which include flow processes and concentration, and to estimate velocity, shear, and residence-time distribution in food processing operations as presented by Krokida*et al.* (2001).

The latest research on the rheological characteristics of products made from fruit and vegetables has been presented by Diamante and Umemoto (2015). Isikli and Karababa (2005) demonstrated the rheological characterization of fenugreek paste for temperature variation with the help of mathematical model. Brummer *et al.* (2003) investigated the flow behaviour of fenugreek gum with the help of physicochemical properties and illustrated the extraction and purification process of it. Mansour and El-Adawy (1994) examined the nutritional potential of germinated fenugreek seeds and also studied the functional properties due to heat treatment.

One of the most popular and widely used models in the food processing sector is the power-law fluid model. Despite being only aempirical relationship between stress and velocity gradients, this model has proved useful in studying the flow behaviour of non-Newtonian fluids. The power law constitutive fluid model has been employed extensively by many researchers like Schowalter (1960), Andersson *et al.* (1992), Aziz *et al.* (2015), Abdullah *et al.* (2018) and Saritha *et al.* (2018).

Modern technology demands have sparked a great deal of research interest in fluid flow investigation, which examine the interactions between various physical phenomena. One such research, which is crucial to engineering and metallurgy, such as thermal oil recovery, drag reduction, transpiration cooling, etc. examines heat transfer in boundary layer flow across a stretched sheet. Sakiadis (1961) was the first to perform this kind of work, and Crane (1970) expanded it to include a stretched sheet. Several scholars have expanded the latter work to incorporate the impact of heat and mass transport characteristics under various physical conditions Gupta and Gupta (1977), Chen and Char (1988), Tsou *et al.*(1967), McLeod and Rajagopal (1987).

The mathematical modelling of fenugreek paste based on rheological flow parameters for processing applications point of view is considered in this study. The study aims to examine the effects of various physical flow

parameters on the velocity and temperature profiles and to compare the flow patterns and temperature distribution for different values of flow behaviour index to get physical insight of the problem.

2. Mathematical Formulation

An incompressible, steady state of fenugreek paste contained in a saturated porous media that obeys power-law fluid model across a non-isothermal stretching sheet is taken into consideration for this investigation. The flow is contained at y > 0 and the fluid motion is generated in the stretching sheet with the help of two equal and opposite forces along the x-axis keeping origin stationary. To estimate the temperature difference between the ambient fluid and the surrounding surface, flow's temperature-dependent heat source/sink parameter is considered. The non-isothermal boundary conditions viz, surface with prescribed power law surface temperature is taken into account in this study. Equations describing the flow of non-Newtonian fenugreek paste are as follows:

$$u_x + v_y = 0 \quad (2.1)$$

$$uu_x + vu_y = -\frac{\mathrm{K}}{\rho}\left(-{u_y}^n\right)_y - \frac{\nu}{K'}\mathrm{u} \quad (2.2)$$

$$\rho c_p\left(uT_x + vT_y\right) = \left(kT_y\right)_y + \mathrm{Q}(T - T_\infty) \quad (2.3)$$

The appropriate boundary conditions are given by

$$At\ \mathrm{y} = 0\colon\ \mathrm{u} = bx\,,\ v = 0, T = T_W = T_\infty + \mathrm{A}\left(\frac{x}{l}\right) \quad (2.4)$$

$$\mathrm{As}\ y \to \infty\colon u \to 0\,, T \to T_\infty \quad (2.5)$$

where, u- velocity in the x-direction, v- velocity in the y-direction, ρ- fluid density, ν-kinematic viscosityK' − permeability of the porous medium, n-flow index, K − consistency coefficient, c_p − specific heat at constant pressure, Q −heat source when Q > 0, Q −heat sink when Q < 0, T_W - plate temperature, T_∞ -plate temperature far away from plate, k - thermal conductivity, A-constant.

The stream function $u = \Psi_y$ and $v = -\Psi_x$is defined to proceed with the analysis. The continuity equation is shown to be self-satisfying. We also define dimensionless temperature and similarity transformations as:

$$\Psi = \left(\frac{\rho b^{1-2n}}{K}\right)^{\frac{-1}{n+1}} x^{\frac{2n}{n+1}} f(\eta), \eta = y\left(\frac{\rho b^{2-n}}{K}\right)^{\frac{1}{n+1}} x^{\frac{1-n}{1+n}}, \theta(\eta)$$

$$= \frac{T - T_\infty}{T_w - T_\infty} \tag{2.6}$$

$$where\ T_w - T_\infty = A\left(\frac{x}{l}\right) \tag{2.7}$$

Thermal conductivity varies with the temperature in the following form $k = k_\infty\big(1 + \varepsilon\theta(\eta)\big)$, where ε is a small parameter and $k_\infty$is the conductivity of the fluid far away from the sheet.

The following physical parameters are introduced

$$K_1 = \frac{\nu}{K'}\ Pr = \frac{\rho c_p}{k_\infty}\left(\frac{\rho^2 b^{3(n-1)}}{K^2}\right)^{\frac{1}{n+1}} x^{\frac{2(n-1)}{n+1}} f(\eta), \beta = \frac{q}{\rho c_p b} \tag{2.8}$$

Here, K_1- porosity parameter, Pr - Prandtl number, β- heat source/sink parameter.

Equations (2.2) and (2.3) are transformed with help of the similarity variables (2.6) and physical parameters (2.8) as follows:

$$nf'''(-f'')^{n-1} + 2\mathrm{n}(n+1)^{-1} ff'' - (f')^2 - K_1 f' = 0 \tag{2.9}$$

$$(1 + \varepsilon\theta)\theta'' + \varepsilon(\theta')^2 + Pr(2\mathrm{n}(n+1)^{-1} f\theta' - (f' - \beta)\theta) = 0 \tag{2.10}$$

The boundary conditions (2.4) and (2.5) in view of (2.6) are reduced as

$$At\ \eta = 0\text{: f} = 0,\ f' = 1, \theta = 1 \tag{2.11}$$

$$As\ \eta \to \infty\text{: } f' \to 0,\ \theta \to 0 \tag{2.12}$$

3. Method of Solution

Matlab's built-in numerical method "bvp4c" is a collocation method for solving differential equations with non-linear boundary conditions where the parameter q is unknown. Unlike the shooting method, this one is based on an algorithm and can effectively solve differential equations. The approximation of y(x) for any x in [a, b] according to boundary conditions can be computed effectively. This approach involves substituting a finite point that reasonably satisfies the problem instead of the infinity criteria at the boundary.

The self-similar governing equations (2.9) and (2.10) are transformed to differential equations of the first order as follows:

$$f = y_1,\ f' = y_2,\ \ f'' = y_3,\ \theta = y_4,\ \theta' = y_5 \tag{3.1}$$

$$y_1' = y_2,\ y_2' = y_3, y_4' = y_5 \quad (3.2)$$

$$y_3' = \frac{1}{n}(-y_3)^{1-n}\left[(y_2)^2 + K_1 y_1 - \frac{2n}{n+1} y_1 y_3\right] \quad (3.3)$$

$$y_5' = \frac{1}{(1+\varepsilon y_4)}\left[-\varepsilon(y_5)^2 - Pr\left\{\frac{2n}{n+1} y_1 y_5 - (y_2 - \beta) y_4\right\}\right] \quad (3.4)$$

The boundary Conditions (2.11) and (2.12) are transformed as

$$y_1(0) = 0,\ y_2(0) = 1,\ y_4(0) = 1, y_5(0) = -1 \quad (3.5)$$

$$y_2(\infty) = 0, y_4(\infty) = 0 \quad (3.6)$$

In order to calculate the aforementioned equations and the various related flow feature parameters, the MATLAB built-in solver 'bvp4c' is used.

4. Results and discussion

The profiles of horizontal velocity$(f'(\eta))$ and temperature$\big(\theta(\eta)\big)$ for the fenugreek paste in porous medium across a non-isothermal stretching sheet is examined. The impact of involved flow parameters, viz. flow index (n), porosity parameter (K_1), Prandtl number $P(r)$, thermal conductivity parameter (ε) and heat source/sink parameter$(\beta)$are examined to get clear physical insight of the problem. The numerically computed values of velocity$(f'(\eta))$ and temperature$\big(\theta(\eta)\big)$ are presented graphically in Figs. 4.1 - 4.7.

Figs. 4.1 and 4.2 demonstrate the impact of flow index (n) and porosity parameter (K_1) on the profiles of horizontal velocity$(f'(\eta))$. From Fig. 4.1 it's clear that the horizontal velocity decreases monotonically and tends to zero with the increase of space variable η from the boundary. The reducing values of flow index of fenugreek paste exhibiting pseudoplastic nature helps to enhance the velocity profiles and consequently boundary layer thickness diminishes. It is noticed from Fig. 4.2 that the growth of porosity parameter (K_1) reduces the horizontal velocity. The influence of porosity helps to resist the fluid motion and thus enhance the deceleration of the flow.

The influence of flow index (n) and porosity parameter (K_1) on the temperature profiles are depicted in Figs. 4.3 and 4.4. From Fig. 4.3 its clear that the temperature of the fluid enhances with the reducing values of flow index (n) and monotonically diminishes to zero in the free stream region and thus reduces the boundary layer thickness. The growth of porosity parameter (K_1) though initially reduces the temperature profile but gradually it enhances with increasing distance of space variable η.

The effect of Prandtl number (Pr) on the temperature profile $\big(\theta(\eta)\big)$ is shown in Fig. 4.5. The temperature profile reduces with the growth of Prandtl number and tends to zero at the boundary. The result is justified as Prandtl number reduces boundary layer thickness. The impact of heat source/sink parameter (β) on the temperature profile $\big(\theta(\eta)\big)$ is displayed in Fig. 4.6. It is noticed that the temperature profile diminishes with the growth of β. The result is obvious as more fluid enters into the system, the fluid temperature decreases. The influence of thermal conductivity on the temperature profile $\big(\theta(\eta)\big)$is shown in Fig. 4.7. The growing thermal conductivity parameter(ε) enhances the temperature profile $\big(\theta(\eta)\big)$ for the fenugreek paste.

Table 4.1: Rheological parameters of Fenugreek paste [7]

Product	T (^{0}C)	k (Pa s^n)	n
Fenugreek Paste	10	3.7490	0.595
	20	5.3440	0.567
	30	12.4200	0.515

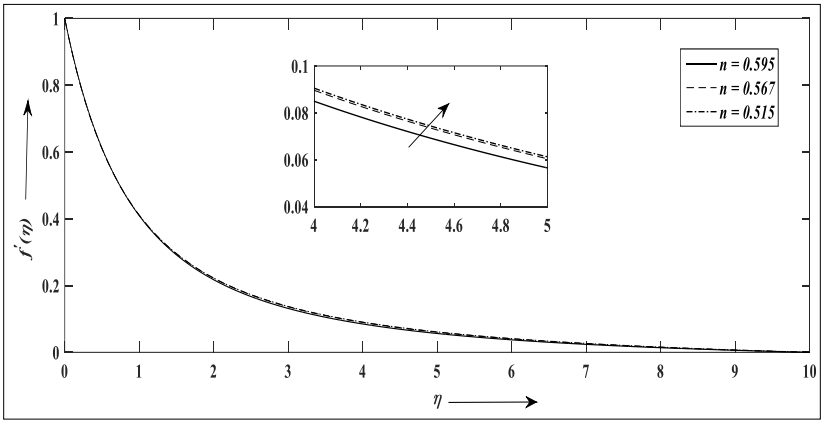

Fig 4.1: $f'(\eta)$ versus η for variation of n taking $K_1 = 0$

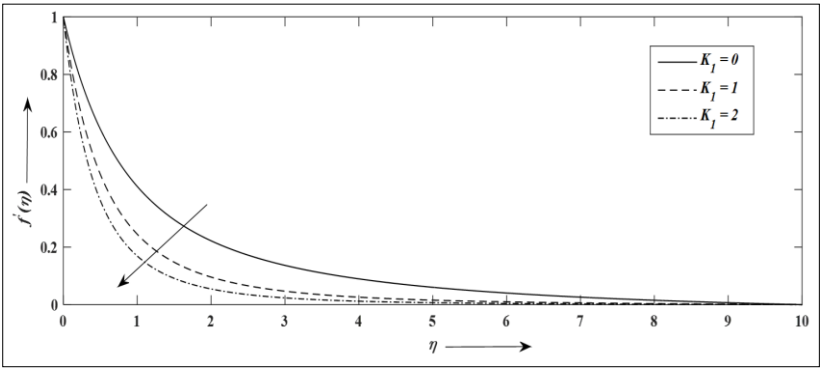

Fig 4.2: $f'(\eta)$ versus η for variation of K_1 taking $n = 0.567$

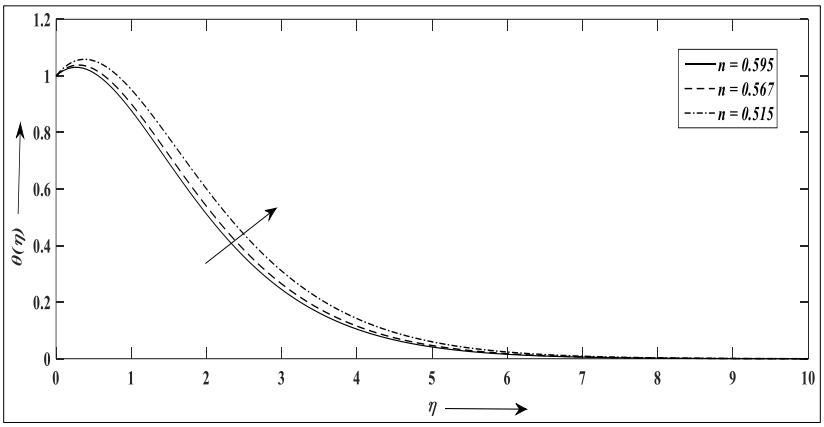

Fig 4.3: $\theta(\eta)$ versus η for variation of n taking $K_1 = 0, \beta = 0, Pr = 1, \varepsilon = 0$

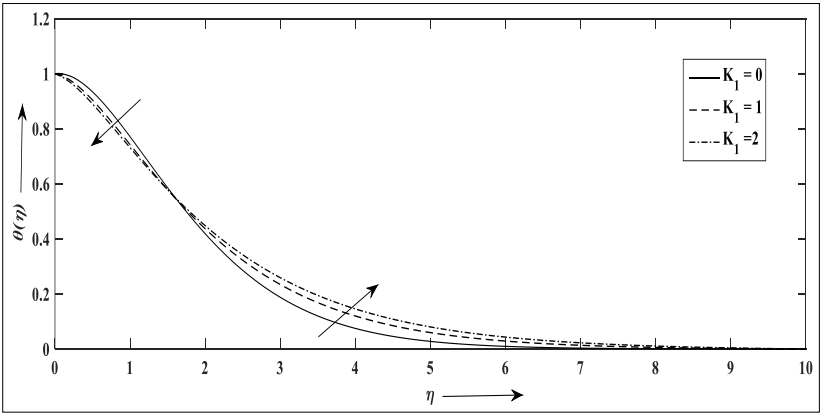

Fig 4.4: $\theta(\eta)$ versus η for variation of K_1 taking $n = 0.567, \beta = 0.1, Pr = 1, \varepsilon = 0.1$

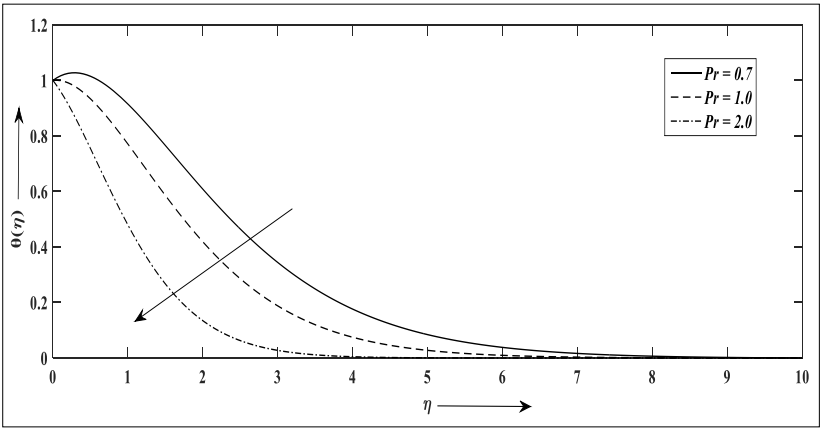

Fig 4.5: $\theta(\eta)$ versus η for variation of P_r taking $n = 0.567, \beta = 0.1, K_1 = 0, \varepsilon = 0.1$

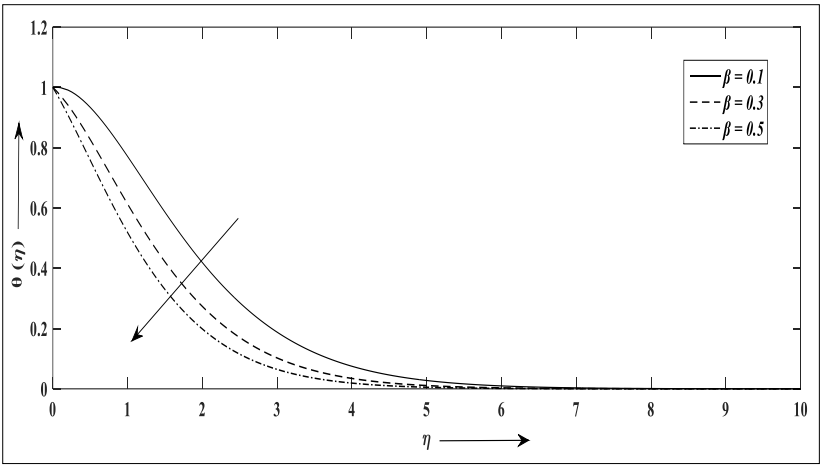

Fig 4.6: $\theta(\eta)$ versus η for variation of β taking $n = 0.567, K_1 = 0, \mathrm{Pr} = 1, \varepsilon = 0.1$

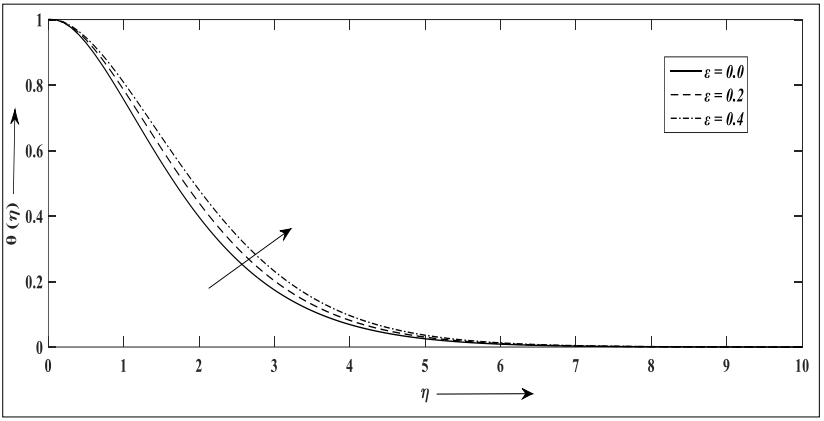

Fig 4.7: $\theta(\eta)$ versus η for variation of ε taking $n = 0.567, K_1 = 0, \Pr = 1, \beta = 0.1$

5. Conclusion

The following conclusions can be drawn from this study:

- The horinzontal velocity diminishes with the growth of flow index and porosity parameter and consequently boundary layer thickness reduces.
- The reducing values of flow index enhances the temperature of the fenugreek paste across the non-isothermal stretching sheet.
- The temperature profile for fenugreek paste reduces initially with the growth of porosity parameter but gradually it enhances with growing distance of space variable.
- The growth of Prandtl number reduces the temperture profile and thus boundary layer thickness diminishes.
- Thermal conductivity parameter enhances the temperature profile but the rising values of source/sink parameter reduces the fluid temperature.

6. Scope For Future Work

Due to multiple potential applications in engineering and the food industry, there is lots of scope for further research. Fluid flow concerns with diverse geometries can also be considered based on the requirements of the food processing industries. This study investigated a few fluid characteristics; however, future research might cover many more rheological fluid qualities vital to the engineering and food industries. The flow simulation may give a clear picture of the results.

References

1. Abdullah, N., Chin, N.I., Yusof, Y.A. and Talib, R.A. (2018). Modelling of rheological behaviour of guava, pomelo and soursop juice concentrates via shear rate-temperature-concentration super positioning. J Food Sci Technol, vol. 55(3), pp: 1207-1213.
2. Andersson, H.I., Bech, K.H. and Dandapat, B.S. (1992). Magneto hydrodynamic flow of a power law fluid over a stretching sheet. International Journal of Non-Linear Mechanics, 72, 929-936.
3. Aziz, A., Ali, Y., Aziz, T. and Siddique, J. (2015). Heat Transfer analysis for stationary boundary layer slip flow of a power low fluid in a Darcy porous medium with plate suction/injection. PLoS ONE. Vol.10 (9), doi:10.1371/journal.pone.0138855.
4. Brummer, Y., Cui, W., & Wang, Q. (2003). Extraction, purification and physicochemical characterization of fenugreek gum. Food Hydrocolloids, 17, 229-236.
5. Chen, C. K. and Char, M. I.: (1988) "Heat transfer on a continuous stretching surface with suction or blowing", J. Math. Anal. Appl. 35, 568 - 580.
6. Crane, L.J. (1970). Flow past a stretching plane. Angew Math. Phy. 21, 645-647.
7. Diamante, L., Umemoto, M. (2015). Rheological properties of Fruits and Vegetables: A Review. International Journal of Food Properties, 18, 1191-1210.
8. Gupta P.S. and Gupta A.S. (1977). Heat and mass transfer on a stretching sheet with suction or blowing. Can. J. Chem. Engng. 55, 744-746.
9. Isikli, N.D. and Karababa, E. (2005) Rheological characterization of fenugreek paste (cemen) Journal of Food Engineering 69, 185-190.
10. Krokida, M. K., Maroulis, Z. B., &Saravacos, G. D. (2001). Rheological properties of fluid fruit and vegetable puree products: compilation of literature data. International Journal of Food Properties, 4(2), 179-200.
11. Mansour, E. H., & El-Adawy, T. A. (1994). Nutritional potential and functional properties of heat treated and germinated fenugreek seeds. Lebensmittel-Wissenschaft und Technologie, 27, 568-573.
12. McLeod. B. and Rajagopal, K. R. :(1987) "On the non-uniqueness of the flow of a Navier - Stokes fluid due to stretching boundary", Arch.Rat.Mech.Anal 98, 385-493.
13. Ofoli, R. Y. (1990). Interrelationships of rheology, kinetics, and transport phenomena in food processing. In H. Faridi & J. M. Faubion (Eds.), Dough Rheology and Baked Product Texture. New York. AVI.

14. Sakiadis, B.C. (1961). Boundary layer behavior on continuous solid surfaces: I. Boundary layer equations for two dimensional and axisymmetric flow. AZChE Journal 7, 26-28.
15. Saritha, K., Rajasekhar, M.N. and Reddy, B.S. (2018). Combined effects of soret and dufour on mhd flow of a Power-law fluid over flat plate in slip flow regime. International Journal of Applied Mechanics and Engineering, 23(3), 689-705.
16. Schowalter, W.R. (1960). The application of boundary layer theory to power law pseudo plastic fluids: similar solutions", AIChE Journal. vol. 6(1), 24-28.
17. Schryver, T. (2002). Fenugreek. Total Health, 24(4), 42-44.
18. Tsou, F., Sparrow, E. and Goldstein, R.J. (1967). Flow and heat transfer in the boundary layer on a continuous moving surface. Znt. J. Heat Mass Transfer 10, 219-235.

Chapter - 4
The Potential of the 〖So〗^ξ Value

Authors

Elen Borang
Department of Mathematics, Dibrugarh University,
Dibrugarh & Bhola Nath College, Dhubri, Assam, India

Sujata Goala
Department of Mathematics, Dibrugarh University,
Dibrugarh & Gargaon College, Sibsagar, Assam, India

Chapter - 4

The Potential of the So^{ξ} Value

Elen Borang and Sujata Goala

Abstract

A key challenge in economic allocation problems is finding a balance between marginalism and egalitarianism. In cooperative game theory, this trade-off can be understood as deciding whether to distribute payoffs based on the Shapley value, which reflects each player's marginal contributions, or the Equal Division rule, which splits the value equally among all players. This chapter examines a particular class of solutions for cooperative TU-games that admit a potential function, particularly the potential associated with the Shapley value. In this work, we propose a modified potential function and establish its recursive relationship with the So^{ξ} value. Furthermore, we prove the uniqueness of the So^{ξ} value using the same potential function.

Keywords: So^{ξ} value, Cooperative TU-games, Potential.

1. Introduction

In economic contexts, players often form coalitions to maximize their collective gains. A key challenge lies in determining how to fairly allocate the cooperative surplus among the participating players. Game theory offers a set of mathematical tools to systematically analyse such distribution problems in cooperative settings. Cooperative game theory addresses the allocation problem by determining how to distribute the total payoff among participating players in a fair and stable manner. The field of cooperative game theory has developed several distinct solution concepts, each providing different approaches to value distribution in coalitions.

The Shapley value [5] and the Equal Division rule [6] are arguably the two most prominent solution concepts in cooperative game theory. They differ fundamentally in how they assess players' contributions to coalitions. The Shapley value follows a marginalistic approach, assigning payoffs based on each player's pure marginal contribution, whereas the Equal Division rule adopts an egalitarian perspective, allocating the total payoff equally among all players.

Hart and Mas-Colell [4] were the first to introduce the potential approach in cooperative transferable utility games. In a seminal result, they demonstrated that the Shapley value [5] can be obtained as the vector of marginal contributions derived from a particular potential function, and further showed that this marginal contribution vector of the function coincides with the Shapley value.

In this chapter, we examine the So^{ξ} value from several perspectives. First, we derive a revised potential function corresponding to this value. We then prove the uniqueness of the So^{ξ} value using a potential function.

2. Preliminaries

A cooperative game with transferable utility (TU-game) is a pair (N, v) where $v: 2^N \to R$ is the characteristic function such that $v(\emptyset) = 0$. The set of all TU games over N is denoted by $G(N)$. A player $i \in N$ called the Null player if $v(S \cup i) = v(S)$ for all $S \subseteq N \setminus i$. A player $i \in N$ called the Nullifying player if $v(S) = 0$ for all $S \subseteq N$ such that $i \in S$. The basic assumption in cooperative games is the formation of grand coalition N. The number of players in coalition S is denoted by $s = |S|$. For a game $(N, v) \in G(N)$ and a coalition $T \in 2^N \setminus \{\emptyset\}$, the subgame with player set T is the game $(T, v|_T)$ defined by $v|_T(S) = v(S)$ for all $S \in 2^T$. A solution of a game is an n-vector which assigns payoffs to each player in N. An allocation rule (efficient) is a function $\Phi : G(N) \to R^n$ which allocates the value of the grand coalition to the players in some reasonable manner. There are many solution concepts which have been proposed over the years. The one point solutions are called values. The Shapley value is the most popular value for TU games. The Shapley value Φ^{Sh} due to shapely [5] is defined by

$$\Phi_i^{Sh}(v) = \sum_{S \subseteq N \setminus i} \frac{(n-s-1)!\, s!}{n!} [v(S \cup i) - v(S)].$$

The Equal Division (ED) [6] rule is another important value for TU games defined by

$$\Phi_i^{ED}(v) = \frac{v(N)}{n} \; for\ all\ i \in \mathrm{N}$$

In the study of TU-games, solution concepts are often characterized by the following well-known properties:

- Efficiency, if $\sum_{i \in N} \Phi_i(v) = v(N)$.
- Anonymity, if for any permutation $\pi: N \to N$, one has $\Phi_i(v) = \Phi_{\pi(i)}(\pi v)$, where the TU game πv is defined by $\pi v(\pi S) = v(S)$.

- Symmetry, if for all symmetric players $i, j \in N$, where $v(S \cup i) = v(S \cup j)$ for all $S \subseteq N \setminus \{i, j\}$ we have $\Phi_i(v) = \Phi_j(v)$.
- Linearity, if for each pair $v, w \in G(N)$, and $\alpha, \beta \in R$, $\Phi(\alpha v + \beta w) = \alpha\, \Phi(\mathrm{v}) + \beta\, \Phi(\mathrm{w})$.
- Null Player Property, for each $i \in N$, who is a null player, $\Phi_i(v) = 0$.
- Nullifying Player Property, $i \in N$, for each who is a nullifying player, $\Phi_i(v) = 0$.
- Desirability, for all N, $v \in G(N)$, and $i, j \in N$ such that $v(S \cup i) - v(S) \geq v(S \cup j) - v(S)$ for all $S \subseteq N \setminus \{i, j\}$ we have $\Phi_i(v) \geq \Phi_j(v)$.
- Positivity, for all N, $v \in G(N)$, and $i \in N$ such that v is monotonic, $\Phi_i(v) \geq 0$.

In shapely [5], the Shapley value is characterized by four key axioms: Efficiency, Anonymity, Linearity, and the Null Player Property. In contrast, the Equal Division rule is characterized in van den Brink [6] using a similar set of axioms: Efficiency, Anonymity, and Linearity and the Nullifying Player Property. In [1], Casajus and Huettner proposed a ξ-parameterized family of solutions, denoted as the class of Solidarity values, whose extremes coincide with the Shapley value and the Equal Division rule. This value is referred to as the So^{ξ} value, defined by,

$$So_i^{\xi}(v) = \xi_n.\frac{v(N)}{n} + \sum_{S \subseteq N \setminus i} \rho_{n,s}.\left[(1 - \xi_{s+1}).v(S \cup i) - (1 - \xi_s).v(S)\right]$$

for all $i \in N$ and $v \in G(N)$, where $\xi_l = \frac{l.\xi}{(l-1).\xi+1}$, for $l \in N$, $\xi \in R \setminus \{-\frac{1}{q}, q \in \mathrm{N}\}$ and

$$\rho_{n,s} = \frac{(n-s-1)!\,s!}{n!}.$$

Hart and Mas-Colell [4] introduced the potential function approach to characterize the Shapley value. The potential function is defined as a real-valued function P such that the sum of the marginal contributions of all players, as determined by P, equals the total worth of the grand coalition. Remarkably, the Shapley value can be expressed as the vector of marginal contributions derived from a specific potential function. Given a function $P: G \to R$ that associates a real number $P(N, v)$ to every game $(N, v) \in G$,

the marginal contribution $D_iP(N,v)$ of a player $i \in N$ is denoted by

$$D_iP(N,v) = P(N,v) - P\big(N \setminus i, v|_{N\setminus i}\big) \quad (1)$$

A function $P: G \to R$ with $P(\emptyset, v) = 0$ is called potential function if it satisfies

$\sum_{i \in N} D_iP(N,v) = v(N)$, for all games $(N,v) \in G$.

Theorem 1: [3] There exists a unique potential function P. For every game (N,v) the resulting payoff vector $D_iP(N,v)$ of marginal contributions coincides with the Shapley value of the game.

3. The ξ-Potential Function

Hart and Mas-Colell [4] demonstrated that there exists a unique potential function P such that the vector of marginal contributions assigned by P coincides with the Shapley value of the game which is already stated in Theorem 1. Later, Dragan [2] proposed a modified potential function Q, which does not enforce efficiency normalization, to characterize the Banzhaf value. However, due to the egalitarian nature of the So^{ξ} value, directly allocating marginal contributions to individual players is inappropriate. To address this, we introduce a revised potential function defined as follows.

Definition 1: A function $P: G \to R$ with $P^{\xi}(\emptyset, v) = 0$ is called a ξ-potential function if it satisfies for all games (N,v),

$$\sum_{i \in N} D_iP^{\xi}(N,v) = v(N) - \frac{\xi_{n-1}}{n-1}\sum_{i \in N} v(N \setminus i).$$

Clearly, $D_iP^{\xi}(N,v) = P^{\xi}(N,v) - P^{\xi}(N \setminus i, v) + \frac{\xi_{n-1}}{n-1}\sum_{i \in N} v(N \setminus i)$.

Consequently,

$$\sum_{i \in N} D_iP^{\xi}(N,v) = \sum_{i \in N} So_i^{\xi}(N,v) + \sum_{i \in N} \frac{\xi_{n-1}}{n-1}\, v(N \setminus i)$$

$= v(N) + \sum_{i \in N} \frac{\xi_{n-1}}{n-1}\, v(N \setminus i)$

$\Longrightarrow \sum_{i \in N}[D_iP^{\xi}(N,v) + \frac{\xi_{n-1}}{n-1}\, v(N \setminus i)] = v(N)$.

From Definition (1), for all subgames $(S, v|_S)$:

$$\sum_{i \in S} D_iP^{\xi}(S, v|_S) = v(S) - \frac{\xi_{s-1}}{s-1}\sum_{i \in S} v(S \setminus i)\,.$$

$$\Rightarrow \sum_{i\in S}\left[P^{\xi}(S,v|_S) - P^{\xi}\left(S\setminus i, v|_{S\setminus i}\right)\right] = v(S) - \frac{\xi_{s-1}}{s-1}\sum_{i\in S} v(S\setminus i).$$

$$sP^{\xi}(S,v|_S) - \sum_{i\in S} P^{\xi}\left(S\setminus i, v|_{S\setminus i}\right) = v(S) - \frac{\xi_{s-1}}{s-1}\sum_{i\in S} v(S\setminus i).$$

$$P^{\xi}(S,v|_S) = \frac{1}{s}\left[\sum_{i\in S} P^{\xi}\left(S\setminus i, v|_{S\setminus i}\right) + v(S) - \frac{\xi_{s-1}}{s-1}\sum_{i\in S} v(S\setminus i)\right] \quad (2)$$

$\forall\, S \subseteq N$ with $P^{\xi}(\emptyset, v) = 0$.

Proposition 1: For any game $(N, v) \in G$,

$$P^{\xi}(N,v) = \frac{1}{n}v(N) + \sum_{S\subsetneq N}\frac{(s-1)!\,(n-s)!}{n!}(1-\xi_s)v(S) \quad (3)$$

Proof: We prove by induction, $P^{\xi}(\emptyset, v) = 0$ is obvious.

Assume that,

$$P^{\xi}\left(N\setminus i, v|_{N\setminus i}\right) = \frac{\xi_{n-1}}{n-1}v(N\setminus i) + \sum_{S\subsetneq N\setminus i}\frac{(s-1)!\,(n-s-1)!}{(n-1)!}(1-\xi_s)v(S).$$

From the recursive Definition (2) of the ξ -potential function,

$$P^{\xi}(N,v) = \frac{1}{n}\left[\sum_{i\in N} P^{\xi}\left(N\setminus i, v|_{N\setminus i}\right) + v(N) - \frac{\xi_{n-1}}{n-1}\sum_{i\in N} v(N\setminus i)\right]$$

$$= \frac{1}{n}\left[\frac{\xi_{n-1}}{n-1}v(N\setminus i) + \sum_{S\subsetneq N\setminus i}\frac{(s-1)!\,(n-s-1)!}{(n-1)!}(1-\xi_s)v(S).\right] + \frac{v(N)}{n} - \frac{\xi_{n-1}}{n(n-1)}\sum_{i\in N} v(N\setminus i)$$

$$= \frac{v(N)}{n} + \left[\frac{\xi_{n-1}}{n(n-1)} - \frac{\xi_{n-1}}{n(n-1)}\right]\sum_{i\in N} v(N\setminus i) + \frac{1}{n}\sum_{i\in N}\sum_{S\subsetneq N\setminus i}\frac{(s-1)!(n-s-1)!}{(n-1)!}(1-\xi_s)v(S)$$

$$= \frac{v(N)}{n} + \frac{1}{n}\sum_{i\in N}\sum_{S\subsetneq N\setminus i}\frac{(s-1)!\,(n-s-1)!}{(n-1)!}(1-\xi_s)v(S)$$

$$= \frac{v(N)}{n} + \frac{1}{n}\sum_{S\subsetneq N\setminus i}\frac{(s-1)!(n-s-1)!}{(n-1)!}(1-\xi_s)v(S).$$

Remark: Although the potential of the Shapley value is known from the work of Hart and Mas-Colell [3], the potential corresponding to the Equal Division (ED) value has not been explored in the literature. In particular, when $\xi = 1$, our framework yields the potential corresponding to the ED value, whereas for $\xi = 0$, it reduces to the potential of the Shapley value.

Definition 2: The vector of adjusted marginal contributions according to the ξ -potential function coincides with the So^{ξ} value, we denote by $A_i P^{\xi}(N, v)$ the adjusted marginal contribution for all $i \in N$

As

$$A_i P^{\xi}(N, v) = P^{\xi}(N, v) - P^{\xi}(N \setminus i, v) + \frac{\xi_{n-1}}{n-1} v(N \setminus i).$$

$$A_i P^{\xi}(N, v) = D_i P^{\xi}(N, v) + \frac{\xi_{n-1}}{n-1} v(N \setminus i). \quad (4)$$

Theorem 2: There exist a unique ξ -potential function P^{ξ} on G(N). The payoff vector $AP^{\xi}(N, v) \equiv \left(A_i P^{\xi}(N, v)\right)_{i \in N}$ coincides with the So^{ξ} value $So^{\xi}(N, v)$ for every game$(N, v) \in \mathrm{G(N)}$.

Proof. The existence and uniqueness of the ξ -potential function P^{ξ} follow directly from equation (3). To show that $AP^{\xi}(N, v) = So^{\xi}(N, v)$ for every game $(N, v) \in \mathrm{G(N)}$, it is sufficient to check that all the axioms in casajus [1] which uniquely determine the So^{ξ} value are also satisfied by AP^{ξ}. Efficiency of AP^{ξ} is just from the definition of the ξ -potential function.

i.e.

$$\sum_{i \in N} A_i P^{\xi}(N, v) = \sum_{i \in N} D_i P^{\xi}(N, v) + \sum_{i \in N} \frac{\xi_{n-1}}{n-1} v(N \setminus i)$$

$$= v(N) - \frac{\xi_{n-1}}{n-1} \sum_{i \in N} v(N \setminus i) + \sum_{i \in N} \frac{\xi_{n-1}}{n-1} v(N \setminus i)]$$

$$= v(N).$$

Secondly, we can obtain the additivity P^{ξ} by (3) that is $P^{\xi}(N, v + w) = P^{\xi}(N, v) + P^{\xi}(N, w)$

for any game $(N, v), (N, w) \in \mathrm{G(N)}$.

Let, $v, w \in V(N)$, $u = v + w$ so that $u(S) = v(S) + w(S)$

We prove additivity by induction on the number of players n.

Suppose, $N = \{i\}$, then

$P^{\xi}(\{i\}, v) = \frac{1}{n} v(\{i\})$, $P^{\xi}(\{i\}, w) = \frac{1}{n} w(\{i\})$ and $P^{\xi}(\{i\}, v + w) = \frac{1}{n}(v + w)(\{i\}) = \frac{1}{n}[v(\{i\}) + w(\{i\})]$.

Therefore, $P^{\xi}(\{i\}, v + w) = P^{\xi}(\{i\}, v) + P^{\xi}(\{i\}, w)$.

Assume P^{ξ} is additive for all games with fewer than n players.

Let N be a set of n players. Using the recursive formula (2) for game $u = v + w$.

$$P^{\xi}(N, v + w) = \frac{1}{n}\left[\sum_{i \in N} P^{\xi}\left(N \setminus i, (v + w)|_{N \setminus i}\right) + (v + w)(N) - \frac{\xi_{n-1}}{n - 1}\sum_{i \in N}(v + w)(N \setminus i)\right]$$

$$= \frac{1}{n}\left[\sum_{i \in N} P^{\xi}\left(N \setminus i, (v + w)|_{N \setminus i}\right) + v(N) + w(N) - \frac{\xi_{n-1}}{n - 1}\sum_{i \in N}(v + w)(N \setminus i)\right]$$

$$= \frac{1}{n}\left[\sum_{i \in N} P^{\xi}\left(N \setminus i, v|_{N \setminus i}\right) + v(N) - \frac{\xi_{n-1}}{n - 1}\sum_{i \in N} v(N \setminus i)\right]$$

$$+ \frac{1}{n}\left[\sum_{i \in N} P^{\xi}\left(N \setminus i, w|_{N \setminus i}\right) + w(N) - \frac{\xi_{n-1}}{n - 1}\sum_{i \in N} w(N \setminus i)\right]$$

$$= P^{\xi}(N, v) + P^{\xi}(N, w).$$

Hence, it is trivial to verify the additivity of DP^{ξ} as well as AP^{ξ} by equations (1) and (4).

Next, let i and j be symmetric players in game (N, v). We first show that $P^{\xi}\left(S \setminus j, v|_{S \setminus j}\right) = P^{\xi}\left(S \setminus i, v|_{S \setminus i}\right)$ for all $S \subseteq N, S \ni i, j$. It is trivial for $S = \{i, j\}$. Suppose that it holds for all such subgames $2 \leq s < n$.

We have:

$$P^{\xi}\left(N \setminus j, v|_{N \setminus j}\right) - P^{\xi}\left(N \setminus i, v|_{N \setminus i}\right)$$

$$= \frac{1}{n-1}\left[\sum_{k\in N\setminus j} P^{\xi}\left(N\setminus\{j,k\}, v|_{N\setminus\{j,k\}}\right) + v(N\setminus j) - \frac{\xi_{n-1}}{n-1}\sum_{k\in N\setminus j} v(N\setminus\{j,k\})\right]$$

$$-\frac{1}{n-1}\left[\sum_{k\in N\setminus i} P^{\xi}\left(N\setminus\{i,k\}, v|_{N\setminus\{i,k\}}\right) + v(N\setminus i) - \frac{\xi_{n-1}}{n-1}\sum_{k\in N\setminus i} v(N\setminus\{i,k\})\right]$$

$$= \frac{1}{n-1}\left[\sum_{k\in N\setminus j} P^{\xi}\left(N\setminus\{j,k\}, v|_{N\setminus\{j,k\}}\right) - \sum_{k\in N\setminus i} P^{\xi}\left(N\setminus\{i,k\}, v|_{N\setminus\{i,k\}}\right)\right]$$

=0

Since, $v(N\setminus i) = v(N\setminus j)$, the symmetry of AP^{ξ} is verified as follows.

$$A_i P^{\xi}(N,v) - A_j P^{\xi}(N,v)$$

$$= D_i P^{\xi}(N,v) + \frac{\xi_{n-1}}{n-1} v(N\setminus i) - \left[D_j P^{\xi}(N,v) + \frac{\xi_{n-1}}{n-1} v(N\setminus j)\right]$$

$$= P^{\xi}\left(N\setminus j, v|_{N\setminus j}\right) - P^{\xi}\left(N\setminus i, v|_{N\setminus i}\right)$$

$$= 0.$$

Next, let $i \in N$ be a ξ -Player. , $i.e.$,

$$\left(1 + \frac{\xi_s}{s}\right) v(S) = v(S\cup i) \quad \forall S \subseteq N\setminus i.$$

$For j \neq i, j \in N$, using the proposition (3) we have to prove that $AP_j^{\xi}(N,v) = AP_j^{\xi}(N\setminus j, v)$

Now,

$$AP_j^{\xi}(N,v) = P^{\xi}(N,v) - P^{\xi}(N\setminus j, v) + \frac{\xi_{n-1}}{n-1} v(N\setminus j)$$

$$= \frac{v(N)}{n} + \sum_{S \subseteq N} \frac{(n-s)!\,(s-1)!}{n!}(1-\xi_s)v(S)$$

$$- \left[\frac{v(N \setminus j)}{n-1} + \sum_{S \subseteq N \setminus j} \frac{(n-s-1)!\,(s-1)!}{(n-1)!}(1-\xi_s)v(S)\right]$$

$$+ \frac{\xi_{n-1}}{n-1} v(N \setminus j)$$

$$= \xi_n \frac{v(N)}{n} + (1-\xi_n)\frac{v(N)}{n} - \left(\frac{1-\xi_{n-1}}{n-1}\right) v(N \setminus j)$$

$$+ \sum_{S \subseteq N \setminus j} \frac{(n-s)!\,(s-1)!}{n!}[(1-\xi_{s+1})v(S \cup j)$$

$$- (1-\xi_s)v(S)]$$

$$= \xi_n \frac{v(N)}{n} + \sum_{S \subseteq N \setminus j} \frac{(n-s)!\,(s-1)!}{n!}[(1-\xi_{s+1})v(S \cup j) - (1-\xi_s)v(S)]$$

$$= \xi_n \left(1 + \frac{\xi_{n-1}}{n-1}\right) v(N \setminus i)$$

$$+ \sum_{S \subseteq N \setminus j, i \in S} [(1-\xi_{s+1})v(S \cup j) - (1-\xi_s)v(S)]$$

$$+ \sum_{S \subseteq N \setminus j, i \notin S} \frac{(n-s)!\,(s-1)!}{n!}[(1-\xi_{s+1})v(S \cup j)$$

$$- (1-\xi_s)v(S)]$$

$$= \frac{\xi_{n-1}}{n-1} v(N \setminus i)$$

$$+ \sum_{S \subseteq N \setminus j} \frac{(n-s)!\,(s-1)!}{n!}[(1-\xi_s)v(S \cup j \setminus i) - (1-\xi_{s-1})v(S \setminus i)]$$

$$+\sum_{S\subseteq N\setminus j, i\notin S}\frac{(n-s-1)!\,s!}{n!}[(1-\xi_s)v(S\cup j)-(1-\xi_{s-1})v(S)]$$

$$=\frac{\xi_{n-1}}{n-1}v(N\setminus i)+\sum_{S\subseteq N\setminus\{i,j\}}\left[\frac{(n-s)!\,(s-1)!}{n!}+\frac{(n-s-1)!\,(s)!}{n!}\right][(1-\xi_s)v(S\cup j)-(1-\xi_{s-1})v(S)]$$

$$=\frac{\xi_{n-1}}{n-1}v(N\setminus i)+\sum_{S\subseteq N\setminus\{i,j\}}\frac{(n-s-1)!\,(s-1)!}{(n-1)!}[(1-\xi_{s+1})v(S\cup j)-(1-\xi_s)v(S)] \quad (5)$$

Again,

$$AP_j^{\xi}(N\setminus j,v)=P^{\xi}(N\setminus j,v)-P^{\xi}(N\setminus ij,v)+\frac{\xi_{n-2}}{n-2}v(N\setminus\{i,j\})$$

$$=\frac{v(N\setminus i)}{n-1}-\frac{v(N\setminus\{i,j\})}{n-2}+\frac{\xi_{n-2}}{n-2}v(N\setminus\{i,j\})+\sum_{S\subseteq N\setminus\{i,j\}}\frac{(n-s-1)!\,(s-1)!}{(n-1)!}[(1-\xi_{s+1})v(S\cup i)-(1-\xi_s)v(S)]$$

$$=\frac{\xi_{n-1}}{n-1}v(N\setminus i)+\frac{(1-\xi_{n-1})}{n-1}v(N\setminus i)-\frac{(1-\xi_{n-2})}{n-2}v(N\setminus\{i,j\})+\sum_{S\subseteq N\setminus\{i,j\}}\frac{(n-s-1)!\,(s-1)!}{(n-1)!}[(1-\xi_{s+1})v(S\cup i)-(1-\xi_s)v(S)]$$

$$=\frac{\xi_{n-1}}{n-1}v(N\setminus i)+\sum_{S\subseteq N\setminus\{i,j\}}\frac{(n-s-1)!\,(s-1)!}{(n-1)!}[(1-\xi_{s+1})v(S\cup i)-(1-\xi_s)v(S)] \quad (6)$$

Hence, from equations (5) and (6), we get

$$AP_j^{\xi}(N,v)=AP_j^{\xi}(N\setminus j,v).$$

Therefore, $AP^{\xi}(N,v)$ coincides with the $So^{\xi}(N,v)$ on G(N).

References

1. Casajus, A., & Huettner, F., (2014a). On a class of solidarity values. European Journal of Operational Research, 236(2), 583-591.
2. Dragan, I., (1996). New mathematical properties of the Banzhaf value. European J. Oper. Res. 95, 451-463.
3. Hart, S. & Mas-Colell, A., (1988). The potential of the Shapley value. In: A.E. Roth (ed), The Shapley value, Essays in Honor of L.S. Shapley. Cambridge University Press, 127-137.
4. Hart, S. & Mas-Colell A., (1989). Potential, value and consistency. Econometrica, 57, 589-614.
5. Shapley, L.S., (1953). A value for n-person games. In: Contributions to the Theory of Games, II. Ed. by W.H. Kuhn, and A.W. Tucker. (Annals of Math. Studies 28). Princeton, 303-306.
6. van den Brink, J. R., (2004). Null or zero players: the difference between the Shapley value and the egalitarian solution.

Chapter - 5
A Discussion on Some Extensions of Reversible Rings and Their Connections with Weak-α Symmetric ring"

Author

Manjuri Dutta
Assistant Professor, Dimoria College (Autononmous),
Guwahati, Assam, India

Chapter - 5

A Discussion on Some Extensions of Reversible Rings and Their Connections with Weak-α Symmetric ring"

Manjuri Dutta

Abstract

In this article, we have studied the connections of a weak α-symmetric ring to some other classes of rings with respect to the ring endomorphism α. Moreover, we have attempted to provide some counterexamples to justify these relationships.

Keywords: weak α-symmetric ring, semi commutative ring

Introduction

Throughout, R denotes a ring with unity 1 that satisfies the associative condition. End(R) and Nil(R) stands for the set of ring endomorphisms of R and the set of nilpotent elements of R, respectively. A ring is called reduced if it has no non-zero elements. The set Nil(R) contains no non zero nilpotent elements whenever the ring R is reduced. Again in 1999, P.M.Cohn [3] termed a ring R as reversible ring if $xy = 0 \Longrightarrow yx = 0$ for x, y in R. A ring which is commutative or reduced is always symmetric as well as reversible. But from these two above definitions, it can be said that a symmetric ring is reversible whether the ring is commutative or not. To establish it, D.D. Anderson and V. Camillo provided the examples of a non symmetric reversible ring (Example I.5) and commutative non reduced symmetric ring (Example II.5) in [1]. Again in 2010, L. Ouyang and H. Chen [14] called a ring as weak symmetric if for any x, y, z in R, $xyz \in Nil(R) \Rightarrow xzy \in Nil(R)$. They proved that symmetric rings are clearly weak symmetric ring and a weak symmetric ring was provided as a counter example 2.2 of [14] to validate this generalization but which is not symmetric. Again, R is semicommutative if xy = 0 for x, $y \in R$, implies for any r of R, xry = 0. A reversible ring is also semmicommutative. But the converse of the above does not hold as Example 1.5 and Example 1.10 (3) of [7].

In [8], Krempa defined that a ring endomorphism is rigid if $x\alpha(x) = 0 \Rightarrow x = 0$ for x in R. He also defined that R is known as α- rigid whenever there is

an endomorphism α in R such that it satisfies α- rigid condition. Also, in [6], R is said to be α-compatible ring whenever xy = 0 ⇔xα (y) = 0 for x and y in R. In [13], L.Ouyang defined weak α-compatible ring as xy ∈ Nil(R) ⇔ xα (y) ∈ Nil(R). Again T.K. Kwak [9] called an ring endomorphism α as right (respectively left) symmetric if xyz = 0 ⇒ xzα(y) = 0 (respectively α(y)xz = 0) where x, y, z in R. If there is a right (respectively left) α-symmetric endomorphism, then the ring R will be a right (respectively left) α-symmetric. R is known as α-symmetric, if α shows the right and left α- symmetric conditions at the same time. Example 2.2 of [9] is provided to show that the right and left α- symmetric rings are different from each other. Thus, the term α-symmetric ring generalized the concept of α- rigid ring. On the other hand, a new term α-reversibility of ring is introduced in [15]. They defined that a ring R is right (respectively left) α-reversible if it satisfies yα (x) = 0 (respectively α (y)x = 0) whenever it is given that xy = 0 for x and y in R. R is named as α-reversible if R follows left and right α-reversible condition together. They also furnished the Example 2 in [15] to show the difference between right and left α-reversibility. They proved that each α-symmetric ring is α-reversible. L. Ouyang introduced a new concept called weak α-rigid endomorphism, on the basis of the set Nil(R) and generalized α-rigid ring as weak α-rigid [13]. Similarly, the term weak α-reversiblility of a ring endomorphism is introduced in [2]. An endomorphism α is weak reversible if xy ∈ Nil(R)⇒yα (x) ∈ Nil(R) for x and y in R. If there is a weak α- reversible endomorphism, then R is termed as weak α-reversible.

1. Weak *α*-symmetric ring:

A ring R is termed as a weak α-symmetric whenever xyzϵNil(R) for any x, y, z in R implies xzα(y)ϵNil(R) [14]. If we consider this given definition as right weak α-symmetric ring, then as usual whenever xyzϵNil(R) for any x, y, z in R implies α(y)xzϵNil(R) will be considered as left weak α-symmetric ring. Remark 2.1 shows that there is no difference between left or right symmetricity of α in the study of weak α-symmetric ring. For any αϵ End(R), domains are weak α-symmetric. Moreover weak α-symmetric ring is an extension of symmetric ring as well as α-compatible ring.

In the next section we will explore various results of weak α-symmetric ring on the basis of its definition related to some classes and extension of reversible ring.

2. Results

Remark 2.1: R is right weak α- symmetric ⇒ R is left weak α-symmetric ring and vice versa.

Proof: By the definition of right weak α- symmetric ring, xyz ∈ Nil(R) implies xzα(y) ∈ Nil(R). There is some n∈ ℕ such that $(xz\alpha(y))^n = 0$. Thus $\alpha(y)\{xz\alpha(y)\ldots xz\alpha(y)\}xz = 0$ implies $(\alpha(y)xz)^{n+1} = 0 \Rightarrow \alpha(y)xz \in Nil(R)$.

Proposition 2.2: A symmetric and α-compatible ring is weak α-symmetric.

Proof: Let us consider x,y and z in R so that xyz ∈ Nil(R). Then $(xyz)^m = 0$ for some m ∈ ℕ. It implies xyzxyz…xyzxyz=0⇒ xyzxyz…xyzxzy=0 as R is symmetric. Now xyzxyz…xyzxzα(y) = 0 given that R is α-compatible. Again, by using symmetric condition of R, xzα(y)xyz…xyz = 0. Now continuing the same process, we get $(xz\alpha(y))^n = 0$. Thus xzα(y) ∈ Nil(R).

The following example is provided to justify that we cannot omit the α-compatibility in a symmetric ring R to get it as a weak α-symmetric ring.

Example 2.3: Let us consider that R = $\mathbb{Z} \oplus \mathbb{Z}$ and which is ring under component wise addition and multiplication. Here, R is symmetric as the fact that R is reduced. We define α from R to R such that α ((x, y)) = (y, x) where (x, y) ∈ R. It can be simply verified that R is not α-compatible ring. Here (1,0)(1, 0) α ((0,1)) = (1, 0) is non nilpotent element in spite of (1,0)(0, 1)(1, 0) ∈ Nil(R). Consequently, R = $\mathbb{Z} \oplus \mathbb{Z}$ is not weak α-symmetric.

Proposition 2.4: A α-symmetric and semicommutative ring is weak α -symmetric.

Proof: Let us assume x, y and z ∈ R so that xyz ∈ Nil(R). So, there is some n ∈ ℕ for which $(xyz)^n = 0$. It implies (xyz)(xyz)…(xyz)(xzα(y)) =0 as R is α-symmetric. It implies (xyzxyzxyzx)(zxzα(y))α(y) = 0 using the same. Again, by semicommutative condition of R, (xyzxyz…xyzxz)α(y)(xzα(y))α(y) = 0. Continuing the same process, finally we obtain xzα(y) ∈ Nil(R).

It is very easy to prove the next Lemma.

Lemma 2.5: If x ∈ Nil(R) ⇒ α(x) ∈ Nil(R) where α∈ End(R). Converse is also true whenever α is monomorphism.

Lemma 2.6: R is semicommutative ⇒ R is weak symmetric ring.

Proof: Let x, y, z ∈ R so that xyz ∈ Nil(R). It implies ⇒ $(xyz)^k = 0$ for some k ∈ ℕ. So x(yz…xyz) = 0 ⇒ xz(yzxyz…xyz = 0 because, R is semicommutative. Again, repeating this process and using semicommutivity of R we will get xzy ∈ Nil(R).

Lemma 2.7: If R is weak symmetric, then xyz ∈ Nil(R) ⇒ any arrangement of product of x; y and z is also in Nil(R).

Proof: Here xyz ∈ Nil(R) implies xzy ∈ Nil(R) by definition of weak symmetric ring. Again xzy ∈ Nil(R) implies 1(xz)y ∈ Nil(R) ⇒ yxz ∈ Nil(R) ⇒ 1(yx)z ∈Nil(R) ⇒ 1.z.(yx) = zyx ∈ Nil(R) as R is weak symmetric. Continuing the process, we can find that any arrangement of x, y, z in Nil(R).

Proposition 2.8: Weak α-symmetric ring ⇒ weak α-reversible ring.

Proof: We can easily prove this proposition by the definitions. The next proposition shows the sufficient condition for the converse part of the above.

Proposition 2.9: A weak symmetric and weak α- reversible ring is always weak α-symmetric.

Proof: Let x, y, z ∈ R so that xyz ∈ Nil(R). Then xzy ∈ Nil(R) as the ring is weak symmetric. Now α(y)xz ∈ Nil(R) as R is weak α- reversible. By using Lemma 2.7, xzα(y) ∈ Nil(R).

Proposition 2.10: A weak symmetric and weak α-reversible ring is always weak α-symmetric.

Proof: Let x, y, z ∈ R so that xyz∈ Nil(R). Then xzy∈ Nil(R) as the ring is weak symmetric. Now α(y)xz ∈ Nil(R) as R is weak α-reversible. By using Lemma 2.7, xzα(y) ∈ Nil(R).

We can directly get the next result as a corollary of above proposition.

Corollary 2.11: A weak symmetric and weak α-compatible ring is always weak α-symmetric.

Proposition 2.12 If R is weak α-symmetric, then R is weak α-rigid where α is any monomorphism.

Proof: Let x ∈ Nil(R). Then $x^2 = 1.x.x \in Nil(R) \Rightarrow 1.x\ \alpha(x) \in Nil(R)$ using weak α-symmetric condition of R. It implies $1\ \alpha(x)\alpha(x) = \alpha\ (x^2) \in Nil(R)$. Therefore, there is some m ∈ N for which $(\alpha\ (x^2))^m = \alpha\ (x^{2m}) = 0$. Since α is one-one, $x^{2m} = 0 \Rightarrow x \in Nil(R)$.

The following example explains that the condition monomorphism of ring endomorphism α cannot be omitted in above proposition.

Example 2.13: Let us consider that F be any field and R = F[x]. Let α: R → R such that α(f(x)) = f(0) for all f(x) ∈ F[x]. Clearly α is not a monomorphism. We know that R is a domain. We can easily show that for any α ∈ End(R), domains are weak α-symmetric. Thus, F[x] is weak α- symmetric. Again, R is domain implies it is reduced ring. For f(x) = x ≠ 0 but f(x)α(f(x)) = 0. So clearly it is not α-rigid. Again Proposition 2.2 of [13] stated that R is α-rigid if and only if R is weak α-rigid and reduced. Thus, R is not weak α -rigid.

Lemma 2.14: R is semicommutative ⇒ Nil(R) forms an ideal.

Proof: Proof is given in [10].

Proposition 2.15: A semicommutative and weak α-rigid ring is weak α-symmetric.

Proof: Let x, y, z ∈ R so that xyz ∈ Nil(R). Then yxz ∈ Nil(R) by Lemma 2.6 and Lemma 2.7 Now by α (yxz) ∈ Nil(R) by using Lemma 2.5**.** So $xz(yxz)(\alpha)^2(y) \in$Nil(R) by using Lemma 2.14 It implies xzα(y)α(xzα(y)) ∈ Nil(R). Now using weakα- rigid condition of R, xzα(y) ∈ Nil(R).

In the following example, we show that weak α-rigid ring may not be weak α-symmetric.

Example 2.16: Let R be any ring and S $=\left\{\begin{pmatrix} X & Y \\ 0 & Z \end{pmatrix} : X, Y, Z \epsilon M_2(R)\right\}$. S forms a ring under usual matrix addition and multiplication. Here α: S→S be defined such that $\alpha\left(\begin{pmatrix} X & Y \\ 0 & Z \end{pmatrix}\right) = \begin{pmatrix} X & -Y \\ 0 & Z \end{pmatrix}$. Let $\begin{pmatrix} X & Y \\ 0 & Z \end{pmatrix} \alpha\left(\begin{pmatrix} X & Y \\ 0 & Z \end{pmatrix}\right) \epsilon$Nil(S). It implies $\left(\begin{pmatrix} X^2 & -XY+YZ \\ 0 & Z^2 \end{pmatrix}\right)^k = 0$ for some k∈ℕ . So $X^{2k} = Y^{2k} = 0$. Now clearly $\left(\begin{pmatrix} X & Y \\ 0 & Z \end{pmatrix}\right)^{2k} = \begin{pmatrix} 0 & * \\ 0 & 0 \end{pmatrix} \epsilon$Nil(S) ⇒ $\begin{pmatrix} X & Y \\ 0 & Z \end{pmatrix} \epsilon$Nil(S).

Again, conversely let $\begin{pmatrix} X & Y \\ 0 & Z \end{pmatrix}$ Nil(S). It is easy to show that $\begin{pmatrix} X & Y \\ 0 & Z \end{pmatrix} \alpha\left(\begin{pmatrix} X & Y \\ 0 & Z \end{pmatrix}\right) \epsilon$ Nil(S). So S is weak α-rigid ring. Here $\begin{pmatrix} E_{12} & 0 \\ 0 & 0 \end{pmatrix}\begin{pmatrix} E_{11} & 0 \\ 0 & 0 \end{pmatrix}\begin{pmatrix} E_{21} & 0 \\ 0 & 0 \end{pmatrix} = 0 \epsilon$Nil(S).

But $\begin{pmatrix} E_{11} & 0 \\ 0 & 0 \end{pmatrix} = \begin{pmatrix} E_{12} & 0 \\ 0 & 0 \end{pmatrix}\begin{pmatrix} E_{21} & 0 \\ 0 & 0 \end{pmatrix} \alpha\left(\begin{pmatrix} E_{11} & 0 \\ 0 & 0 \end{pmatrix}\right) \notin$ Nil(S). Consequently, S is not a weak α-symmetric.

Proposition 2.17: A weak α -symmetric and weak α -compatible ring is weak symmetric ring.

Proof: Let x, y, z ∈ R so that xyz ∈ Nil(R). It implies xz α (y) ∈ Nil(R) by definition of weak α -symmetric ring. Now xzα (y) ∈ Nil(R) ⇒ xzy ∈ Nil(R) as it is weak α -compatible ring.

From Corollary 2.11 and Proposition 2.17, we can conclude the following:

Proposition 2.18: If R is a weak α -compatible ring. Then the following two statements are equivalent:

i) R is a weak symmetric.

ii) R is a weak α -symmetric.

Example 2.3: shows that weak symmetric is not weak α-symmetric. The ring $R = \mathbb{Z} \oplus \mathbb{Z}$ is semmicommutative as well as symmetric. Consequently, it is weak symmetric ring by using the Lemma 2.12. Here $(1,0)(0, 1) \in Nil(\mathbb{Z} \oplus \mathbb{Z})$, but $(0,1)\alpha((1, 0)=(0,1)\epsilon Nil(\mathbb{Z} \oplus \mathbb{Z})$. So, it is not weak α-reversible ring. Therefore, by Proposition 2.8, we can conclude that $\mathbb{Z} \oplus \mathbb{Z}$ is not weak symmetric.

References

1. Anderson, D. D., & Camillo, V. (1998). Armendariz rings and Gaussian r ings. Communications in algebra, 26(7), 2265-2272.
2. Bahlekeh, A. (2014). Nilpotent Elements and Extended Reversible Rings. Southeast Asian Bulletin of Mathematics, 38(2).
3. Cohn, P. M. (1999). Reversible rings. Bulletin of the London Mathematical Society, 31(6), 641-648.
4. Dutta, M., & Singh, K. H. (2021). On some generalizations of reduced and rigid modules. In IOP Conference Series: Materials Science and Engineering (Vol. 1020, No. 1, p. 012024). IOP Publishing.
5. Lunqun, O., & Jingwang, L. (2011). On weak (α, δ)-compatible rings. Int. J. Algebra, 5(26), 1283-1296.
6. Hashemi, E., & Moussavi, A. (2005). Polynomial extensions of quasi-Baer rings. Acta Mathematica Hungarica, 107(3), 207-224.
7. Kose, H., Ungor, B., & Halicioglu, S. (2012). A generalization of reduced rings. Hacettepe Journal of Mathematics and Statistics, 41(5), 689-696.
8. Krempa, J. (1996). Some examples of reduced rings. In Algebra colloq (Vol. 3, No. 4, pp. 289-300).
9. Kwak, T. K. (2007). Extensions of extended symmetric rings. Bulletin of The Korean Mathematical Society, 44(4), 777-788.
10. Kim, N. K., & Lee, Y. (2003). Extensions of reversible rings. Journal of Pure and Applied Algebra, 185(1-3), 207-223.
11. Lambek, J. (1971). On the representation of modules by sheaves of factor modules. Canadian Mathematical Bulletin, 14(3), 359-368
12. Liu, Z., & Zhao, R. (2006). On weak Armendariz rings. Communications in Algebra®, 34(7), 2607-2616.

13. Ouyang, L. (2008). Extensions of generalized α-rigid rings. International Electronic Journal of Algebra, 3(3), 103-116

14. Ouyang, L., & Chen, H. (2010). On weak symmetric rings. Communications in Algebra, 38(2), 697-713.

15. Pourtaherian, H., & Rakhimov, I. S. (2011). On skew version of reversible rings. International Journal of Pure and Applied Mathematics, 73(3), 267-280.

Chapter - 6
Continuous Wavelet Transforms Associated With Hermite Transform

Author

Pranami Phukan
Department of Mathematics, Biswanath College,
Biswanath Chariali, Assam, India

Chapter - 6

Continuous Wavelet Transforms Associated With Hermite Transform

Pranami Phukan

Abstract

A review on the continuous Hermite wavelet transform and some basic properties of Hermite transform. We also discussed boundedness properties of Hermite wavelet transform.

1. Introduction

Many authors have defined wavelet transforms associated with different integral transforms. In ([6], [5]) Pathak and Dixit, Pathak and Pandey defined the wavelet transform which are associated with the Hankel and Laguree transform respectively. In [7] Upadhyay and Tripathi defined continuous wavelet transform corresponding to Watson transform. In 2017 Prasad and Mandal [4] studied the Kontorovich-Lebedev wavelet transform and derived many important properties related to the KL-wavelet transform. In [1] Pathak and Abhishek studied the continuous and discrete wavelet transform associated with index Whittaker transform. Hans-Jurgen Glaeske [3] defined the translation and convolution operator associated with Hermite transform and proved so many important results related to these operators. Now, however to best our knowledge wavelet associated with the Hermite transform is not defined. So, we are interested to define the wavelet associated to Hermite transform and study the continuous as well as discrete wavelet transforms associated with this.

The wavelet transform [8] of the function $f \in L_{2,\mu}(\boldsymbol{R})$ with respect to the wavelet $\phi \in L_{2,\mu}(R)$ is defined by 14

$$(W_\phi f)(\rho,\sigma) = \int_{-\infty}^{\infty} f\,(t)\overline{\phi_{\rho,\sigma}(t)}dt, \rho \in \boldsymbol{R}, \sigma > 0, \tag{1.1}$$

where, $\phi_{\rho,\sigma}(t) = \sigma^{-\frac{1}{2}}\phi(\frac{t-\rho}{\sigma})$. (1.2)

In terms of translation τ_p defined by

$\tau_\rho \phi(t) = \phi(t-\rho), \rho \in \boldsymbol{R}$,

and dilation D_σ is defined by

$D_\sigma \phi(t) = \sigma^{-\frac{1}{2}} \phi(\frac{t}{\sigma}), \sigma > 0$,

we can write, $\phi_{\rho,\sigma}(t) = \tau_\rho D_\sigma \phi(t)$. (1.3)

From equation 1.1 and 1.3 it is clear that wavelet transform of the function f on R is an integral transform for which the kernel is the dilated translate of ϕ.

We can also express equation 1.1 as the convolution

$$\big(W_\phi f\big)(\rho,\sigma) = \big(f * g_{0,\sigma}\big)(\rho) \tag{1.4}$$

where, $g(t) = \overline{\phi(-t)}$.

Since associated with each integral transform there exists a special kind of convolution, one can construct wavelet transform corresponding to an integral transform using the associated convolution.

We construct wavelet and wavelet transform on the interval $(-\infty, \infty)$ by using the theory of Hermite transforms [2] and associated convolution involving the function

$H_n^{(\mu)}(x) = exp(\frac{-x^2}{2}) \tilde{H}_n^{(\mu)}(x), x \in \boldsymbol{R}$,

where $\tilde{H}_n^{(\mu)}(x)$ is the normalized Hermite polynomial, where $\alpha > -1$, is given by

$$\tilde{H}_n^{(\mu)}(x) = \begin{cases} \frac{H_{2\mu}^{(\mu)}(x)}{H_{2\mu}^{(\mu)}(0)} = \tilde{R}_k^{(\mu-\frac{1}{2})}(x^2), & n = 2k \\ \frac{H_{2\mu+1}^{(\mu)}(x)}{(H_{2k+1}^{(\mu)}(x))_{(0)}} = xR_k^{(\mu+\frac{1}{2})}(x^2), & n = 2k+1 \end{cases}$$

and

$$H_n^{(\mu)}(x) = \begin{cases} (-1)^k 2^{2k} k!\, L_k^{(\mu-\frac{1}{2})}(x^2), & n = 2k \\ (-1)^k 2^{2k+1} k!\, x L_k^{(\mu+\frac{1}{2})}(x^2), & n = 2k+1 \end{cases}$$

Set

$d\mu(x) = e^{-x^2} |x|^{2\mu} dx$. (1.5)

Let us consider the measurable function $f(x)$ on the interval $(-\infty, \infty)$.

Then the Hermite transform is defined by

$$H[f](n) = \hat{f}(n) = \int_{-\infty}^{\infty} f(x)\tilde{H}_n(x)d\mu(x), n \in \boldsymbol{N}. \quad (1.6)$$

The inverse Hermite transforms defined by

$$f(x) = \sum_{n=0}^{\infty} \hat{f}(n)\tilde{H}_n^{(\mu)}(x)[\tilde{h}_n^{(\mu)}]^{-1}. \quad (1.7)$$

Where, $h_n^{(\mu)} = 2^{2n}\Gamma([\frac{n}{2}] + 1)\Gamma([\frac{(n+1)}{2}] + \mu + \frac{1}{2})$.

Let the space of those real measurable functions f on $(-\infty, \infty)$ be $L_{p,\mu}(-\infty, \infty)$, $1 \leq p < \infty$ for which

$$||f||_{p,\mu} = \{\int_{-\infty}^{\infty} |f(x)|^p d\mu(x)\}^{\frac{1}{p}}, p < \infty. \quad (1.8)$$

$$||f||_{p,\mu} = esssup_{x\in R}|f(x)|, p = \infty. \quad (1.9)$$

An inner product on $L_{2,\mu}$, is defined by 38

$$\langle f, g\rangle = \int_{-\infty}^{\infty} f(x)\overline{g(x)}d\mu(x). \quad (1.10)$$

2. Hermite Translation And Convolution

In this section, Hermite translation and associated convolution will be discussed. To define the Hermite convolution we have to introduce Hermite translation. For this purpose we need the basic function.

$$K_H^{(\mu)}(x, y, z) \sim \sum_{n=0}^{\infty}[\tilde{h}_n^{(\mu)}]^{-1}\tilde{H}_n^{(\mu)}(x)\tilde{H}_n^{(\mu)}(y)\tilde{H}_n^{(\mu)}(z). \quad (2.1)$$

Hence by equation 1.6 and 1.7, we have

$$\int_{-\infty}^{\infty} K_H^{(\mu)}(x, y, z)\tilde{H}_n^{(\mu)}(z)d\mu(z) = \tilde{\tilde{H}}_n^{(\mu)}(x)\tilde{H}_n^{(\mu)}(y). \quad (2.2)$$

Clearly $K_H^{(\mu)}(x, y, z)$ is symmetric in x, y and z.

Setting $n = 0$ in equation 2.2, we have

$$\int_{-\infty}^{\infty} K_H^{(\mu)}(x, y, z)d\mu(z) = 1. \quad (2.3)$$

The Hermite translation τ_y of $f \in L_{p,\mu}(-\infty, \infty)$, $1 \leq p < \infty$ is defined

$$\tau_y f(x) = f(x, y) = \int_{-\infty}^{\infty} f(z)K_H^{(\mu)}(x, y, z)d\mu(z), 1 \leq p < \infty. \quad (2.4)$$

Lemma 2.1: For $f \in L_{p,\mu}$ and $1 \leq p < \infty$,

$$||\tau_y^{(\mu)} f||_{p,\mu} \leq ||f||_{p,\mu}. \quad (2.5)$$

and the map: $f \to \tau_y f$ is continuous and linear in $L_{p,\mu}$.

Proof: Proof is referred from [3].

Let $p, q, r \in (-\infty, \infty)$ and $\frac{1}{r} = \frac{1}{p} + \frac{1}{q} - 1$. Then the Hermite convolution [3] of $f \in L_{p,\mu}(-\infty, \infty)$ and $g \in L_{g,\mu}(-\infty, \infty)$ is defined by following equation

$$(f * g)(y) = \int_{-\infty}^{\infty} \tau_y^{(\mu)}(f; x) g(x) d\mu(x). \tag{2.6}$$

By using the relation defined in equation 2.4, convolution $(f * g)$ can be defined as

$$(f * g)(x) = \int_{-\infty}^{\infty} \int_{-\infty}^{\infty} f(z) g(x) dm_{x,y}^{(\mu)}(z)$$

$$= \int_{-\infty}^{\infty} \int_{-\infty}^{\infty} f(z) g(x) K_H^{(\mu)}(x, y, z) d\mu(x) d\mu(z). \tag{2.7}$$

Also recall the following Lemma from [3].

Lemma 2.2: Let $p, q, r \in (-\infty, \infty)$ and $\frac{1}{r} = \frac{1}{p} + \frac{1}{q} - 1$, $f \in L_{p,\mu}(-\infty, \infty)$ and $g \in L_{q,\mu}(-\infty, \infty)$. 60Then the convolution $(f * g)$ defined by equation 2.7 satisfies the following norm inequality:

$$(i) \quad ||f * g||_{r,\mu} \leq ||f||_{p,\mu} ||g||_{q,\mu}. \tag{2.8}$$

Moreover $f, g \in L_{2,\mu}$, we get

$$(ii) \quad (f * g)^{\wedge}(n) = \hat{f}(n) \hat{g}(n). \tag{2.9}$$

Lemma 2.3: For any $f \in L_{2,\mu}$ the following Parseval Identity holds for Hermite transform:

$$\sum_n [\tilde{h}_n^{(\mu)}]^{-1} |\hat{f}(n)|^2 = ||f||_{2,\mu}^2 \tag{2.10}$$

Proof: Proof is referred from theorem 1 in ref. [2].

For any $f_1, f_2 \in L_{2,\mu}(-\infty, \infty)$ the below Parseval Identity holds for Hermite transform. See ref. [2].

$$\sum_n [\tilde{h}_n^{(\mu)}]^{-1} f_1(n) f_2(n) = \int_{-\infty}^{\infty} f_1(x) f_2(x) d\mu(x)$$

and

$$\sum_n [\tilde{h}_n^{(\mu)}]^{-1} f_1(n) f_2(n) = \int_{-\infty}^{\infty} H^{-1}[f_1(n)][f_2(n)] d\mu(x).$$

3. Continuous Hermite Wavelet Transform

For a function $\phi \in L_{p,\mu}(-\infty, \infty)$, defined the dilation D_σ by

$$D_\sigma \phi(t) = \phi(\sigma t), \sigma > 0. [cite_s tart] \tag{3.1}$$

Using the Hermite translation 2.4 and above dilation, the Hermite wavelet

$\phi_{\rho,\sigma}(t)$ is defined as follows:

$$\phi_{\rho,\sigma}(t) = \tau_\rho D_\sigma \phi(t) = \tau_\rho \phi(\sigma t) \tag{3.2}$$

$$= \int_0^\infty \phi(\sigma z) K_H^{(\mu)}(\rho, t, z) d\mu(z) \tag{3.3}$$

where $\rho \geq 0$ and $\sigma > 0$. The integral is convergent by virtue of inequality 2.5.

Definition 3.1: Admissible Hermite wavelet

The function $\phi(\alpha) \in L_{p,\mu}(-\infty, \infty)$ is said to be admissible Hermite wavelet if $\phi(\alpha)$ satisfies the following admissibility condition

$$C_\phi = \sum_{n=0}^\infty \frac{|\hat{\phi}(n)|^2}{|n|} < \infty,$$

where $\hat{\phi}(n)$ is the Hermite transform of ϕ.

Continuous Hermite wavelet transform

Using the wavelet $\phi_{\rho,\sigma}$ we now define the continuous Hermite wavelet transform.

$$(\tilde{H}_\phi^{(\mu)} f)(\rho, \sigma) = \langle f(t), \phi_{\rho,\sigma}(t)$$

$$= \int_{-\infty}^\infty f(t) \overline{\phi_{\rho,\sigma}(t)} d\mu(t) \tag{3.4}$$

$$= \int_{-\infty}^\infty \int_{-\infty}^\infty f(t) \overline{\phi(\sigma z)} K_H^{(\mu)}(\rho, t, z) d\mu(z) d\mu(t) \tag{3.5}$$

provided the integral is convergent. Since by inequality 2.5 and definition $\phi_{\rho,\sigma} \in L_{p,\mu}$ whenever $\phi \in L_{p,\mu}$. By virtue of Lemma 2.2, the integral 3.5 is convergent for $f \in L_{q,\mu}, \frac{1}{p} + \frac{1}{q} = 1$.

The Hermite wavelet transform can be expressed in the form of Hermite transform as follows. 89

$$H[(\tilde{H}_\phi^{(\mu)} f)(\rho, \sigma)] = \hat{f}(n) \hat{\phi}(\sigma, n)$$

Also, the Hermite wavelet transform can be written as

$$(\tilde{H}_\phi^{(\mu)} f)(\rho, \sigma) = (f * \phi(\sigma, \alpha))(\rho)$$

The continuity and boundedness results follow from the following theorem. 93

Theorem 3.1: Let $f(\alpha) \in L_{p,\mu}$ and $\phi(\alpha) \in L_{q,\mu}, \sigma > 0$ with $1 \leq p, q < \infty$ and $\frac{1}{p} + \frac{1}{q} = 1$ and $(\tilde{H}_\phi^{(\mu)} f)(\rho, \sigma)$ be continuous Hermite wavelet transform

3.5. 94Then 9

i) $||(\widetilde{H}_{\phi}^{(\mu)[cite_start]}f)(\rho,\sigma)||_{r,\mu} \leq ||f||_{p,\mu}||\phi(\sigma,\alpha)||_{q,\mu}, \frac{1}{r} = \frac{1}{p} + \frac{1}{q} -$ $1,1 \leq p,q,r < \infty.$

ii) $||(\widetilde{H}_{\phi}^{(\mu)[cite_start]}f)(\rho,\sigma)||_{\infty,\mu} \leq ||f||_{p,\mu}||\phi(\sigma,\alpha)||_{q,\mu}, \frac{1}{p} + \frac{1}{q} = 1$

Proof: (ii) Using representation 3.5, we have

$(\widetilde{H}_{\phi}^{(\mu)}f)(\rho,\sigma) = \int_{-\infty}^{\infty}\int_{-\infty}^{\infty} f(t)\overline{\phi(\sigma z)}K_H^{(\mu)}(\rho,t,z)d\mu(z)d\mu(t)$

$= \int_{-\infty}^{\infty}\int_{-\infty}^{\infty} f(t)\overline{\phi(\sigma z)}K_H^{(\mu)^{\frac{1}{p}}}(\rho,t,z)K_H^{(\mu)^{\frac{1}{q}}}(\rho,t,z)d\mu(z)d\mu(t)$

using Holder's inequality, we get

$|(\widetilde{H}_{\phi}^{(\mu)}f)(\rho,\sigma)| \leq (\int_{-\infty}^{\infty}\int_{-\infty}^{\infty}|f(t)|^p K_H^{(\mu)}(\rho,t,z)d\mu(z)d\mu(t))^{\frac{1}{p}} \times$

$(\int_{-\infty}^{\infty}\int_{-\infty}^{\infty}|\phi(\sigma z)|^q K_H^{(\mu)}(\rho,t,z)d\mu(z)d\mu(t))^{\frac{1}{q}}$

$= (\int_{-\infty}^{\infty}|f(t)|^p d\mu(t)\int_{-\infty}^{\infty}K_H^{(\mu)}(\rho,t,z)d\mu(z))^{\frac{1}{p}} \times$

$(\int_{-\infty}^{\infty}|\phi(\sigma z)|^q d\mu(z)\int_{-\infty}^{\infty}K_H^{(\mu)}(\rho,t,z)d\mu(t))^{\frac{1}{q}}$

by using equation 2.3, it follows that

$|(\widetilde{H}_{\phi}^{(\mu)}f)(\rho,\sigma)| \leq ||f||_{p,\mu}||\phi(\sigma,\alpha)||_{q,\mu};$

so that

$||(\widetilde{H}_{\phi}^{(\mu)[cite_start]}f)(\rho,\sigma)||_{\infty,\mu} \leq ||f||_{p,\mu}||\phi(\sigma,\alpha)||_{q,\mu}.$

the inequality 1.1 follows from inequality 2.8.

Theorem 3.2: If ϕ is a basic Hermite wavelet and Ψ is any bounded function, then $(\phi * \Psi)$ is also a hermite wavelet.

Proof.

$C_{(\phi*\Psi)} = \sum_{n=0}^{\infty}\frac{|(\phi*\Psi)^\wedge(n)|^2}{n}$

$= \sum_{n=0}^{\infty}\frac{|(\phi)^\wedge(n)(\Psi)^\wedge(n)|^2}{n}$

$\leq |(\Psi)^\wedge(n)|\sum_{n=0}^{\infty}\frac{|(\phi)^\wedge(n)|^2}{n} < \infty$

Hence $(\phi * \Psi)$ is a Hermite wavelet.

References

1. Pathak, Ashish and Abhishek, Continuous and discrete wavelet transform associated with Index Whittaker transform (Preprint).
2. Markett, Clemens, The product formula and convolution structure associated with the generalized Hermite polynomials, Journal of Approximation Theory, 73, 199-217 (1993).
3. Glaeske, Hans-Jurgen, Convoution structure of Hermite transforms, Algebra Analysis and related topics, Banach Center Publications, Vol 53 (1), 113-120 (2000).
4. Prasad, Akhilesh, Mandal, U. k. wavelet transform associated with Kontorvich-Lebedev transform, Int. J. Wavelets Multiresolut. Inf. Process. 15 (2017), no. 2.
5. R. S. Pathak and C. P. Pandey, Laguerre wavelet transform, Integral Transforms Spec. Funct. 20 (7) (2009) 505-518.
6. R. S. Pathak and M. M. Dixit, Continuous and discrete Bessel wavelet transforms, J. Comput. Appl. Math. 160 (12) (2003) 241-250.
7. S. K. Upadhyay and Alok Tripathi, Continuous Watson wavelet transform, Integral Transforms Spec. Funct. 23 (2012), no. 9, 639-647.
8. C. K. Chui, An introduction to wavelets, Academic Press, New York, 1992.
9. E. C. Titchmarch, Introduction to theory of Fourier integrals, 2nd edition, Oxford University Press, Oxford, U.K. (1948).

Chapter - 7
q-Bessel Wavelet Transform on Exponentially Growing Spaces

Author

Pratima Devi

Mathematics Department, North Eastern Regional Institute of Science and Technology, Nirjuli, Arunachal Pradesh, India

Chapter - 7

q-Bessel Wavelet Transform on Exponentially Growing Spaces

Pratima Devi

Abstract

The q-Bessel wavelet Transform on χ_μ and Q_μ type spaces of exponential growth are investigated and their properties discussed by using the theory of q-Bessel Fourier Transform. Using this said theory, the integral equation of Fredholm type is defined and some examples associated with this integral equation are given.

Keywords: q-Bessel Fourier transform, dilation, translation convolution, wavelet transform, q-Bessel wavelet transform, spaces χ_μ and Q_μ, Fredholm integral equation

1. Introduction

The q-Bessel Fourier transform is defined by

$$(h_\mu f)(y) = \int_0^\infty (xy)^{\frac{1}{2}} j_\alpha(xy;q^2) f(x) d_q x \ , \ y \in (0,\infty), \mu \geq \frac{-1}{2}, \qquad (1)$$

Where j_α is the q-bessel function.

If $f \in L^1_{\alpha,q}(\mathbb{R}_{q,+})$ and $h_\mu f \in L^1_{\alpha,q}(\mathbb{R}_{q,+})$, then inverse q-bessel fourier transform is defined by

$$f(x) = \int_0^\infty (xy)^{\frac{1}{2}} j_\alpha(xy,q^2)(h_\mu f)(y) d_q y \qquad (2)$$

Let $\in L^1_{\alpha,q}(\mathbb{R}_{q,+})$, $g \in L^1_{\alpha,q}(\mathbb{R}_{q,+})$ then q-Bessel Fourier convolution of f and g is

$$(f\#g)(x) = \int_0^\infty f(y)(\tau_x g)(y) d_q y \qquad (3)$$

Where,

$$(\tau_x g)(y) = \int_0^\infty g(z) D_{\alpha,q}(x,y,z)\, d_q z \qquad (4)$$

and

$D_{\alpha,q}(x,y,z) =$

$\int_0^\infty t^{-\mu-\frac{1}{2}}(xt)^{\frac{1}{2}}j_\alpha(xt;q^2)(yt)^{\frac{1}{2}}j_\alpha(yt;q^2)(zt)^{\frac{1}{2}}j_\alpha(zt;q^2)d_qt \;\; x,y,z \in (0,\alpha)$, provided that the above integrals exist.

If f and g in $L^1_{\alpha,q}(\mathbb{R}_{q,+})$, then

$$h_\mu(f\#g)(x) = x^{-\mu-\frac{1}{2}}(h_\mu f)(x)\big(h_\mu g\big)(x). \tag{5}$$

Space χ_μ which consists of all smooth complex- valued function $\phi(x)$, $x \in (0,\infty)$ satisfies the following norm

$$\alpha(\phi) = sup_{x\in(0,\infty)}\left|e^{kx}\left(x^{-1}\frac{d}{d_qx}\right)^m\left(x^{-\mu-\frac{1}{2}}\phi(x)\right)\right| < \infty\,, \tag{6}$$

For every $k,m \in \mathbb{N}_0$.

The semi norm for $\phi \in \chi_\mu$ is given by

$$\eta^\mu_{k,m}(\phi) = sup_{x\in(0,\infty)}|e^{kx}x^{-\mu-\frac{1}{2}}S^m_\mu\phi(x)|\,, k,m \in \mathbb{N}_0, \tag{7}$$

where, $S_\mu = x^{-\mu-\frac{1}{2}}\frac{d}{d_qx}x^{2\mu+1}\frac{d}{d_qx}x^{-\mu-\frac{1}{2}}$, induces on χ_μ the same toplology as defined by $\{\gamma^\mu_{k,m}\}_{k,m\in\mathbb{N}_0}$.

From [1], $\mathcal{Q}_\mu$ as the space of all complex-valued functions Φ which is like [4] and satisfy the following two conditions.

1) $z^{-\mu-\frac{1}{2}}\Phi(z)$ is an even entire function.

2) For every $k,m \in \mathbb{N}_0$, the following norm is given by

$$\omega^\mu_{k,m}(\Phi) = sup_{|Imz|\le k}(1+|z|^2)^m|z^{-\mu-\frac{1}{2}}\phi(z)| < \infty. \tag{8}$$

The boundedness properties of Bessel functions are given below:

i) $|z^{-\mu}j_\alpha(z)| \le Ce^{|Imz|}, z \in \mathbb{C}$ (9)

ii) $\left|z^{\frac{1}{2}}H^{(1)}_\mu(z)\right| \le Ce^{-Imz}, z \in \mathbb{C}, |z| \ge 1$ (10)

Where $H^{(1)}_\mu$ denotes the q-bessel fourier transform of first kind of order μ and C is a positive constant depending on μ in (9) and (10).

From [6], the q-Bessel wavelet transform of a function $f \in L^2_{\alpha,q}(\mathbb{R}_{q,+})$ with respect to q-Bessel wavelet $\psi \in L^2_{\alpha,q}(\mathbb{R}_{q,+})$ is

$$\big(B^{\alpha,q}_\psi f\big)(b,a) = \int_0^\infty f(t)\tau_b\psi_a(x) = a^{\mu-\frac{1}{2}}\int_0^\infty f(t)\psi(\tfrac{t}{a},\tfrac{b}{a})d_qt \tag{11}$$

If $\psi \in L^2_{\alpha,q}(\mathbb{R}_{q,+})$ and $\in L^2_{\alpha,q}(\mathbb{R}_{q,+})$, then using the techniques of [5], we have

$$\left(B^{\alpha,q}_{\psi} f\right)(b,a) = \int_0^{\infty} (bx)^{\frac{1}{2}} j_{\alpha}(bx;q^2) x^{-\mu-\frac{1}{2}} \left(h_{\mu} f\right)(x) \left(h_{\mu}\psi\right)(ax) d_q x \quad (12)$$

2. The q-Bessel Wavelet Transform on the spaces χ_{μ} and Q_{μ}

Lemma 2.1: *If* $\psi \in \chi_{\mu}(I)$, $I = (0,\infty)$ then we have the following estimate

$$\left| \left(a^{-1} \frac{d}{d_q a}\right)^p (h_{\mu}\psi)(a(\xi + i(k+1))) \right| \leq \sum_{r=0}^{p} \binom{p}{r} C_{\mu} a^{\mu+\frac{1}{2}-2r} |\xi + i(k+1)|^{\mu-2r+2p+\frac{1}{2}}$$

$$\gamma^{\mu}_{k+1,0}(\psi) \Gamma(2\mu - 2r + 2p + 1), \quad (13)$$

where $a > 0$, $\mu > r - p - \frac{1}{2}$ *and* $C_{\mu} = C \times A_{\mu,r}$ *with arbitrary constant* C *and* $A_{\mu,r} = \left(\mu + \frac{1}{2}\right)\left(\mu + \frac{1}{2} - 2\right) \ldots \left(\mu + \frac{1}{2} - 2(r-1)\right)$.

Proof: We have,

$$\left(v^{-1} \frac{d}{d_q v}\right)^p \left(h_{\mu}\psi\right)(v) = \left(v^{-1} \frac{d}{d_q v}\right)^p \int_0^{\infty} (vy)^{\frac{1}{2}} j_{\alpha}(vy;q^2) \psi(y) d_q y$$

$$= \int_0^{\infty} \left(v^{-1} \frac{d}{d_q v}\right)^p (vy)^{-\mu} j_{\alpha}(vy;q^2) (vy)^{\mu+\frac{1}{2}} \psi(y) d_q y$$

$$= \int_0^{\infty} \sum_{r=0}^{p} \binom{p}{r} \left(v^{-1} \frac{d}{d_q v}\right)^p (v^{-\mu} j_{\alpha}(vy;q^2) v^{\mu+\frac{1}{2}} y^{\frac{1}{2}} \psi(y) d_q y. \quad (14)$$

Therefore, we obtain

$$\left(v^{-1} \frac{d}{d_q v}\right)^p \left(h_{\mu}\psi\right)(v) =$$

$$\sum_{r=0}^{p} \binom{p}{r} (-1)^{p-r} A_{\mu,r} v^{\mu+\frac{1}{2}-2r} \int_0^{\infty} (vy)^{-(\mu+q+r)} j_{\alpha+q-r}(vy;q^2) y^{\mu+2q-2r+\frac{1}{2}} \psi(y) d_q y \quad .$$

The following estimate can be obtained from (9),

$$\left| \left(v^{-1} \frac{d}{d_q v}\right)^p \left(h_{\mu}\psi\right)(v) \right| \leq$$

$$\sum_{r=0}^{p} \binom{p}{r} C_{\mu} |v|^{\mu+\frac{1}{2}-2r} sup_{y\in(0,\infty)} \left| e^{(k+1)y} y^{-\mu-\frac{1}{2}} \psi(y) \right| \int_0^{\infty} e^{-y} y^{2\mu+2q-2r+1} d_q y.$$

If $|Im\ v| \leq k$

$$\leq \sum_{r=0}^{p} \binom{p}{r} C_{\mu} |v|^{\mu+\frac{1}{2}-2r} \gamma^{\mu}_{k+1,0}(\psi) \Gamma(2\mu - 2r + 2q + 1).$$

Putting $v = a(\xi + i(k+1))$, we get

$$\left|\left(a^{-1}\frac{d}{d_q a}\right)^p (h_\mu\psi)\left(a(\xi+i(k+1))\right)\right|$$

$\leq \sum_{r=0}^{p}\binom{p}{r}C_\mu a^{\mu-2r+\frac{1}{2}}|\xi+i(k+1)|^{\mu-2r+2p+\frac{1}{2}}\gamma^{\mu}_{k+1,0}(\psi)\Gamma(2\mu-2r+2p+1)$.

Theorem 2.2: q-Bessel wavelet transform B^{α}_{ψ} is a continuous linear map from $\chi_\mu(I)$ to $\chi_\mu(I\times I)$ for $\mu \geq \frac{-1}{2}$.

Proof: Let $\phi \in \chi_\mu(I)$. Then by using [12] and [1] , we have

$$(-1)^p\left(b^{-1}\frac{d}{d_q b}\right)^p b^{-\mu-\frac{1}{2}}\left(B^{\alpha,q}_{\psi}\phi\right)(b,a)$$

$$=\frac{1}{2}\int_{-\infty}^{\infty} b^{-\mu-p}(\xi+i\eta)^{p+\frac{1}{2}}H^{(1)}_{\mu+p}(b(\xi+i\eta))$$

$$\times((\xi+i\eta)^{-\mu-\frac{1}{2}}(h_\mu\phi)(\xi+i\eta))(h_\mu\phi)(\xi+i\eta)(h_\mu\psi)(a(\xi+i\eta))d_q\xi$$

Therefore,

$$\left|(-1)^p\left(a^{-1}\tfrac{d}{d_q a}\right)^l\left(b^{-1}\tfrac{d}{d_q b}\right)^p b^{-\mu-\frac{1}{2}}\left(B^{\alpha,q}_{\psi},\phi\right)(b,a)\right|$$

$$\leq \int_{-\infty}^{\infty} b^{-\mu-p-\frac{1}{2}}\left|\left(b(\xi+i\eta)\right)^{\frac{1}{2}}H^{(1)}_{\mu+p}\left(b(\xi+i\eta)\right)\right|\left|(\xi+i\eta)^p\left((\xi+i\eta)^{-\mu-\frac{1}{2}}\left(h_\mu\phi\right)(\xi+i\eta)\right)\right|$$

$$\left|\left(a^{-1}\tfrac{d}{d_q a}\right)^1\left(h_\mu\psi\right)\left(a(\xi+i\eta)\right)\right|d_q\xi$$

$$\leq b^{-\mu-q-\frac{1}{2}}Ce^{-b\eta}\int_{=\infty}^{\infty}\left|(\xi+i\eta)^p\left((\xi+i\eta)^{-\mu-\frac{1}{2}}\left(h_\mu\phi\right)(\xi+i\eta)\right)\right|\left|\left(a^{-1}\frac{d}{d_q a}\right)^1\left(h_\mu\psi\right)\left(a(\xi+i\eta)\right)\right|d_q\xi$$

Using Lemms 2.1 and putting$\eta = k+1$

We have

$$\left|e^{kb}\left(a^{-1}\tfrac{d}{d_q a}\right)^{-1}\left(b^{-1}\tfrac{d}{d_q b}\right)^p b^{-\mu-\frac{1}{2}}\left(B^{\alpha,q}_{\psi},\phi\right)(b,a)\right|$$

$$\leq C.C_{\mu}b^{-\mu-p-\frac{1}{2}}a^{\mu-2r+\frac{1}{2}}e^{-b}\sum_{r=0}^{l}\binom{l}{r}\gamma_{k+1}^{\mu}(\psi)\Gamma(2\mu-2r+2l+1)$$
$$\times\int_{-\infty}^{\infty}|\xi+i(k+1)|^{\mu-2r+2l+p+\frac{1}{2}}|(\xi$$
$$+i(k+1))^{-\mu-\frac{1}{2}}(h_{\mu}\phi)(\xi+i(k+1))|\,d_q\xi$$

Now, let

$$z=\xi+i(k+1)\left|e^{kb}\left(a^{-1}\frac{d}{d_qa}\right)^{-1}\left(b^{-1}\frac{d}{d_qb}\right)^{p}b^{-\mu-\frac{1}{2}}\left(B_{\psi}^{\alpha,q},\phi\right)(b,a)\right|$$
$$\leq C'_{\mu}b^{-\mu-p-\frac{1}{2}}a^{\mu-2r+\frac{1}{2}}e^{-b}\sum_{r=0}^{l}\binom{l}{r}\gamma_{k+1}^{\mu}(\psi)\Gamma(2\mu-2r+2l$$
$$+1)$$
$$\times sup_{|Imz|\leq k+1}(1+|z|^2)^m\left|z^{-\mu-\frac{1}{2}}\left(h_{\mu}\phi\right)(z)\right|\int_{-\infty}^{\infty}(1$$
$$+|z|^2)^{-m}|z|^{\mu-2r+2l+p+\frac{1}{2}}d_qz$$

Is convergent for large value of m. [1, Theorem2.1], we get

$$\left|e^{kb}\left(a^{-1}\frac{d}{d_qa}\right)^{-1}\left(b^{-1}\frac{d}{d_qb}\right)^{p}b^{-\mu-\frac{1}{2}}\left(B_{\psi}^{\alpha,q},\phi\right)(b,a)\right|\leq$$
$C'_{\mu}b^{-\mu-P-\frac{1}{2}}a^{\mu-2r+\frac{1}{2}}e^{-b}\sum_{r=0}^{l}\binom{l}{r}\gamma_{k+1}^{\mu}(\psi)\Gamma(2\mu-2r+2l+1)\{\eta_{k+2,0}^{\mu}(\phi)+\eta_{k+2,m}^{\mu}(\phi)\}$.

Theorem 2.3: The q-Bessel wavelet transform $B_{\psi}^{\alpha,q}$ is a continuous linear mapping from $\mathcal{Q}_{\mu}(I)$ to $\mathcal{Q}_{\mu}(I\times I)$.

Proof: Let $\phi\in\mathcal{Q}_{\mu}$. Suppose $\left(B_{\psi}^{\alpha,q}\phi\right)(z,a)=\Phi(z,a)$ where $z=b+ib',b,b'\in I$ and $a\in I$.

$a^{-\mu-\frac{1}{2}}z^{-\mu-\frac{1}{2}}\Phi(z,a)=$
$\int_0^{\infty}(zx)^{-\mu}j_{\alpha}(zx;q^2)x^{\mu+\frac{1}{2}}(h_{\mu}\phi)(x)(ax)^{-\mu-\frac{1}{2}}(h_{\mu}\psi)(ax)d_qx.$

Taking the absolute value of the above equation, we get

$$|a^{-\mu-\frac{1}{2}}z^{-\mu-\frac{1}{2}}\Phi(z,a)|$$
$$\leq\int_0^{\infty}|(zx)^{-\mu}j_{\alpha}(zx)|\left|x^{\mu+\frac{1}{2}}\left(h_{\psi}\phi\right)(x)\right|\left|(ax)^{-\mu-\frac{1}{2}}\left(h_{\mu}\psi\right)(ax)\right|d_qx$$

$$\leq C \int_0^{\infty} e^{x|Imz|} \left| x^{\mu+\frac{1}{2}} \left(h_\mu \phi\right)(x) \right| \left| (ax)^{-\mu+\frac{1}{2}} \left(h_\mu \psi\right)(ax) \right| d_q x$$

$$\leq C \, sup_{x\in l} \left| e^{xk} x^{-\mu-\frac{1}{2}} \left(h_\mu \phi\right)(x) \right| sup_{x\in l} \left| e^{akx} (ax)^{-\mu-\frac{1}{2}} \left(h_\mu \psi\right)(ax) \right|$$

$$\int_0^{\infty} e^{-axk} x^{2\mu+1} \, d_q x.$$

For $x > 1, l > \mu + \frac{3}{2}$ and in this view of [Theorem 2.1], we have

$$|a^{-\mu-\frac{1}{2}} z^{-\mu-\frac{1}{2}} \Phi(z,a)| \leq C w_{k+1}^{\mu}(\phi) w_{k+1}^{\mu}(\psi) \frac{\Gamma(2\mu+1)}{(ak)^{2\mu+1}}. \tag{15}$$

For $x \in (0,1)$, using the argument of [1, Theorem 2.1], we have

$$|a^{-\mu-\frac{1}{2}} z^{-\mu-\frac{1}{2}} \Phi(z,a)| \leq C w_{1,n}^{\mu}(\phi) w_{1,n}^{\mu}(\psi) \frac{\Gamma(2\mu+1)}{(ak)^{2\mu+1}}. \tag{16}$$

Where $n \in \mathbb{N}$ and $n > \mu + 1$. Taking (15) and (16), $B_\psi^{\alpha,q}$ is continuous from $\mathcal{Q}_\mu(I)$ to $\mathcal{Q}_\mu(I \times I)$.

Lemma 2.4: Let ψ be a q-bessel wavelet, then it can be written in the terms of q-bessel fourier transform as

$$\tau_b \psi_a(x) = b^{\mu+\frac{1}{2}} h_\mu [(bu)^{-\mu} j_\alpha(bu; q^2) \left(h_\mu \psi\right)(au)](x),$$

where, a, b are dilation and translation parameters respectively.

Proof: Using (11) and putting $\frac{t}{a} = u$, we get

$$\tau_b \psi_a(x) = a^{\mu-\frac{1}{2}} \int_0^{\infty} \psi(z)$$

$$\left(\int_0^{\infty} (au)^{-\mu-\frac{1}{2}} (xu)^{\frac{1}{2}} j_\alpha(x\mu; q^2)(bu)^{\frac{1}{2}} j_\alpha(bu; q^2)(zau)^{\frac{1}{2}} j_\alpha(azu) a d_q u \right) d_q$$

$$= \int_0^{\infty} \left(\int_0^{\infty} (zau)^{\frac{1}{2}} j_\alpha(azu) \psi(z) d_q z \right) u^{-\mu-\frac{1}{2}} (xu)^{\frac{1}{2}} j_\alpha(xu; q^2)(bu)^{\frac{1}{2}} j_\alpha(bu) d_q u.$$

$$= \int_0^{\infty} u^{-\mu-\frac{1}{2}} (xu)^{\frac{1}{2}} j_\alpha(xu; q^2)(bu)^{\frac{1}{2}} j_\alpha(bu) (h_\mu \psi)(au) d_q u.$$

$$= b^{\mu+\frac{1}{2}} h_\mu [(bu)^{-\mu} j_\alpha(bu; q^2) \left(h_\mu \psi\right)(au)](x).$$

Theorem 2.5: If $f \in \chi'_\mu$ and $\psi \in \chi_\mu$ then $b^{-\mu-\frac{1}{2}} (B_\psi^{\alpha,q} f)(b,a) \in \theta_{\chi\mu'}$, where χ'_μ and $\theta_{\chi\mu}$ denote the dual and multiplier of χ_μ respectively.

Proof: Suppose $f \in \chi'_\mu$ and $\varphi \in \chi_\mu$. Then

$$\left(B_\psi^{\alpha,q} f\right)(a,b) = (f \# \overline{\psi_a})(b)$$

$=< f, \tau_b \psi_a >$

$=< \sum_{k=0}^{r} S_\mu^k \left(e^{rx} x^{-\mu-\frac{1}{2}} f_k \right), \tau_b \psi_a >$

$=< \sum_{k=0}^{r} e^{yx} x^{-\mu-\frac{1}{2}} f_k, \tau_b (S_\mu^k \psi_a) >$

Using Lemma 2.4, we get

$$\left(B_\psi^{\alpha,q} f\right)(b,a)$$

$$= \sum_{k=0}^{r} \int_0^\infty e^{yx} x^{-\mu-\frac{1}{2}} f_k(x) b^{\mu+\frac{1}{2}} h_\mu \left[(bt)^{-\mu} j_\alpha(bt;q^2) h_\mu \left(S_\mu^k \psi\right)(at)\right](x) d_q x$$

$$= \sum_{k=0}^{r} \int_0^\infty e^{rx} x^{-\mu-\frac{1}{2}} f_k(x) b^{\mu+\frac{1}{2}} h_\mu \left[(bt)^{-\mu} j_\alpha(bt;q^2) h_\mu \psi(at)(at)^{2k}\right](x) d_q x$$

$$\left| \left(b^{-1} \frac{d}{d_q b} \right)^n b^{-\mu-\frac{1}{2}} \left(B_\psi^{\alpha,q} f\right)(a,b) \right|$$

$$= \sum_{k=0}^{r} a^{2k} \int_0^\infty \left| e^{rx} x^{-\mu-\frac{1}{2}} f_k(x) h_\mu \left((bt)^{-\mu-n} j_{\alpha+n}(bt;q^2) t^{2(k+n)} \left(h_\mu \psi\right)(at) \right) \right.$$

$$\left.(x)\right| d_q x$$

$\leq$

$$sup_{x\in l} \left| e^{(r+1)x} x^{-\mu-\frac{1}{2}} h_\mu \left((bt)^{-\mu-n} j_{\alpha+n}(bt;q^2) t^{2(k+n)} (h_\mu \psi)(at) \right)(x) \right| \times$$

$$r a^{2r} \int_0^\infty |e^{-x} f_k(x)| d_q x$$

$\leq$

$$C' a^{2r} sup_{x\in l} \left| e^{(r+1)x} x^{-\mu-\frac{1}{2}} h_\mu \left((bt)^{-\mu-n} j_{\alpha+n}(bt;q^2) t^{2(k+n)} h_\mu \psi(at) \right)(x) \right|$$

Since $\psi \in \chi_\mu \Rightarrow (h_\mu \psi)(at) \in \mathcal{Q}_\mu$ and $(bt)^{-\mu-n} j_{\alpha+n}(bt;q^2) \in \theta \mathcal{Q}_\mu$ (Multiplier of $\mathcal{Q}_\mu$).

Therefore $t^{2(n+k)} (bt)^{-\mu-n} j_{\alpha+n}(bt;q^2)(h_\mu \psi)(at) \in \mathcal{Q}_\mu$. We get the following expression

$$\left| \left(b^{-1} \frac{d}{d_q b} \right)^n (1 + a^{2r})^{-1} b^{-\mu-\frac{1}{2}} \left(B_\psi^{\alpha,q} f\right)(a,b) \right| \leq C' e^{lb} .$$

This shows that $(1 + a^{2r})^{-1} b^{-\mu-\frac{1}{2}} (B_\psi^{\alpha,q} f)(b,a) \in \theta_{\chi_\mu}$.

3. Applications

In this section we introduce the Fredholm integral equation associated with q-bessel convolution on χ_μ space.

The Fredholm integral equation is defined by

$$\int_0^\infty f(t)g(x,t)d_qt + \lambda f(x) = u(x) \tag{18}$$

where $g(x)$ and $u(x)$ are given functions and λ is a known Parameter. From (3), we can write (18) as

$$(f\#g)(x) + \lambda f(x) = u(x) \tag{19}$$

Theorem 3.1: Let $f \in L^1_{\alpha,q}(0,\infty)$ and $g \in L^1_{\alpha,q}(0,\infty)$. Then solution of (19) is

$$f(x) = \int_0^\infty (x\xi)^{\frac{1}{2}} j_\alpha(x\xi;q^2) \frac{(h_\mu u)(\xi)}{(\xi^{-\mu-\frac{1}{2}}(h_\mu g)(\xi)+\lambda)} d_q\xi \tag{20}$$

Proof: Taking q-bessel fourier transform of (19) and using (5), we get

$$\xi^{-\mu-\frac{1}{2}}\big(h_\mu f\big)(\xi) + \lambda\big(h_\mu f\big)(\xi) = \big(h_\mu u\big)(\xi)$$

$$\big(h_\mu f\big)(\xi) = \frac{(h_\mu u)(\xi)}{(\xi^{-\mu-\frac{1}{2}}(h_\mu g)(\xi)+\lambda)} \tag{21}$$

From the inversion formula (2), we can find the solution

$$f(x) = \int_0^\infty (x\xi)^{\frac{1}{2}} j_\alpha(x\xi;q^2) \frac{(h_\mu u)(\xi)}{(\xi^{-\mu-\frac{1}{2}}(h_\mu g)(\xi)+\lambda)} d_q\xi.$$

Theorem 3.2: Let $f \in \chi_\mu$, $g \in \chi_\mu$. Then

$$(f\#g)(x) + \lambda f(x) \in \chi_\mu. \tag{22}$$

Proof: The q-bessel fourier convolution is a continuous linear mapping from $\chi_\mu \times \chi_\mu$ into χ_μ. This implies that $(f\#g) \in \chi_\mu$.

Since, $f \in \chi_\mu$, therefore $(f\#g)(x) + \lambda f(x) \in \chi_\mu$.

Example 3.1: We take $u(x) = x^{\mu+\frac{1}{2}}e^{-ax^2}$ with $Re\ a > 0, Re\ \mu > -1$ and $f = g$ in (18). Then from (21), we have $[(h_\mu f)(\xi)]^2 = \xi^{\mu+\frac{1}{2}} h_\mu(x^{\mu+\frac{1}{2}}e^{-ax^2})(\xi)$

$$= \frac{\xi^{2\mu+1}}{(2a)^{\mu+1}} e^{-\xi^2/4a}.$$

From [3], we have $f(x) = 2^{\frac{\mu+1}{2}} x^{\mu+1}e^{-2ax^2}$.

This $x^{\mu+1}e^{-2ax^2} \in \chi_\mu$ and the solution $f(x) = 2^{\frac{\mu+1}{2}} x^{\mu+1}e^{-2ax^2} \in \chi_\mu$.

Theorem 3.4: Let $\psi \in \chi_\mu \subset L^p_{\alpha,q}(0,\infty)$ be a q-bessel wavelet. Then

$$f(b) = \int_0^\infty j_\alpha(b\xi; q^2)(b\xi)^{1/2} \frac{(h_\mu u)(\xi)}{(\xi^{-\mu-\frac{1}{2}}(h_\mu \psi_a)(\xi)+\lambda)} d_q\xi. \quad (23)$$

Proof: Putting $q = \psi_a(b)$ in (19) and from (21), we have

$$\big(h_\mu f\big)(\xi) = \frac{(h_\mu u)(\xi)}{(\xi^{-\mu-\frac{1}{2}}(h_\mu \psi_a)(\xi)+\lambda)} \quad (24)$$

With the help of inversion formula of q-Bessel fourier transform, we get (23).

Example 3.2: Solve the integral equation

$$\int_0^\infty f(t)\psi\left(\frac{t}{a}, \frac{b}{a}\right) d_q t = u(b),$$

Where $\psi(x) = 2^v \Gamma(v+1) x^{-v-\frac{1}{2}} j_{\alpha+v+1}(x)$.

Solution: From (24) , we get

$$\big(h_\mu f\big)(\xi) = (h_\mu u)(\xi) \frac{1}{\xi^{-\mu-\frac{1}{2}} h_\mu (2^v \Gamma(v+1) x^{-v-\frac{1}{2}} j_{\alpha+v+1}(x))(a\xi)}$$

$$= \big(h_\mu u\big)(\xi) \frac{1}{[1-(a\xi)^2]^v}, Re\ v > -1, Re\ \mu > -1.$$

Taking $v = \left(\mu + \frac{1}{2}\right)$, (5), we have

$$\big(h_\mu f\big)(\xi) = h_\mu \left(u \# \pi^{-\frac{1}{2}} 2^{-\mu} \Gamma\left(\frac{1}{2} - \mu\right) \left(\frac{x}{a}\right)^{\mu-\frac{1}{2}} sin\frac{x}{a} \right)(\xi)$$

$$f(x) = u \# \pi^{-\frac{1}{2}} 2^{-\mu} \Gamma\left(\frac{1}{2} - \mu\right) \left(\frac{x}{a}\right)^{\mu-\frac{1}{2}} sin\frac{x}{a}.$$

Reference

1) Betancor J. J. and Mesa L. R, "*Hankel convolution on distribution space with exponential growth*", Studia Mathematica 121(1) (1996) 35-52.

2) Debnath L., "*Wavelet Transforms and their Applications*", Birkh¨auser, Boston, MA, 2002.

3) Erd´elyi A., "*Tables of Integral transforms*", II, McGraw-Hill, New York, 1953.

4) Pavlovi´c Miroslav, "*Characterizations Of The Harmonic Hardy Space h1 On The Real Ball"*, Filomat 25(3) (2011) 137-143.

5) Chui C. K., "*An Introduction to Wavelets"* , Academic Press, 1992.

6) Upadhyay S. K., Yadavand R. N., Debnath L., "*On continuous Bessel wavelet transformation associated with the Hankel-Housdroff operator*",

Integral transforms and Special functions 23(5) (2012) 315-323.

7) Watson G. N., "*A Treatise on the Theory of Bessel Functions*", 2nd ed., Cambridge Univ. Press, London/ New York, 1966.

8) Zemanian A. H., "*Generalized Integral Transformations"*, Inter science Publ., New york, 1968.

9) Upadhyay S. K., and Singh Reshma. "*Bessel wavelet transform on the spaces with exponential growth*." *Filomat* 31.8 (2017): 2459-2466.

Chapter - 8
Shapley Function for Intuitionistic Fuzzy Cooperative Games

Author

Rajib Biswakarma
Department of Mathematics, Silapathar College,
Silapathar, Assam, India

Chapter - 8

Shapley Function for Intuitionistic Fuzzy Cooperative Games

Rajib Biswakarma

Abstract

The concept of intuitionistic fuzzy Shapley functions is introduced for cooperative games characterized by intuitionistic fuzzy coalitions and intuitionistic fuzzy characteristic functions are expressed in Choquet integral form. The framework extends the classical Shapley function on a class of cooperative fuzzy games. We derive the specific expressions for intuitionistic fuzzy Shapley functions across different classes of intuitionistic fuzzy games and discuss their existence and uniqueness. A numerical example is also provided to demonstrate how optimal allocation for the players can be determined.

Keywords: Cooperative game, Intuitionistic fuzzy coalition, Shapley function, Intuitionistic fuzzy Shapley function, Choquet integral

1. Introduction

A cooperative game with transferable utility (TU), or simply a TU-game, is defined as a pair (N, v), where N is a set of n players, called the grand coalition and v: the characteristic function defined on $P(N)$ that assigns every subset (coalition) a real number called its worth giving zero worth to the empty coalition. Let G_0 denote the class of TU-game. A solution for any cooperative game is a function on G_0 which assigns to the TU-game a distribution of payoffs for its players. If there is no ambiguity on the player set N we denote by $G_0(N)$ the class of all TU games with the fixed N. Among the various one-point solutions for TU-games, the Shapley value, the Solidarity value, Banzhaf value and Share functions are perhaps the most popular ones. These methods have been successfully applied in various domains, including enterprise management and economics, to ensure fairness and stability in coalition formations. However, real-world scenarios often involve significant uncertainty and vagueness, as coalitions may form under incomplete or imprecise information. Players may only partially participate in coalitions, with their contribution levels lying somewhere between complete membership

and total non-participation. Fuzzy cooperative games, pioneered by Aubin, address this issue by introducing fuzzy coalitions where players' participation is represented by membership grades in the interval $[0,1]$. Since then, numerous solution concepts have been developed to handle fuzzy characteristic functions and fuzzy coalition values. Despite these advancements, fuzzy set theory is limited in capturing the full spectrum of uncertainty involved in coalition formation. In particular, it cannot adequately describe the nuanced states of "participation," "non-participation," and "hesitation" simultaneously. Intuitionistic fuzzy sets, introduced by Atanassov, address this gap by incorporating three dimensions of information: the degree of membership, the degree of non-membership, and the degree of hesitation. These sets provide a richer framework for modeling situations where players may express uncertainty about their willingness to cooperate or the outcomes of collaboration.

While intuitionistic fuzzy sets have been explored in multi-attribute decision-making and non-cooperative games, their application in cooperative game theory remains relatively underdeveloped. Recent works, such as those by Elena Mielcovave extended the traditional transferable utility game framework to accommodate intuitionistic fuzzy values, offering new perspectives on coalition behavior under uncertainty.

Building on this foundation, this paper introduces intuitionistic fuzzy Shapley functions, a novel approach to payoff distribution in cooperative games with intuitionistic fuzzy coalitions and intuitionistic fuzzy characteristic functions. These Shapley function aim to distribute payoffs in a manner that accounts for players' degrees of participation, non-participation, and hesitation. By integrating the principles of intuitionistic fuzzy sets with the flexibility of Shapley functions, this study addresses critical gaps in the literature and provides a robust framework for decision-making in uncertain environments. The proposed approach not only extends existing theories but also introduces new axioms and properties for intuitionistic fuzzy Shapley function. Illustrative examples are included to demonstrate the practicality and effectiveness of the proposed model.

2. Preliminaries

This section presents the key definitions and results which are relevant to the development of this paper.

2.1 Intuitionistic Fuzzy Sets

The concept of an intuitionistic fuzzy set (IFS), introduced by Atanassov, is a generalization of a fuzzy set that provides a richer framework for handling

uncertainty by incorporating both membership and non-membership degrees along with a hesitation degree

Definition 1: An intuitionistic fuzzy set $\tilde{A}$ in a universe of discourse X is defined as:

$\tilde{A} = \{\langle x, \mu_{\tilde{A}}(x), \nu_{\tilde{A}}(x)\rangle : x \in X\}$,

In this:

- $\mu_{\tilde{A}}(x): X \to [0,1]$ is the membership degree of x in $\tilde{A}$, representing the extent to which x belongs to $\tilde{A}$.
- $\nu_{\tilde{A}}(x): X \to [0,1]$ is the non-membership degree of x in $\tilde{A}$ representing the extent to which x does not belong to $\tilde{A}$.
- For each $x \in X$ the condition $0 \leq \mu_{\tilde{A}}(x) + \nu_{\tilde{A}}(x) \leq 1$ must hold.
- The hesitation degree, $\pi_{\tilde{A}}(x)$ reflects the uncertainty or lack of knowledge about the membership status of x in $\tilde{A}$. It is defined as:

$\pi_{\tilde{A}}(x) = 1 - \mu_{\tilde{A}}(x) - \nu_{\tilde{A}}(x)$,

where $\pi_{\tilde{A}}(x) \geq 0$.

1) Properties: If $\nu_{\tilde{A}}(x) = 1 - \mu_{\tilde{A}}(x)$, the intuitionistic fuzzy set reduces to a classical fuzzy set.

2) $\pi_{\tilde{A}}(x) = 0$ indicates no hesitation, while $\pi_{\tilde{A}}(x) > 0$ indicates uncertainty about x's membership.

Definition 2: The ϵ-cut of an intuitionistic fuzzy set (IFS), is defined as:

$$\tilde{A}_\epsilon = \{x \in X | \mu_{\tilde{A}}(x) \geq \epsilon \text{ and } \nu_{\tilde{A}}(x) \leq 1 - \epsilon\}$$

Definition 3: The strong ϵ-cut of an intuitionistic fuzzy set (IFS), is defined as:

$$\tilde{A}_\epsilon = \{x \in X | \mu_{\tilde{A}}(x) > \epsilon \text{ and } \nu_{\tilde{A}}(x) \leq 1 - \epsilon\}$$

For any intuitionistic fuzzy set, we have:

$$\tilde{A}_0 = \{x \in X | \mu_{\tilde{A}}(x) \geq 0 \text{ and } \nu_{\tilde{A}}(x) \geq 0\} = X$$

Theorem 1: For any two Intuitionistic fuzzy set $\tilde{A}$, $\tilde{B}$

1) $\tilde{A} \subseteq \tilde{B}$ holds if and only if $\tilde{A}_\epsilon \subseteq \tilde{B}_\epsilon$ for all $\epsilon \in (0,1]$.
2) $\tilde{A} = \tilde{B}$ holds if and only if $\tilde{A}_\epsilon = \tilde{B}_\epsilon$ for all $\epsilon \in (0,1]$.

2.2 Triangular Intuitionistic Fuzzy Number (TIFN)

Definition 4: [?] A TIFN on the real number set R is an intuitionistic fuzzy set denoted as:

$$\tilde{a} = \langle a; a_1^-, a_1^+; a_2^-, a_2^+ \rangle$$

The membership function and the non-membership function of $\tilde{a}$ are defined:

$$\mu_{\tilde{a}}(x) = \begin{cases} 0 & \text{for } x < a_1^-, x > a_1^+ \\ \dfrac{x - a_1^-}{a - a_1^-} & \text{for } a_1^- \le x < a \\ 1 & \text{for } x = a \\ \dfrac{a_1^+ - x}{a_1^+ - a} & \text{for } a \le x < a_1^+ \end{cases}$$

$$\nu_{\tilde{a}}(x) = \begin{cases} 1 & \text{for } x < a_2^-, x > a_2^+ \\ \dfrac{a - x}{a - a_2^-} & \text{for } a_2^- \le x < a \\ 0 & \text{for } x = a \\ \dfrac{x - a}{a_2^+ - a} & \text{for } a \le x < a_2^+ \end{cases}$$

$$\pi_{\tilde{a}}(x) = 1 - \mu_{\tilde{a}}(x) - \nu_{\tilde{a}}(x),$$

Definition 5: [?] Let us consider an TIFN $\tilde{a} = \langle a; a_1^-, a_1^+, a_2^-, a_2^+ \rangle$ defined on the real line R as described before. The ϵ-cut of IFN is defined by:

$$\tilde{a}_\epsilon = \{(x, \mu_{\tilde{a}}(x), \nu_{\tilde{a}}(x)) | \mu_{\tilde{a}}(x) \ge \epsilon \text{ and } \nu_{\tilde{a}}(x) \le 1 - \epsilon\} \forall \epsilon \in [0,1].$$

ϵ-cut Representation of TIFN:

The ϵ-cut representation of $\tilde{a}$ generates the following pair of intervals and is denoted

by:

$$\tilde{a}_\epsilon = ([a_{1\epsilon}^-, a_{1\epsilon}^+]; [a_{2\epsilon}^-, a_{2\epsilon}^+]),$$

Where the interval $[a_{1ò}^-, a_{1ò}^+]$ is defined as follows

$$a_{1ò}^- = \begin{cases} \inf\{x | x \in \mu_ò\} & \text{if } ò > 0 \\ \inf\{x | x \in [a - a_1^-, a + a_1^+]\} & \text{if } ò = 0 \end{cases}$$

$$a_{1\grave{o}}^{+}=\begin{cases}\sup\{\lambda \mid x\in\mu_{\grave{o}}\} & \text{if } \grave{o}>0\\ \sup\{\lambda \mid x\in[a-a_1^{-},a+a_1^{+}]\} & \text{if } \grave{o}=0\end{cases}$$

Here $\mu_{\grave{o}}$ is defined by $\mu_{\grave{o}}=\{\lambda \mid \mu_{\tilde{a}}(x)\geq \grave{o}\}$

And in a similar manner the interval [$a_{2\grave{o}}^{-}$, $a_{2\grave{o}}^{+}$] is defined as follows

$$a_{2\grave{o}}^{+}=\begin{cases}\sup\{\lambda \mid x\in\nu^{\grave{o}}\} & \text{if } 1-\grave{o}>0\\ \sup\{\lambda \mid x\in[a-a_2^{-},a+a_2^{+}]\} & \text{if } 1-\grave{o}=0\end{cases}$$

$$a_{2\grave{o}}^{-}=\begin{cases}\inf\{\lambda \mid x\in\nu^{\grave{o}}\} & \text{if } \grave{o}>0\\ \inf\{\lambda \mid x\in[a-a_1^{-},a+a_1^{+}]\} & \text{if } \grave{o}=0\end{cases}$$

Where v_{ϵ} is defined by

$$\nu_{\grave{o}}=\{\lambda \mid \nu_{\tilde{a}}(x)\leq 1-\grave{o}\}=\{\lambda \mid 1-\nu_{\tilde{a}}(x)\geq \grave{o}\}$$

2.3 Operations on TIFNs with Hukuhara Difference

Let three TIFNs be defined as:

$\tilde{a}=\langle a;a_1^{-},a_1^{+};a_2^{-},a_2^{+}\rangle$, $\tilde{b}=\langle b;b_1^{-},b_1^{+};b_2^{-},b_2^{+}\rangle$, $\tilde{c}=\langle c;c_1^{-},c_1^{+};c_2^{-},c_2^{+}\rangle$.

1) Addition

$\tilde{a}+\tilde{b}=\langle a+b;a_1^{-}+b_1^{-},a_1^{+}+b_1^{+};a_2^{-}+b_2^{-},a_2^{+}+b_2^{+}\rangle$,

2) Difference: (Imaginary and extended Hukuhara differences)

$\tilde{c}=\tilde{a}-_H\tilde{b}$. is called Imaginary Hukuhara difference if

$b_i^{+}-a_i^{-}>b_i^{+}-a_i^{+}$ $(i=1,2)$

The extended Hukuhara difference of TIFNs is defined as:

$$\tilde{c}=\tilde{a}-_{eH}\tilde{b}=\langle a-b;a_1^{-}-b_1^{-},a_1^{+}-b_1^{+};a_2^{-}-b_2^{-},a_2^{+}-b_2^{+}\rangle$$

3. Scalar Multiplication: $k\tilde{a}$ $\begin{cases}\langle ka;ka_1^{-},ka_1^{+};ka_2^{-},ka_2^{+}\rangle, & \text{if } k\geq 0\\ \langle ka;ka_1^{+},ka_1^{-};ka_2^{+},ka_2^{-}\rangle, & \text{if } k<0\end{cases}$

Definition 6: Let $\tilde{a}=\langle a;a_1^{-},a_1^{+};a_2^{-},a_2^{+}\rangle$ and $\tilde{b}=\langle b;b_1^{-},b_1^{+};b_2^{-},b_2^{+}\rangle$ be two TIFNs, where

$$S_\lambda(\tilde{a}) = \frac{\lambda(a_1^- + 2a + a_1^+)}{4} + \frac{(1-\lambda)(a_2^- + 2a + a_2^+)}{4}$$

$$S_\lambda(\tilde{b}) = \frac{\lambda(b_1^- + 2b + b_1^+)}{4} + \frac{(1-\lambda)(b_2^- + 2b + b_2^+)}{4}$$

are λ weighted mean area of $\tilde{a}$ and $\tilde{b}$ respectively $\lambda \in [0,1]$ than,

$\tilde{a}$ and $\tilde{b}$ be two TIFNs, where $S_\lambda(\tilde{a})$ and $S_\lambda(\tilde{b})$ are weighted mean area of $\tilde{a}$ and $\tilde{b}$ respectively, $\lambda \in [0,1]$.

- If $S_\lambda(\tilde{a}) > S_\lambda(\tilde{b})$, then $\tilde{a} > \tilde{b}$
- If $S_\lambda(\tilde{a}) < S_\lambda(\tilde{b})$, then $\tilde{a} < \tilde{b}$
- If $S_\lambda(\tilde{a}) = S_\lambda(\tilde{b})$, then $\tilde{a} = \tilde{b}$

2.4 Intuitionistic Fuzzy Cooperative Games

Definition 7: Let $N = \{1,2,\ldots,n\}$ be the set of players. An intuitionistic fuzzy coalition on N, which is identified with a function $f: N \to [0,1] \times [0,1]$. Then for an intuitionistic fuzzy coalition

and

$$S_{T_0} = \{\langle i, \mu_{T_0}(i), \nu_{T_0}(i)\rangle \mid i \in N\}$$

In this

$S_{T_0} = \{(i, \mu_{T_0}(i), \nu_{T_0}(i)) : i \in N\}$

- $\mu_{T_0}(i) \in [0,1]$: Degree of membership.
- $\nu_{T_0}(i) \in [0,1]$: Degree of non-membership.
- $\pi_{T_0}(i) = 1 - \mu_{T_0}(i) - \nu_{T_0}(i)$: Degree of hesitation.
- The support is denoted by $Supp(S_{T_0}) = \{i \in N : \mu_{T_0}(i) > 0, 1 - \nu_{T_0}(i) > 0\}$ cardinality is written as $|Supp(S_{T_0})|$

Definition 8: A function $\tilde{v}: P(N) \to \tilde{\mathcal{R}}$ satisfying $\tilde{v}(\emptyset) = \langle 0; 0,0; 0,0\rangle$ is called intuitionistic fuzzy characteristic function. The s*et all* games with intuitionistic fuzzy characteristic function on $P(N)$ is denoted by $\tilde{G}_0(N)$.

Let $\tilde{v}(S_0)$ indicate the intuitionistic fuzzy characteristic function value for any coalition $S_0 \in P(N)$ where the TIFN

$\tilde{v}(S_0) = \langle v(S_0); v_1^-(S_0), v_1^+(S_0); v_2^-(S_0), v_2^+(S_0)\rangle$ is called the worth of the coalition S_0

Definition 9: Let $(N, \tilde{v})$ be the $n \geq 2$ - persons intuitionistic fuzzy cooperative game with $\tilde{v} : IF(N) \to \mathrm{R}$ characteristic function of TIFNs on *IF(N),* the set of all intuitionistic fuzzy coalitions of *N* such that $\tilde{v}(\varnothing) = \langle 0;0,0;0,0\rangle.$ The set of all n-persons intuitionistic fuzzy cooperative games $(N, \tilde{v})$ is denoted by $\tilde{G}(N)$. For notational simplicity, we denote $(N, \tilde{v})$ by $\tilde{v}$.

Definition 10: Let $\tilde{v} \in \tilde{G}(N)$ and $W_0 \in P(N)$. A coalition $S_0 \subseteq W_0$ is called an intuitionistic fuzzy carrier in W_0 for $\tilde{v}$ if: $\tilde{v}(S_0 \cap T_0) = \tilde{v}(T_0), \quad \forall T_0 \in P(W_0)$

The set of all carriers in W_0 for $\tilde{v},$ denoted by $IC(W_0 |_{\tilde{v}}),$ is given by:

$$IC(W_0 |_{\tilde{v}}) = \{S_0 \subseteq W_0 |\ \tilde{v}(S_0 \cap T_0) = \tilde{v}(T_0), \forall T_0 \subseteq W_0\}$$

Definition 11: Let $\tilde{v} \in \tilde{G}(N)$ and $W_0 \in P(N)$\$.*If* \$$\tilde{v}(S_0 \cup \{i\}) = \tilde{v}(T_0)$ for all $S_0 \subseteq W_0$, $\{i\},$ then $i \in W_0$ is called an intuitionistic fuzzy null player in W_0

Definition 12: Let $S_N \in IF(N)$ and $\tilde{v} \in \tilde{G}(N)$ An intuitionistic fuzzy coalition $S_T \subseteq S_N$ is called an intuitionistic fuzzy carrier in S_N for $\tilde{v}$ if $\tilde{v}(S_{T_0} \cap S_{K_0}) = \tilde{v}(S_{K_0})$ for all $S_{K_0} \subseteq S_N$ The set of all intuitionistic fuzzy carriers in S_N for $\tilde{v}$ is denoted by $IFC(S_N |_{\tilde{v}}).$

Definition 13: Let $S_N \in IF(N)$ and $\tilde{v} \in \tilde{G}(N).$*If*$\tilde{v}(S_{T_0} \cup S_N(i)) = \tilde{v}(S_{T_0})$ for all $S_T \subseteq S_N$ with $i \notin Supp(S_{T_0}),$ then *i* is called an intuitionistic fuzzy null player in S_N.

Definition 14: Let $S_{T_0} \subseteq S_N \in IF(N)$ and $i, j \in N.$ For any S_{T_0} define $S_{T_0}^{ij}(k)$ =

$\{\langle k, \mu_{T_0^{[ij]}}(k), \nu_{T_0^{[ij]}}(k)\rangle, \mu_{T_0^{[ij]}}(k), \nu_{T_0^{[ij]}}(k) \in [0,1], \quad \pi_{T_0^{[ij]}}(k) = 1 - \mu_{T_0^{[ij]}}(k) - \nu_{T_0^{[ij]}}(k)\}(k) = \{\langle k, \mu_{T_0^{[ij]}}(k), \nu_{T_0^{[ij]}}(k)\rangle\}$

Where he membership functions are defined as follows:

$$\mu_{T_0^{[ij]}}(k) = \begin{cases} \min\{\mu_{S_{T_0}}(i), \mu_N(j)\} & \text{if } k = i \\ \min\{\mu_{S_{T_0}}(j), \mu_N(i)\} & \text{if } k = j \\ \mu_{S_{T_0}}(k) & \text{otherwise} \end{cases}$$

$$\nu_{T_0^{[ij]}}(k) = \begin{cases} \max\{\nu_{S_{T_0}}(i), \nu_N(j)\} & \text{if } k = i \\ \max\{\nu_{S_{T_0}}(j), \nu_N(i)\} & \text{if } k = j \\ \nu_{S_{T_0}}(k) & \text{otherwise} \end{cases}$$

Definition 15: Let $S_{T_0} \subseteq S_N \in IF(N)$ and $i, j \in N$. For any S_{T_0} define $\beta_{ij}[S_{T_0}]$ by

$$\beta_{ij}[S_{T_0}](k) = \begin{cases} S_{T_0}(j) & \text{if } k = i \\ S_{T_0}(i) & \text{if } k = j \\ S_{T_0}(k) & \text{otherwise} \end{cases}$$

Definition 16: Given $S_{T_0} \in IF(N)$, let $Q(S_{T_0}) = \{S_{T_0}(i) \mid \mu_{T_0}(i) > 0, 1 - \nu_{T_0}(i) > 0, i \in N\}$ and let $q(s)$ be the cardinality of $Q(S_{T_0})$ Write the elements of $Q(S)$ n increasing order as $\grave{o}_1 < \ldots < \grave{o}_{q(s)}$ Then a game $\tilde{v} \in \tilde{G}(N)$ is said to be an intuitionistic fuzzy cooperative game with Choquet integral form if and only if:

$$\tilde{v}(S_{T_0}) = \sum_{l=1}^{q(s)} \tilde{v}([S_{T_0}]_{\grave{o}_l})(\grave{o}_l - \grave{o}_{l-1}) \text{ for any } S_{T_0} \in IF(N) \text{ where } \grave{o}_0 = 0.$$

The set of all intuitionistic fuzzy games with Choquet integral form is denoted by $\tilde{G}_C(N)$.

Definition 17: Given, a game $\tilde{v} \in \tilde{G}(N)$ said to be with proportional values if and only if $S_{T_0} \in IF(N), let S_{T_0}^p = \{i \in N \mid S_{T_0}^p(i) = \langle \mu_{T_0}(i) = p, \nu_{T_0}(i) = 1 - p\rangle\}$ for any $p, 1 - p \in [0,1]$

$$\tilde{v}(S_{T_0}) = \sum_{p\in[0,1]} \tilde{v}(S_{T_0}^{p}) \cdot \langle p, 1-p\rangle \quad \forall S_{T_0} \subseteq S_N .$$

The set of all fuzzy games with proportional values is denoted by $\tilde{G}_p(N).$

Lemma 1: Let $\tilde{v} \in \tilde{G}C(N), SW_0 \in IF(N), W_0 \in P(N)$ then the following holds:

$$\tilde{v}(S_{T_0}) \le \tilde{v}(S_{W_0}), \quad \forall S_{T_0} \subseteq S_{W_0}.$$

Proof: Recall from Theorem 1 $S_{T_0} \subseteq S_{W_0}$ if and only if $[S_{T_0}]\grave{o} \subseteq [SW_0]_{\grave{o}}$ $for \grave{o} \in (0,1].$

If $\tilde{v} \in \tilde{G}(N) then \tilde{v}(S_0) \le \tilde{v}(W_0), \quad \forall T_0 \subseteq W_0.$

Therefore $\tilde{v} \in \tilde{G}(N) then \tilde{v}(S_{T_0}) \le \tilde{v}(S_{W_0}), \quad \forall S_{T_0} \subseteq S_{W_0}.$

Lemma 2: Let

$$\tilde{v} \in \tilde{G}C(N), SW_0 \in IF(N), W_0 \in P(N) and S_{T_0} \subseteq S_{W_0}. then \tilde{v}(S_{T_0}) = \tilde{v}(S_{W_0}) iff \tilde{v}([S_{T_0}]\grave{o}) = \tilde{v}([SW_0]_{\grave{o}}).$$

Proof. Recall from Theorem 1 one can easily obtain the conclusion.

Theorem 2. Let

$$\tilde{v}C \in \tilde{G}_C(N) and SW_0, S_N \in IF(N), W_0 \in P(N). If S_{W_0} \in IFC(S_N \mid \tilde{v}_C) then [SW_0]\grave{o} \in IC([S_N]\grave{o}|_{\tilde{v}_C}).$$

Proof.

Definition 18. A function $\tilde{v} \in \tilde{G}(N)$ is called a intuitionistic convex fuzzy game on *IF(N)* if $\tilde{v}(S_{T_0} \cup S_{K_0}) + (S_{T_0} \cap S_{K_0}) \ge \tilde{v}(S_{T_0} + \tilde{v}(S_{K_0})\, for all S_{T_0}, S_{K_0} \subseteq S_N.$

Where,

$$(S_{T_0} \cup S_{K_0})(i) = \langle \mu_{T_0}(i), \nu_{T_0}(i)\rangle \cup \langle \mu_{K_0}(i), \nu_{K_0}(i)\rangle = \langle \max\{\mu_{T_0}(i), \mu_{K_0}(i)\}, \min\{\nu_{T_0}(i), \nu_{K_0}(i)\}\rangle$$

and

$$(S_{T_0} \cap S_{K_0})(i) = \langle \mu_{T_0}(i), \nu_{T_0}(i)\rangle \cap \langle \mu_{K_0}(i), \nu_{K_0}(i)\rangle = \langle \min\{\mu_{T_0}(i), \mu_{K_0}(i)\}, \max\{\nu_{T_0}(i), \nu_{K_0}(i)\}\rangle \quad ,$$

respectively.

Definition 19. An intuitionistic Shapley function on $\tilde{G}(N)$ is a function $\Phi^{Sh}:\tilde{G}(N)\to \mathrm{R}^{P(N)}$ that satisfies the following four axioms i.e., Axiom PN1-PN4.

Axiom PN1 (Efficiency): If $\tilde{v}\in\tilde{G}(N)$ and $S_0\subseteq W_0$ then,

$$\sum_{i\in W_0}\Phi_i^{Sh}(W_0,\tilde{v})=\tilde{v}(W_0),$$

$$\Phi_i^{Sh}(W_0,\tilde{v})=\tilde{0}\$\ forall\$i\notin W_0.$$

Axiom PN2 (Carrier): If $\tilde{v}\in\tilde{G}(N)\$,\$W_0\subseteq N$ and $T_0\in IC(W_0\mid_{\tilde{v}})$ then

$$\Phi_i^{Sh}(W_0,\tilde{v})=\Phi_i^{Sh}(T_0,\tilde{v}).$$

Axiom PN3 (Symmetry): If $\tilde{v}\in\tilde{G}(N)\$,\$W_0\subseteq N\$,\$i,j\in W_0$ and $\tilde{v}(S_0\cup\{i\})=\tilde{v}(S_0\cup\{j\})$ for any $S_0\in P(W_0,\ \{i,j\})$ then $\Phi_i^{Sh}(W_0,\tilde{v})=\Phi_j^{Sh}(W_0,\tilde{v}).$

Axiom PN4 (Linearity): For any $\tilde{u},\tilde{v}\in\tilde{G}(N)\$,\$k,t\in$ and $k\tilde{u}+t\tilde{v}\in\tilde{G}(N)$, then

$$\Phi^{Sh}(W_0,k\tilde{u}+t\tilde{v})=k\Phi^{Sh}(W_0,\tilde{u})+t\Phi^{Sh}(W_0,\tilde{v}).$$

Theorem 3. Let $\tilde{v}\in\tilde{G}(N)$ and $S_0\subseteq W_0\in P(N).$ A function $\Phi^{Sh}:\tilde{G}(N)\to \mathrm{R}^{P(N)}$ defined by:

$$\Phi_i^{Sh}(W_0,\tilde{v})=\{\sum_{S_0\subseteq W_0}\frac{(|S_0|-1)!(|W_0|-|S_0|)!}{|W_0|!}\{\tilde{v}(S_0)\,!\ {}_H\ \tilde{v}(S_0,\ \{i\})\}$$

if $i\in S_0\subseteq W_0$ and $\tilde{0}$ elsewhere, is the unique Shapley function in $W_0\ for\tilde{v}\in\tilde{G}(N).$

Proof: From the concept of the extended Hukuhara difference and the Shapley function, the theorem can be easily proven.

Definition 20: An intuitionistic Shapley function on $\tilde{G}(N)$ is a function

$\Phi^{Sh}:\tilde{G}(N)\to \mathrm{R}^{IF(N)}$ that satisfies the following four axioms i.e., Axiom IS1-IS4.

Axiom IS1 (Efficiency**):** If $\tilde{v}\in\tilde{G}(N)$ and $S_N\in IF(N)$ then

$$\sum_{i\in Supp(S_N)}\Phi_i^{Sh}(S_N,\tilde{v})=\tilde{v}(S_N),$$

$$\Phi_i^{Sh}(S_N,\tilde{v})=\tilde{0}\$\, forall\$i\notin Supp(S_N)$$

Axiom IS2 (Carrier): If $\tilde{v}\in\tilde{G}(N)$ and $S_{T_0}\subseteq S_N\in IF(N)$ is an intuitionistic fuzzy carrier for $\tilde{v}\in\tilde{G}(N)$ then

$$\Phi_i^{Sh}(S_N,\tilde{v})=\Phi_i^{Sh}(S_{T_0},\tilde{v}).$$

Axiom IS3. (Symmetry) If $\tilde{v}\in\tilde{G}(N),S_{T_0}\subseteq S_N\in IG(N),S_{T_0}^{ij}$ is a intuitionistic fuzzy carrier in S_N and $\tilde{v}(S_{T_0})=\tilde{v}(\beta_{ij}[S_{T_0}])$ For any $S_{T_0}\subseteq S_N^{ij}$ then

$$\Phi_i^{Sh}(S_N,\tilde{v})=\Phi_j^{Sh}(S_N,\tilde{v})$$

Axiom IS4. (Linearity) For any $\tilde{u},\tilde{v}\in\tilde{G}(N)\$,\$k,t\in$ and $k\tilde{u}+t\tilde{v}\in\tilde{G}(N)$ then

$$\Phi^{Sh}(S_{T_0},k\tilde{u}+t\tilde{v})=k\Phi^{Sh}(S_{T_0},\tilde{u})+t\Phi^{Sh}(S_{T_0},\tilde{v})$$

Theorem 4. Let $\tilde{v}\in\tilde{G}_C(N)$ and $S_{T_0}\subseteq S_N\in IG(N)$ A function $f^{Sh}:\tilde{G}_C(N)\to \mathrm{R}^{IF(N)}$ defined by

$$f^{Sh}(S_N,\tilde{v})=\sum_{i\in N}f_i^{Sh}(S_N,\tilde{v})=\sum_{i\in N}\sum_{l=1}^{q(s)}\Phi_i^{Sh}([S_N]_{\grave{o}_l},\tilde{v})\cdot(\grave{o}_l-\grave{o}_{l-1})$$

is an intuitionistic fuzzy Shapley function in $S_N\, for\tilde{v}\in\tilde{G}_C(N)$ where

$$\Phi_i^{Sh}([S_N]_{\grave{o}_l},\tilde{v})=\begin{cases}\displaystyle\sum_{W_0\subseteq[S_N]_{\grave{o}_l}}\frac{(|W_0|-1)!(|[S_N]_{\grave{o}_l}|-|W_0|)!}{|[S_N]_{\grave{o}_l}|!}\{\tilde{v}(W_0)-_{eH}\tilde{v}(W_0-i)\}, & \text{if } i\in W_0\subseteq[S_N]_{\grave{o}_l}\\ \tilde{0}, & \text{elsewhere}\end{cases}$$

Proof: Recall from Theorem 2 that there exists a unique Φ^{Sh} satisfying Axiom $(PN_1 - PN_4)$. We use this to prove that the function f_i^{Sh} satisfies Axiom $(IS_1 - IS_4)$.

Axiom IS_1 **(Efficiency):** Let $\tilde{v} \in \tilde{G}_C(N)$ and $S_N \in IF(N)$. Since $\sum_{i \in Supp\, S_N} \Phi_i^{Sh}([S_N]_{\dot{\alpha}_l}, \tilde{v}) = \tilde{v}([S_N]_{\dot{\alpha}_l})$ holds for any $l \in 1,...,q(s),$ we obtain $f_i^{Sh}(S_N, \tilde{v}) = f_i^{Sh}(S_{T_0}, \tilde{v})$.

$$\sum_{i \in N} f_i^{Sh}(S_N, \tilde{v}) = \sum_{l=1}^{q(s)} \sum_{i \in N} \Phi^{Sh}([S_N]_{\dot{\alpha}_l}, \tilde{v}) \cdot (\dot{\alpha}_l - \dot{\alpha}_{l-1})$$

$$= \sum_{l=1}^{q(s)} \tilde{v}([S_N]_{\dot{\alpha}_l})(\dot{\alpha}_l - \dot{\alpha}_{l-1}) = \tilde{v}(S_N).$$

Since $i \notin Supp\, S_N$ implies $i \notin [S_N]_{\dot{\alpha}_l}$ we must have $\Phi_i^{Sh}([S_N]_{\dot{\alpha}_l}, \tilde{v}) = \tilde{0}.$

Axiom IS_2 (Carrier) Let $\tilde{v} \in \tilde{G}_C(N)$ and $S_N \in IF(N)$ and $S_{T_0} \in IFC(S_N|_{\tilde{v}})$ We know $S_{T_0} \in IFC(S_N|_{\tilde{v}}) \Rightarrow T_0 \in IC([S_N]_{\dot{\alpha}}|_{\tilde{v}})$ for any $\dot{\alpha} \in (0,1] \Rightarrow \Phi_i^{Sh}([S_N]_{\dot{\alpha}}, \tilde{v}) = \Phi_i^{Sh}([S_{T_0}]_{\dot{\alpha}}, \tilde{v})$ for any $\dot{\alpha} \in (0,1].$ Hence we obtain $f_i^{Sh}(S_N, \tilde{v}) = f_i^{Sh}(S_{T_0}, \tilde{v})$

Axiom IS_3 (Symmetry)

Let $\tilde{v} \in \tilde{G}_C(N)$ and $S_N \in IF(N)$ We know $S_N^{ij}(i) = S_N^{ij}(j).$ If $S_N^{ij}(i) = \langle j, 0, 1 \rangle \$ and \$ S_N^{ij}(j) = \langle i, 0, 1 \rangle \$ then \$ f_i^{Sh}(S_N^{ij}, \tilde{v}) = f_j^{Sh}(S_N^{ij}, \tilde{v}) = \tilde{0}$

We shall discuss the case where $i, j \in Supp\, S_N^{ij}$. In this case the following is valid:

$$\tilde{v}(S_{T_0}) - v(\beta_{ij}[S_{T_0}]) = 0, \quad \forall S_{T_0} \subseteq S_N^{ij}$$

$$\tilde{v}(S_{T_0}) - v(\beta_{ij}[S_{T_0}]) = \tilde{0}, \quad \forall S_{T_0} \subseteq S_N^{ij} \text{ such that } S_{T_0}(i) = \langle i, \epsilon, 1-\epsilon \rangle, S_{T_0}(j) = \langle j, 0,1 \rangle, \text{ and } S_{T_0}(k) = \langle k, 0,1 \rangle \text{ or } S_{T_0}(k) = \langle i, \epsilon, 1-\epsilon \rangle \forall k \in Supp\, S_N, \forall \epsilon \in (0, \mu_{N[ij]}(i)]$$

$$\{\tilde{v}([S_{T_0}{}']_\epsilon \cup \{i\}) - \tilde{v}([S_{T_0}{}']_\epsilon \cup \{j\})\} \cdot \epsilon = \tilde{0}, \quad \forall S_{T_0}{}' \subseteq S_N^{ij}, \text{ such that } S_{T_0}{}'(i) = \langle i, 0,1 \rangle, S_{T_0}{}'(j) = \langle j, 0,1 \rangle, \text{ and } S_{T_0}{}'(k) = \langle k, 0,0 \rangle \text{ or } S_{T_0}{}'(k) = \langle k, \epsilon, 1-\epsilon \rangle \forall k \in Supp\, S_N, \forall \epsilon \in (0, \mu_{N[ij]}(i)]$$

$$\{\tilde{v}([S_{T_0}{}']_\epsilon \cup \{i\}) - \tilde{v}([S_{T_0}{}']_\epsilon \cup \{j\})\} \cdot \epsilon = \tilde{0}, \quad \forall S_{T_0}{}' \subseteq S_N^{ij}, \text{ such that } S_{T_0}{}'(i) = \langle i, 0,1 \rangle, S_{T_0}{}'(j) = \langle j, 0,1 \rangle, \text{ and } S_{T_0}{}'(k) = \langle k, 0,0 \rangle \text{ or } S_{T_0}{}'(k) = \langle k, \epsilon, 1-\epsilon \rangle \forall k \in Supp\, S_N, \forall \epsilon \in (0, \mu_{N[ij]}(i)]$$

$$\{\tilde{v}([S_{T_0}{}']_\epsilon \cup \{i\}) - \tilde{v}([S_{T_0}{}']_\epsilon \cup \{j\})\} \cdot \epsilon = \tilde{0}, \quad \forall S_{T_0}{}' \subseteq S_N^{ij}, \text{ such that } S_{T_0}{}'(i) = \langle i, 0,1 \rangle, S_{T_0}{}'(j) = \langle j, 0,1 \rangle, \text{ and } S_{T_0}{}'(k) = \langle k, 0,0 \rangle \text{ or } S_{T_0}{}'(k) = \langle k, \epsilon, 1-\epsilon \rangle \forall k \in Supp\, S_N, \forall \epsilon \in (0, \mu_{N[ij]}(i)]$$

$$\{\tilde{v}(T_0 \cup \{i\}) - \tilde{v}(T_0 \cup \{j\})\} = \tilde{0}, \quad \forall T_0 \in P([S_N^{ij}]_\epsilon \setminus \{i, j\}), \forall \epsilon \in (0, \mu_{N[ij]}(i)].$$

Consequently, if $\tilde{v}(S_{T_0}) = \tilde{v}(\beta_{ij}[S_{T_0}])$ for any $S_{T_0} \subseteq S_N^{ij}$ then $\tilde{v}(T_0 \cup \{i\}) = \tilde{v}(T_0 \cup \{j\})$ for any $T_0 \in P([S_N^{ij}]_\grave{o}, \{i, j\})$ and $\grave{o} \in (0, \mu_{N^{[ij]}}(i)]$ Hence we have $\Phi_i^{Sh}([S_N^{ij}]_\grave{o}, \tilde{v}) = \Phi_j^{Sh}([S_N^{ij}]_\grave{o}, \tilde{v})$ for any $\grave{o} \in (0, \mu_{N^{[ij]}}(i)]$ and $\Phi_i^{Sh}([S_N^{ij}]_\grave{o}, \tilde{v}) = \Phi_j^{Sh}([S_N^{ij}]_\grave{o}, \tilde{v}) = \tilde{0}$ for any $\grave{o} \in (\mu_{N^{[ij]}}(i), 1]$. Therefore, $\Phi_i^{Sh}([S_N^{ij}]_\grave{o}, \tilde{v}) = \Phi_j^{Sh}([S_N^{ij}]_\grave{o}, \tilde{v})$ for any $\grave{o} \in (0,1]$ It follows that $f_i^{Sh}(S_N^{ij}, \tilde{v}) = f_j^{Sh}(S_N^{ij}, \tilde{v})$.

Axiom IS_4 (Linearity) Since $\boldsymbol{\Phi}^{Sh}$ is linear so for any $\tilde{u}, \tilde{v} \in \tilde{G}_C(N), k, t \in \square$ and by the definition of f^{Sh} we can easily prove that $f^{Sh}(S_N, k\tilde{u} + t\tilde{v}) = kf^{Sh}(S_N, \tilde{u}) + tf^{Sh}(S_N, \tilde{v})$

This completes the proof.

Example 1: Optimal Allocation Strategies in Intuitionistic Fuzzy Cooperative Games: Consider three companies (players) 1, 2, and 3 i.e., set players *N* = {1, 2, 3} planning to collaborate on a joint project requiring resources. Each company has a different willingness to contribute, expressed in an intuitionistic fuzzy manner due to uncertainty and incomplete information. Company 1 has 10 units of resource R_1, will contribute 6 units, will not contribute 3 units and hesitates to contribute 1 unit. Company 2 has 10 units of resource R_2 will contribute 3 units, will not contribute 6 units, hesitates to contribute 1 unit. Company 3 has 10 units of resource R_3, will contribute 2 units, will not contribute 6 units and Hesitates to contribute 2 unit. Therefore, an intuitionistic fuzzy coalition S_N has been formed.

The coalition formed by these companies is represented as:

$$S_N = \{\langle 1, 0.6, 0.3\rangle, \langle 2, 0.3, 0.6\rangle, \langle 3, 0.2, 0.6\rangle\}$$

Due to uncertainty, the expected profit for each coalition is an trianguler intuitionistic fuzzy number (TIFN):

Table 1

The Crisp Coalition $T_0 \in P(N)$	**The Intuitionistic Fuzzy Characteristic Function** $\tilde{v}(T_0)$
{}	$\tilde{0} = \langle 0; 0, 0; 0, 0\rangle$

{1}	< 5; 3, 8; 2, 6 >
{2}	< 5; 3, 8; 2, 6 >
{3}	< 5; 3, 8; 2, 6 >
{1, 2}	< 5; 3, 9; 2, 7 >
{1, 3}	< 5; 3, 9; 2, 7 >
{2, 3}	< 5; 3, 9; 2, 7 >
{1, 2, 3}	< 6; 3, 9; 2, 7 >

The set $Q(S_N) = \{\grave{o}_1 = 0.2 < \grave{o}_2 = 0.3 < \grave{o}_3 = 0.6\}$

Table 2

$\Phi^{Sh}([S_N]_{\grave{o}}, \tilde{v})$	The intuitionistic fuzzy Shapley function as a TIFN
$\Phi_1^{Sh}([S_N]_{0.2}, \tilde{v})$	$< 2;1,3;\frac{2}{3},\frac{7}{3} >$
$\Phi_1^{Sh}([S_N]_{0.3}, \tilde{v})$	$< \frac{5}{2};\frac{3}{2},\frac{9}{2};1,\frac{7}{2} >$
$\Phi_2^{Sh}([S_N]_{0.3}, \tilde{v})$	$\tilde{0}$
$\Phi_3^{Sh}([S_N]_{0.3}, \tilde{v})$	$\tilde{0}$
$\Phi_1^{Sh}([S_N]_{0.6}, \tilde{v})$	< 5; 3, 8; 2, 6 >
$\Phi_2^{Sh}([S_N]_{0.6}, \tilde{v})$	$\tilde{0}$
$\Phi_3^{Sh}([S_N]_{0.6}, \tilde{v})$	$\tilde{0}$

From Table 1 and Table 2, we get

$f_1^{Sh}([S_N], \tilde{v}) = \langle 2.15; 1.25, 3.45; 0.833, 2.6166 \rangle$

$f_2^{Sh}([S_N], \tilde{v}) = \langle 0.65; 0.35, 1.05; 0.233, 0.8166 \rangle$

and $f_3^{Sh}([S_N], \tilde{v}) = \langle 0.4; 0.2, 0.6; 0.133, 0.466 \rangle$ Since $\tilde{v} \in \tilde{G}_C(N)$ therefore $\tilde{v}(S_N) = \langle 3.2, 1.8, 5.1, 1.2, 3.9 \rangle$.

Obviously $\tilde{v}(S_N) = f_1^{Sh}([S_N], \tilde{v}) + f_2^{Sh}([S_N], \tilde{v}) + f_3^{Sh}([S_N], \tilde{v})$.

3. Conclusion

In this work, I discussed the Shapley function for a class of intuitionistic fuzzy cooperative game. The exploration of other solution concepts for intuitionistic fuzzy cooperative games is left as a direction for future research.

References

1. Aubin, J.P. (1988) Cooperative fuzzy games, Mathematics of Operations Research, 6, 1-13.
2. Aubin, J.P. (1982) Mathematical Methods of Game and Economic Theory, Rev. ed., North-Holland, Amsterdam, 1982.
3. Alvarez-Mozos, M., R. van den Brink, G. van der Laan, O. Tejada (2013) Share functions for cooperative games with levels structure of cooperation, European Journal of Operational Research, 244, 167-179.
4. Aumann, R.J., L.S. Shapley, Values of Non-Atomic Games, Princeton University Press, Princeton, NJ, 1974.
5. Aumann, R. and S. Hart (Ed.) (2002) Handbook of Game Theory with Economic Applications, Elsevier, ISBN: 9780444894281.
6. Banzhaf, J.F. (1965) Weighted Voting Doesn't Work: A Mathematical Analysis, Rutgers Law Review, 19, 317-343.
7. Biswakarma, R., Borkotokey, S. and Mesiar, R. (2017) A Simplified expression of Share Functions for Cooperative games with fuzzy coalitions, Tatra Mt. Math. Pub. 69, 1-16.
8. Biswakarma, R. and Borkotokey, S. (2017) Solidarity Share Functions for Cooperative Games, The International Journal of Applied Mathematical Analysis and Applications, 12, 2, 213-220.
9. Borkotokey, S. Cooperative games with fuzzy coalitions and fuzzy characteristic functions, Fuzzy Sets and Systems, 59 (2008) 138-151.
10. Butnariu, D. (1980) Stability and Shapley value for an n-persons fuzzy game, Fuzzy Sets and Systems, 4, 63-72.
11. Choquet, G., (1953) Theory of capacities, Annales de Institut Fourier, 5, 131-295.
12. Guha D, Chakraborty D (2010) A theoretical development of distance measure for intuitionistic fuzzy numbers. Int J Math Math Sci. Article ID 949143.
13. Li, S., Q. Zhang (2009) A Simplified expression of the Shapley function for fuzzy game, European Journal of Operational Research, 196, 234-245.
14. Meng, F.Y., Q. Zhang (2011) The Shapley Value on a kind of cooperative fuzzy games, Journal of Computational Information System 7: 6, 1846-1854.

15. Meng, F.Y., Q. Zhang (2010) The Shapley function for fuzzy cooperative games with multilinear extension form, European Journal of Operational Research, 23, 644-650.

16. Nan, X. H. Bo, C.L. Wei, Cooperative games with the intuitionistic fuzzy coalitions and intuitionistic fuzzy characteristic functions, in: D.F. Li, X.G. Yang, M. Uetz, G.J. Xu (Eds.), Game Theory and Applications, vol. 758, Springer, Singapore, 2017, pp. 337-352.

17. Nowak, A. S. and T. Radzik, A solidarity value for n- person transferable utility games, Int. J. Game Theory, (1994) 23: 43-48.

18. Shapley, L.S. (1953) A value for n-person games, Annals of Mathematical Studies, 28, 307-317.

19. Sprumont, Y. (1990) Population monotonic allocation schemes for cooperative games with transferable utility, Games and Economic Behavior, 2, 378-394.

20. Tan, C., Z.Z. Jiang, X. Chen, W.H. Ip (2014) A Banzhaf function for fuzzy game, IEEE Transaction on Fuzzy Systems, 22, 1489-1502.

21. Tsurumi, M., T. Tanino, M. Inuiguchi (2001) (Theory and methodology) A Shapley function on a class of cooperative fuzzy games, Eur. J. Oper. Res., 129, 596-618.

22. van der Laan, G., R. van den Brink (1998) Axiomatizations of a class of share functions on n-person games, Theory Dec., 44, 117-148.

23. van der Laan, G., R. van den Brink (1999) The normalized Banzhaf value and the Banzhaf share function, Int. J. Math. Game Theory Algebra, 9, 65-84.

24. van der Laan, G., R. van den Brink (2005) A class of consistent share functions for games in coalition structure, Games and Economic Behavior, 51, 193-212.

25. Veeramani, V., R. Batulan (2010) Some Characterisations of a-cut in intuitionistic fuzzy set theory, Set Theory and Logic.

Chapter - 9
MHD Jeffrey Fluid Flow Over a Exponentially Stretching Sheet with Soret and Dufour Effect in Presence of Heat Generation/ Absorption

Author

Satyabhushan Roy
Department of Mathematics, Cotton University, Guwahati, Assam, India

Chapter - 9

MHD Jeffrey Fluid Flow Over a Exponentially Stretching Sheet with Soret and Dufour Effect in Presence of Heat Generation/ Absorption

Satyabhushan Roy

Abstract

An incompressible non-newtonian jeffrey fluid's heat transfer flow characteristics across a exponentially stretching surface with soret and dufour effects in presence of heat generation and absorption are investigated in this study. With boundary conditions and a transverse magnetic field, the sheet is linearly stretched. The basic governing equations (pdes) are converted into odes using the appropriate similarity variables. Python is utilized to solve the resultant equations. Graphical analysis is used to examine the effects of certain physical factors and dimensionless numbers on the flow field and heat transfer.

1. Introduction

The investigation of flow and heat transfer of a Newtonian fluid induced by a stretching sheet stands as a cornerstone problem in classical fluid mechanics and convective heat transfer, retaining enduring relevance due to its profound and direct applicability to a vast spectrum of industrial manufacturing processes. From the foundational work of Crane [1], who established the seminal paradigm of flow over a linearly stretching surface, the field has seen extensive theoretical and experimental evolution.

Subsequent research, spanning from Gupta and Gupta [2] to Cortell [3] and beyond, has significantly generalized Crane's model, incorporating complexities such as mixed convection, thermal radiation, unsteady kinematics, nonlinear stretching, suction effects, and thermally stratified media, as exemplified by the contributions of Hayat *et al.* [4], El-Aziz [5], Akyldz and Siginer [6], and Mukhopadhyay [7]. Gbadeyan *et al.* [8], who investigated the effects of thermal diffusion (Soret effect) and diffusion thermo (Dufour effect) on combined heat and mass transfer in a mixed convection boundary layer flow over a vertical stretching sheet. Their study considered a porous medium saturated with a viscoelastic fluid under the

influence of a magnetic field. Imran *et al*. [9] conducted an analysis of an unsteady mixed convection flow within a fluid-saturated porous medium adjacent to a heated or cooled semi-infinite vertical stretching sheet, incorporating the effect of a heat source. In a related study, Aly and Ebaid [10] investigated mixed convection boundary layer flow of nanofluids along an inclined plate embedded in a porous medium, employing both analytical and numerical solution approaches.

Further expanding on this theme, Dessie and Kishan [11] examined magneto hydrodynamic (MHD) boundary layer flow and heat transfer of a fluid with variable viscosity through a porous medium towards a stretching sheet. Their analysis also accounted for the effects of viscous dissipation and volumetric heat sources or sinks. Additionally, Narayana [12] carried out a study on the combined effects of thermal radiation and a first-order chemical reaction on unsteady mixed convection flow. This work modeled a viscous, incompressible, electrically conducting fluid moving through a porous medium of variable permeability between two long, vertical, non-conducting wavy channels, with heat generation also considered. These studies represent a select, but indicative, sample of the active research in this domain.

In many engineering and physical systems, significant temperature differences exist between a solid surface and the surrounding ambient fluid. Such pronounced thermal gradients necessitate the inclusion of temperature-dependent volumetric heat sources or sinks in the analytical model, as these internal generation or absorption mechanisms can exert a strong influence on overall heat transfer characteristics studied by Vajravelu and Nayfeh [13]. The study of heat generation or absorption effects in moving fluids is critically important due to its relevance to a range of practical problems, including fluids undergoing exothermic or endothermic chemical reactions studied by Vajravelu and Hadjinicolaou [14], Vajravelu and Nayfeh [13]. Furthermore, natural convection coupled with internal heat generation has direct applications in areas such as combustion modeling was studied by Westphal *et. al*. [15].

Although the precise mathematical modeling of internal heat generation or absorption is complex, simplified formulations can effectively represent its average behavior for most physical scenarios. Historically, the strength of this internal heat effect has been modeled as a constant, as a function of spatial coordinates, or as a function of temperature itself. Early work by Sparrow and Cess [16] incorporated temperature-dependent heat absorption in their analysis of steady stagnation point flow and heat transfer. Moalem [17] investigated the

impact of temperature-dependent heat sources, such as those arising from electrical heating, on heat transfer within a porous medium. Vajravelu and Nayfeh [13] further explored this concept in their study of hydromagnetic convection around a cone and a wedge. More recent contributions include Chamkha [18], who considered a linear temperature-dependent heat source/sink model in a analysis of mixed convection within a porous channel, and Crepeau and Clarksean [19], who employed a space-dependent, exponentially decaying heat generation/absorption model in their work on flow and heat transfer from a vertical plate.

The study of non-Newtonian fluids is of profound significance due to their wide-ranging technical and industrial applications. However, the classical Navier-Stokes equations are insufficient to accurately describe the rheological behavior of such fluids. Owing to the substantial differences between Newtonian and non-Newtonian fluids, numerous constitutive models have been proposed to characterize their complex stress-strain relationships.

Among these, the Jeffrey fluid model represents one of the simplest and most commonly utilized non-Newtonian formulations. It is distinguished by its use of a time derivative rather than a convected derivative in its constitutive equation, a feature common to many other fluid models. Recently, this model has prompted considerable research interest. For instance, Maryam Aleem *et al.* [20] investigated the flow of a Jeffrey fluid through a porous medium bounded by two parallel plates one moving with a variable velocity and the other stationary under the influence of a magnetic field. Babu *et al.* [21] analyzed the magneto-hydrodynamic (MHD) flow of a Jeffrey fluid past a vertical plate embedded in a porous medium, incorporating the effects of heat transfer and rotation.

Further contributions include the work of Sreenadh *et al.* [22], who examined Jeffrey fluid flow in a rotating channel in the presence of Couette flow. Reddappa *et al.* [23] focused on the convective Couette flow of a Jeffrey fluid within an inclined channel where the walls are coated with a porous material. Additional significant studies in this domain can be found in the works of Ahmad and Ishak [24], Prasad *et al.* [25], Nallapu and Radhakrishna macharya [26], and Shehzad *et al.* [27]. Nadeem *et al.* [28].

In view of the preceding literature review, the objective of the present investigation is to analyze the boundary layer flow and heat transfer characteristics of a magnetohydrodynamic (MHD) Jeffrey fluid over an exponentially stretching sheet. The sheet is embedded within a thermally stratified porous medium in presence of Soret and Dufour effect and is subject

to uniform suction at the surface. The governing partial differential equations, along with their corresponding boundary conditions, are transformed into a system of coupled, nonlinear ordinary differential equations using an appropriate set of similarity transformations. The resulting boundary value problem is solved numerically using Python. The effects of key dimensionless parameters such as the magnetic field parameter, Soret and Dufour number, on the dimensionless velocity and temperature profiles are presented graphically and discussed in detail.

2. Formation of the Problem

A stable two-dimensional conductive, invisible viscous flow of Jeffrey fluid on a vertical heated sheet is considered. The flow is restricted to positive side of Y-axis. Two equal and opposing forces are applied along the X-axis, stretching the surface at a velocity U along the X-axis, while maintaining the origin constant. A variable magnetic field $B(x) = B_0 e^{\frac{x}{2L}}$ is applied normally to the surface, where B_0 is constant. The surface temperature and concentration are are denoted by $T_w(x), C_w(x)$ and are immersed in a double stratified medium of changeable ambient temperature and concentration denoted by $T_\infty(x), C_\infty(x)$ respectively. The governing equations takes the following form,

$$\frac{\partial u}{\partial x} + \frac{\partial v}{\partial y} = 0, \tag{1}$$

$$u\frac{\partial u}{\partial x} + v\frac{\partial u}{\partial y} = \frac{\mu}{\rho(1+\lambda_1)}\frac{\partial^2 u}{\partial y^2} - \frac{\sigma B_0^2}{\rho}u + g\beta_t(T - T_\infty) + g\beta_c(C - C_\infty) - \frac{\nu}{K_p}u, \tag{2}$$

$$u\frac{\partial T}{\partial x} + v\frac{\partial T}{\partial y} = \frac{k}{\rho C_p}\frac{\partial^2 T}{\partial y^2} + \frac{D_M K_T}{C_s C_p}\frac{\partial^2 C}{\partial y^2} - \frac{1}{\rho C_p}\frac{\partial q_r}{\partial y} + \frac{1}{\rho c_p}q''', \tag{3}$$

$$u\frac{\partial C}{\partial x} + v\frac{\partial C}{\partial y} = D\frac{\partial^2 C}{\partial y^2} + \frac{D_M K_T}{T_m}\frac{\partial^2 T}{\partial y^2} - K_r(C - C_\infty). \tag{4}$$

The boundary conditions are,

$$u = U, v = -V_w, T = T_w, C = C_w \; at \; y = 0 \tag{5}$$

$$u = 0, T = T_\infty, C = C_\infty \; at \; y = \infty$$

By using Rosseland approximation for thermal radiation, the radiative heat flux is modeled as,

$$q_r = -\frac{4\sigma_1}{3k_1}\frac{\partial T^4}{\partial y}.$$

where k_1 is the mean absorption coefficient and σ_1 is the Stefan Boltzmann

constant. Following Chamkha [18] it is assumed that T^4 can be stated as a linear function of temperature since the temperature difference within the flow are thought to be sufficiently small. This is achieved by omitting higher order terms and expanding T^4 in a Taylor series around T_∞, thus,

$$T^4 \approx 4T_\infty^3 T - 3T_\infty^4.$$

and thus the gradient of heat radiation term can be expressed as

$$\frac{\partial q_r}{\partial y} = -\frac{16\sigma_1 T_\infty^3}{3k_1}\frac{\partial^2 T}{\partial y^2}.$$

Introducing the similarity transformation:

$$\eta = y\sqrt{\frac{U}{2\nu L}}, u = Uf'(\eta), v = -\sqrt{\frac{\nu U}{2L}}\left(f(\eta) + \eta f'(\eta)\right), \quad \theta(\eta) = \frac{T-T_\infty}{T_w-T_\infty}, \phi(\eta) = \frac{C-C_\infty}{C_w-C_\infty}, G_r = \frac{2g\beta_t(T_w-T_0)L}{U^2}, G_m = \frac{2g\beta_C(C_w-C_0)L}{U^2}, S_p = \frac{K_p U}{2Lv}, N = \frac{kk_1}{4\sigma_1 T_\infty^3}, M = \frac{2\sigma B_0^2 L}{\rho U}. \quad (6)$$

and writing the internal heat generation q''' as,

$$q''' = k\left(\frac{Re}{2L^2}\right)[a^*(T_w - T_\infty)e^{-\eta} + b^*(T - T_\infty)] \quad (7)$$

Substituting (6) into (2)-(4) we get the following similarity equations,

$$f''' = 2(1+\lambda_1)(f')^2 + (1+\lambda_1)f'\left(M + \frac{1}{Sp}\right) - (1+\lambda_1)f''f - 2(1+\lambda_1)(Gr\theta + Gm\phi), \quad (8)$$

$$\left(1 + \frac{4}{3N}\right)\theta'' = Prf'\theta - Prf\theta' - DuPr\phi'' + a^*e^{-\eta} + b^*, \quad (9)$$

$$\phi'' = -ScSr\theta'' - Sc(f\phi' - \phi f') + ScKr. \quad (10)$$

The transformed boundary conditions are,

$$f(0) = f_w,\ f'(0) = 1, \theta(0) = 1 - St_1, \phi(0) = 1 - St_2, as\ \eta \to 0,$$

$$f'(\infty) = 0, \theta(\infty) = 0, \phi(\infty) = 0, as\ \eta \to \infty. \quad (11)$$

3. Results & Discussion

The resulting nonlinear ordinary differential expressions (8) and (10) are solved numerically with corresponding boundary conditions through the help of Python. This section provides the effect of various physiological parameters on velocity, temperature and concentration profile for fixed values of M =1, λ_1 =0.3, Pr=0.71, Du=0.1, Sr=0.1, Kr=0.5, $a^* = 0.2 = b^*$.

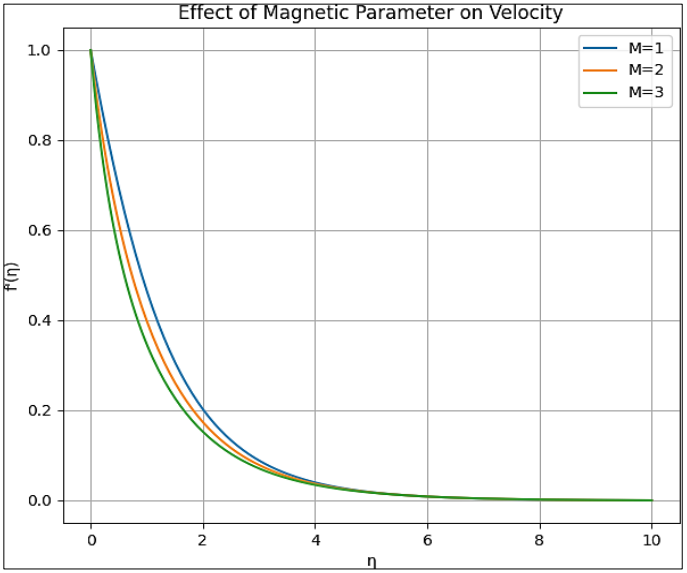

Fig 1

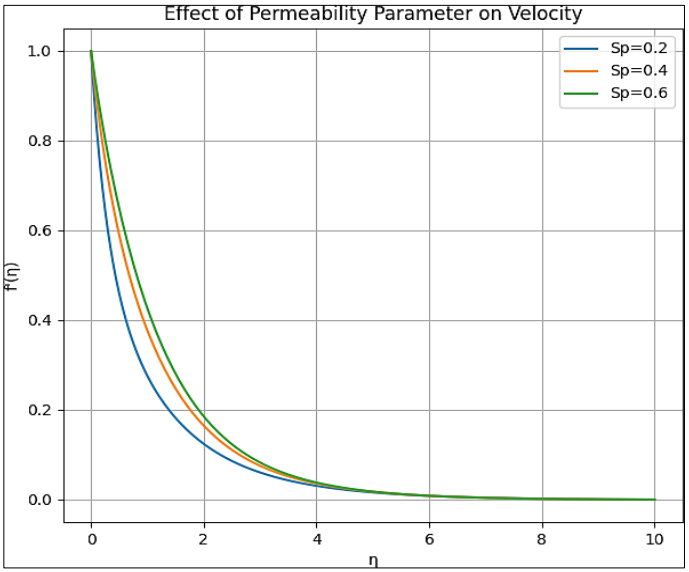

Fig 2

The consequences of M on velocity profile is presented in fig.1. The velocity profile exhibits a characteristic suppression with an increasing magnetic parameter, a phenomenon fundamentally attributed to magneto hydrodynamic (MHD) effects. When a transverse magnetic field is applied to

an electrically conducting fluid in motion, it induces a Lorentz force that opposes the direction of flow. This force functions as a distributed resistive body force within the momentum boundary layer, directly counteracting fluid motion. The resulting retarding effect not only dampens the local velocity but also leads to a concomitant thickening of the momentum boundary layer, thereby reducing the overall velocity gradient at the stretching surface. The consequences of Sp on velocity profile is presented in fig.2. The velocity profile is enhanced with an increase in the permeability parameter, a direct consequence of the modified hydrodynamic resistance within the porous matrix. Elevated permeability signifies a more pervious medium, which reduces the Darcy-type resistive drag impeding fluid motion. Consequently, the Darcy drag force is attenuated, allowing momentum from the stretching surface to diffuse more effectively into the fluid. This results in a steeper velocity gradient near the wall, a higher peak velocity within the boundary layer, and an overall thinning of the momentum boundary layer compared to scenarios with lower permeability.

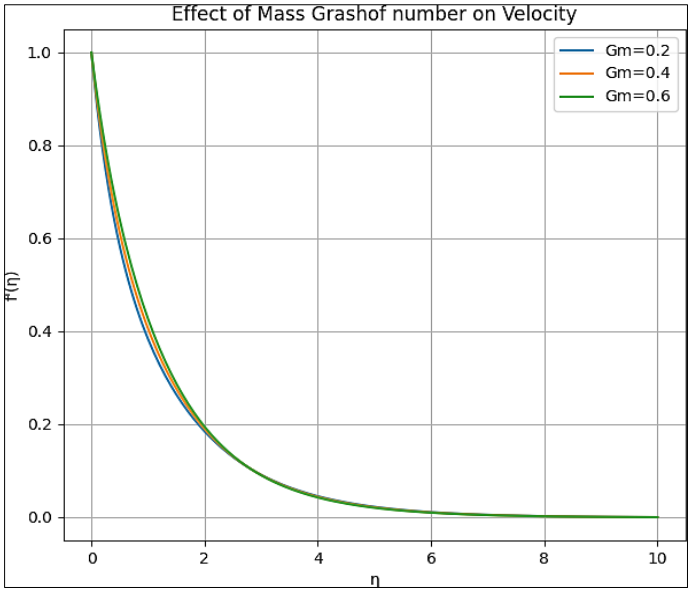

Fig 4

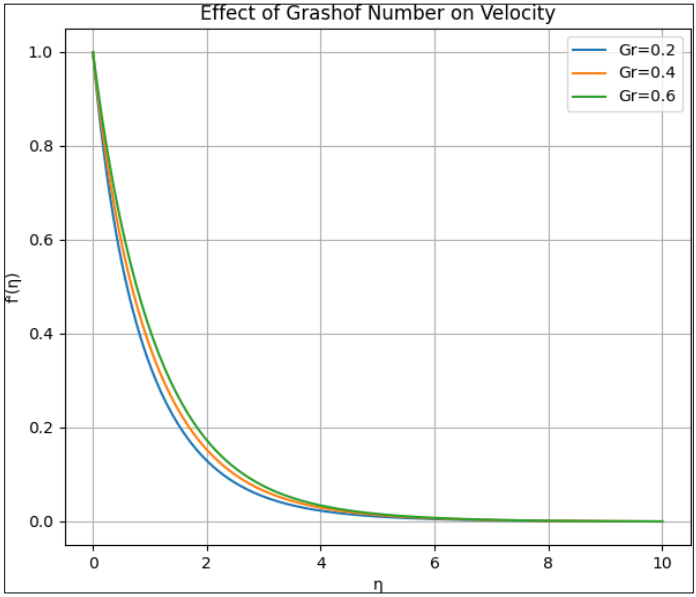

Fig 3

The consequences of Gr and Gm on velocity profile is presented in fig.3. and fig.4. The Grashof number (Gr) and mass (or species) Grashof number (Gm) characterize the relative strength of buoyancy forces-driven by temperature and concentration gradients, respectively to viscous forces in a fluid. When either parameter increases, the buoyancy-driven force within the boundary layer is amplified. This enhanced force acts as an additional accelerating mechanism alongside the primary motion (e.g., stretching), thereby augmenting fluid velocity and resulting in a thicker momentum boundary layer. Essentially, stronger thermal or solutal buoyancy contributes constructively to the flow field, elevating the velocity profile.

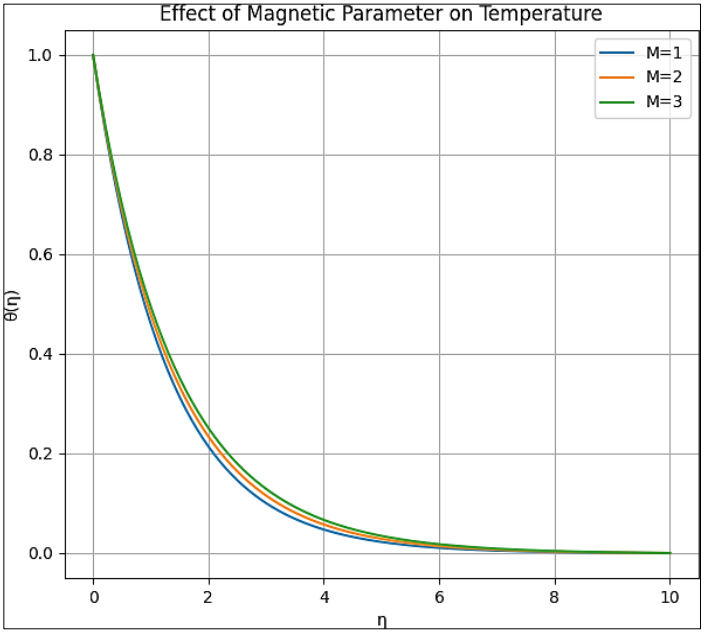

Fig 5

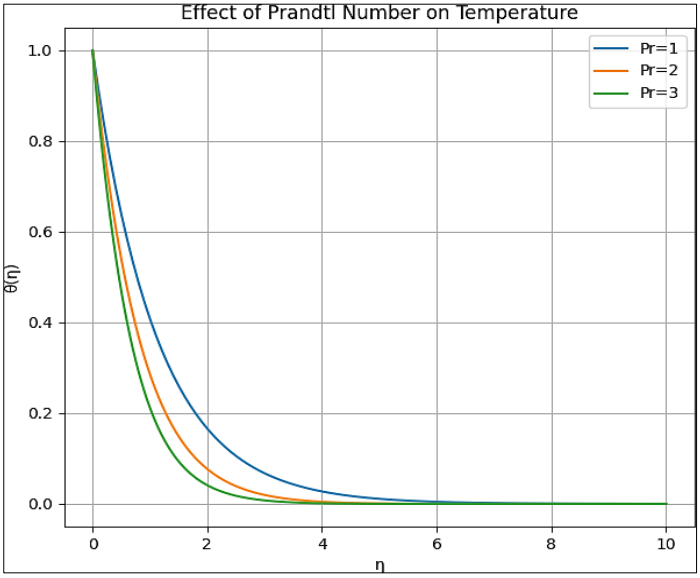

Fig 6

The consequences of M on Temperature profile is presented in fig.5. In magnetohydrodynamic (MHD) boundary layer flow, the temperature profile

increases with an increasing magnetic parameter primarily due to the conversion of kinetic energy into thermal energy via enhanced viscous dissipation. As the magnetic parameter rises, the opposing Lorentz force suppresses fluid velocity, thereby amplifying the velocity gradients within the boundary layer. This elevated shear leads to greater viscous heating, which acts as a volumetric heat source. Simultaneously, the retardation of flow reduces convective cooling, allowing the heat generated internally from viscous dissipation and possibly Joule heating to accumulate, thereby elevating the thermal boundary layer and increasing the temperature distribution. The consequences of Pr on Temperature profile is presented in fig.6. An increase in the Prandtl number (Pr) reduces the temperature in the boundary layer. Since Pr represents the ratio of momentum diffusivity to thermal diffusivity, a higher Pr means heat diffuses more slowly relative to momentum. This results in a thinner thermal boundary layer with a steeper temperature gradient near the surface, confining heat closer to the wall and lowering temperatures within the fluid layer.

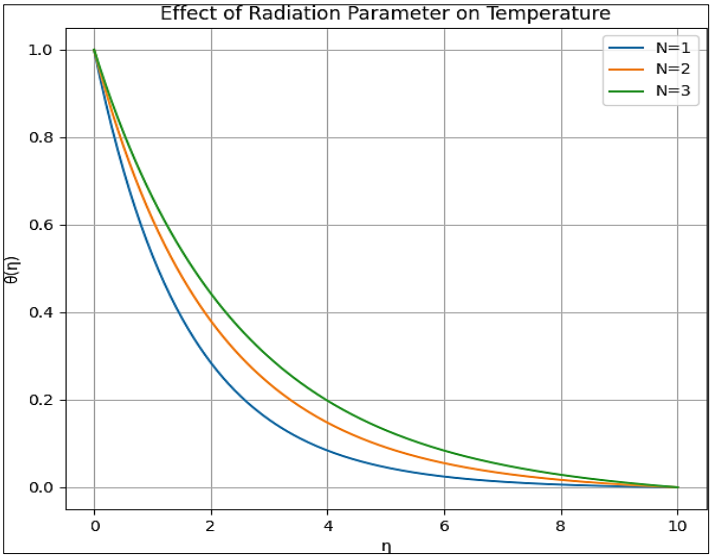

Fig 8

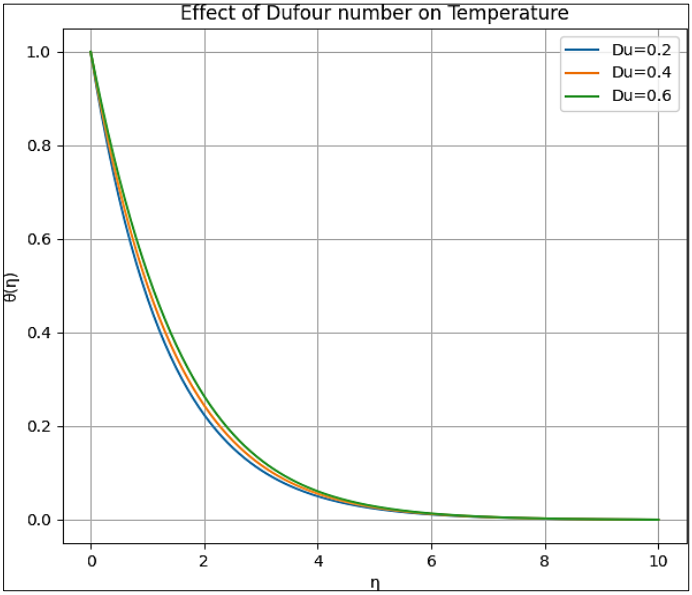

Fig 7

The consequences of Du on Temperature profile is presented in fig.7. The Dufour (or diffusion-thermo) effect describes heat flux driven by a concentration gradient. An increase in the Dufour number enhances this cross-diffusion mechanism, where mass diffusion induces additional thermal energy within the boundary layer. This acts as an internal heat source, raising the fluid temperature. The consequences of N on Temperature profile is presented in fig.8. Thermal radiation contributes an extra mode of energy transfer. A larger radiation parameter increases radiative heat flux toward the fluid. This provides supplementary heating to the thermal boundary layer, effectively raising the temperature distribution while also thickening the thermal boundary layer.

The consequences of Kr on Concentration profile is presented in fig.9. An increase in the chemical reaction parameter (Kr), particularly for a destructive reaction (species consumption), enhances the rate of species depletion within the boundary layer. This leads to a reduction in species concentration as the reaction actively removes the diffusing component. For a generative reaction, the opposite trend would be observed.

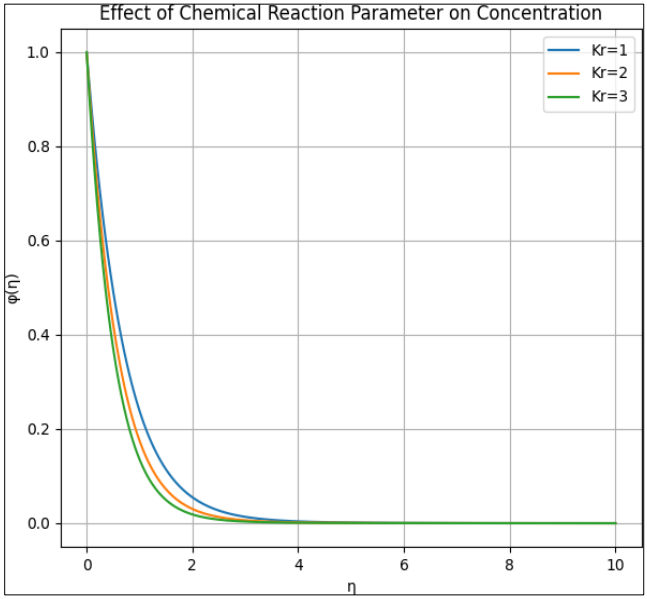
Effect of Chemical Reaction Parameter on Concentration
Kr=1
Kr=2
Kr=3
φ(η)
η
0.0
0.2
0.4
0.6
0.8
1.0
0
2
4
6
8
10

Fig 9

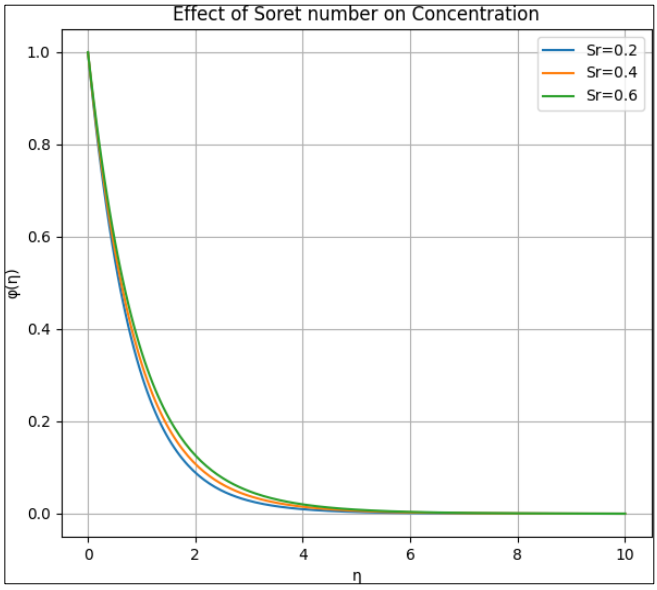
Effect of Soret number on Concentration
Sr=0.2
Sr=0.4
Sr=0.6
φ(η)
η
0.0
0.2
0.4
0.6
0.8
1.0
0
2
4
6
8
10

Fig 10

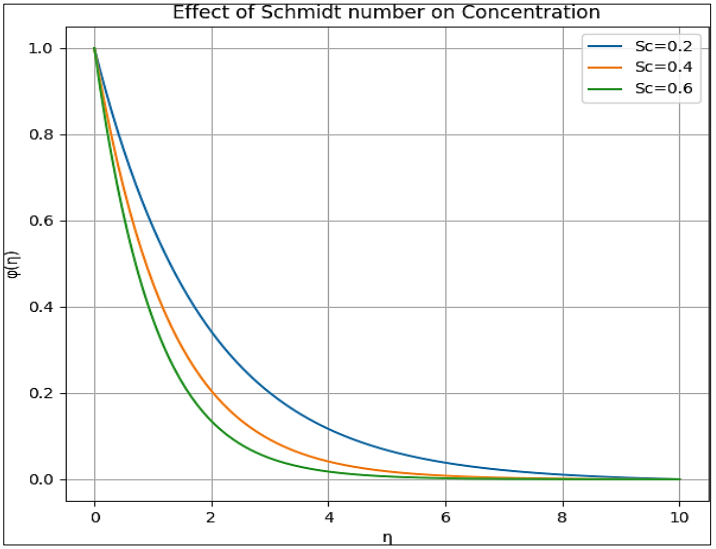

Fig 11

The consequences of Sr on Concentration profile is presented in fig.10. The concentration increases with an increasing Soret number because the Soret effect describes thermal diffusion-the movement of species due to a temperature gradient. A higher Soret number signifies a stronger influence of the temperature gradient on mass transport relative to ordinary Fickian diffusion. In a boundary layer with a heated surface, the temperature decreases moving away from the wall. This thermal gradient drives molecular diffusion from the hot region toward the cold region. Therefore, as the Soret number increases, more species are thermally driven from the hot wall into the boundary layer, enhancing the concentration of the diffusing component within the fluid. The consequences of Sc on Concentration profile is presented in fig.11. The Schmidt number is the ratio of momentum diffusivity (viscosity) to mass diffusivity. A higher Sc indicates that mass diffusivity is low relative to momentum diffusivity. This means mass (species) spreads more slowly. Consequently, the concentration boundary layer becomes thinner, confining the species closer to the wall and resulting in a steeper concentration gradient but a lower concentration at any given point away from the surface compared to a fluid with a lower Sc.

4. Conclusion

The analysis of magnetohydrodynamic (MHD) boundary layer flow over a stretching surface reveals a complex interplay of forces and transport mechanisms, each governed by specific dimensionless parameters. Beginning

with the magnetic parameter (M), its increase induces a resistive Lorentz force that suppresses the velocity profile while simultaneously elevating the temperature due to enhanced viscous dissipation and reduced convective cooling. This foundational MHD effect sets the stage for coupled heat and mass transfer phenomena. Thermal transport is primarily modulated by the Prandtl number (Pr), where higher values suppress the temperature profile by thinning the thermal boundary layer, and the radiation parameter (Rd), which augments temperature by contributing additional radiative energy. Mass transfer is governed by the Schmidt number (Sc), where increased values decrease concentration by inhibiting mass diffusion, and the chemical reaction parameter (Kr), which depletes species concentration in destructive reactions.

Crucially, cross-diffusion effects create direct couplings between thermal and concentration fields: the Dufour number (Df) increases temperature by converting concentration gradients into thermal energy, while the Soret number (Sr) increases concentration by driving species migration along thermal gradients.

In synthesis, the system demonstrates that flow control (via M), heat transfer (via Pr, Rd, Df), and mass transfer (via Sc, Kr, Sr) are not independent but are intricately linked through viscous dissipation, buoyancy, and cross-diffusion. This interconnectedness highlights the necessity of a coupled, multi-parameter approach for accurately modeling and optimizing real-world applications from polymer processing and metallurgy to electrochemical systems and energy device design where magnetic fields, thermal radiation, and coupled heat-mass transfer coexist.

Reference:

1. Crane, L.J. (1970). Flow past a stretching plate, Z. Angew. Math. Phys., 21:645-647.
2. Gupta, P.S. and Gupta, A. S. (1977). Heat and mass transfer on a stretching sheet with suction and blowing, Can. J. Chem. Eng., 55:744-746.
3. Cortell, R. (2007). Viscous flow and heat transfer over a nonlinearly stretching sheet, Appl. Math. Comput., 184:864-873.
4. Hayat, T., Abbas, Z., & Javed, T. (2008). Mixed convection flow of a micropolar fluid over a non-linearly stretching sheet. Physics letters A, 372(5), 637-647.
5. El-Aziz, M. A. (2009). Radiation effect on the flow and heat transfer over an unsteady stretching sheet, International Communications in Heat and Mass Transfer, 36:521-524.

6. Akyildiz, F. T. and Siginer, D. A. (2010). Galerkin-Legendre spectral method for the velocity and thermal boundary layer over a non-linearly stretching sheet, Non-Linear Analysis: Real World Applications, 11:735-741

7. Mukhopadhyay, S. (2013). MHD boundary layer flow and heat transfer over an exponentially stretching sheet embedded in a thermally stratified medium, Alexandria Engineering Journal, 52:259-265.

8. J.A. Gbadeyan, A.S Idowu, A.W. Ogunsola, O.O. Agboola, P.O. Olanrewaju, Heat and mass transfer for Soret and Dufour's effect on mixed convection boundary layer flow over a stretching vertical surface in a porous medium filled with a viscoelastic fluid in the presence of magnetic field, Glob. J.Sci.Front.Res.11(2011)22494626.

9. Imran, S. M., Asghar, S., & Mushtaq, M. (2012). Mixed convection flow over an unsteady stretching surface in a porous medium with heat source. Mathematical Problems in Engineering, 2012(1), 485418.

10. Aly, E. H., & Ebaid, A. (2013). New Analytical and Numerical Solutions for Mixed Convection Boundary-Layer Nanofluid Flow along an Inclined Plate Embedded in a Porous Medium. Journal of Applied Mathematics, 2013(1), 219486.

11. Dessie, H., & Kishan, N. (2014). MHD effects on heat transfer over stretching sheet embedded in porous medium with variable viscosity, viscous dissipation and heat source/sink. Ain shams engineering journal, 5(3), 967-977.

12. Narayana, P. S. (2015). Effects of variable permeability and radiation absorption on magnetohydrodynamic (MHD) mixed convective flow in a vertical wavy channel with traveling thermal waves. Propulsion and Power Research, 4(3), 150-160.

13. Vajravelu, K., & Nayfeh, J. (1992). Hydromagnetic convection at a cone and a wedge. International communications in heat and mass transfer, 19(5), 701-710.

14. Vajravelu, K., & Hadjinicolaou, A. (1993). Heat transfer in a viscous fluid over a stretching sheet with viscous dissipation and internal heat generation. International Communications in Heat and Mass Transfer, 20(3), 417-430.

15. Westphal, B. R., Keiser, D. D., Rigg, R. H., & Laug, D. V. (1995). Production of metal waste forms from spent fuel treatment (No.

ANL/TD/CP-84383; CONF-941207-24). Argonne National Lab., IL (United States).

16. Sparrow, E. M., & Cess, R. D. (1961). Temperature-dependent heat sources or sinks in a stagnation point flow. Applied Scientific Research, 10(1), 185.
17. Moalem, D. (1976). Steady state heat transfer within porous medium with temperature dependent heat generation. International Journal of Heat and Mass Transfer, 19(5), 529-537.
18. Chamkha, A. J. (1997). Non-Darcy fully developed mixed convection in a porous medium channel with heat generation/absorption and hydromagnetic effects. Numerical Heat Transfer, Part A Applications, 32(6), 653-675.
19. Crepeau, J. C., & Clarksean, R. (1997). Similarity solutions of natural convection with internal heat generation.
20. Aleem, M., Asjad, M. I., Ahmadian, A., Salimi, M., & Ferrara, M. (2020). Heat transfer analysis of channel flow of MHD Jeffrey fluid subject to generalized boundary conditions. The European physical journal plus, 135(1), 26.
21. Babu, NVN, Murali. G, Bhati, S.M., (2018). Heat Transfer Analysis on MHD Rotating Jeffery fluid flow past a vertical plate filled in porous medium, IAETSD journal for advanced research in applied sciences, 5(5).
22. Sreenadh, S., & Reddappa, B. (2016). Couette flow of a Jeffrey fluid in a rotating channel. Int J Eng Sci Res Technol, 5(5), 218-227.
23. Reddappa, B., Sreenadh, S., & Naidu, K. K. (2015). Convective Couette flow of a Jeffrey fluid in an inclined channel when the walls are provided with porous lining. Adv. Appl. Sci. Res., 6(12), 69-75.
24. Ahmad, K., & Ishak, A. (2017). Magnetohydrodynamic flow and heat transfer of a Jeffrey fluid towards a stretching vertical surface. Thermal Science, 21(1 Part A), 267-277.
25. Ramachandra Prasad, V., Abdul Gaffar, S., Keshava Reddy, E., Anwar Bég, O., & Krishnaiah, S. (2015). A mathematical study for laminar boundary-layer flow, heat, and mass transfer of a Jeffrey non-Newtonian fluid past a vertical porous plate. Heat Transfer-Asian Research, 44(3), 189-210.
26. Nallapu, S., & Radhakrishnamacharya, G. (2014). Jeffrey fluid flow through porous medium in the presence of magnetic field in narrow

tubes. International Journal of Engineering Mathematics, 2014(1), 713831.

27. Shehzad, S. A., Alsaedi, A., & Hayat, T. (2013). Influence of thermophoresis and Joule heating on the radiative flow of Jeffrey fluid with mixed convection. Brazilian Journal of Chemical Engineering, 30, 897-908.

28. Nadeem, S., Zaheer, S., & Fang, T. (2011). Effects of thermal radiation on the boundary layer flow of a Jeffrey fluid over an exponentially stretching surface. Numerical Algorithms, 57(2), 187-205.

Chapter - 10
A Comprehensive Review of Nanofluids and Hybrid Nanofluids: Properties, Applications, and Recent Advances

Author

Dr. Shiva Rao
Department of Mathematics, Bapujee College, Sarthebari, Assam, India

Chapter - 10

A Comprehensive Review of Nanofluids and Hybrid Nanofluids: Properties, Applications, and Recent Advances

Dr. Shiva Rao

Abstract: Nanofluids, which are fluids engineered by suspending nanoparticles within a base fluid, exhibit enhanced thermal properties and have gained significant traction in various engineering applications. Hybrid nanofluids, which combine multiple types of nanoparticles within a base fluid, present additional benefits that extend the capabilities of nanofluid technology. This paper discusses the unique properties of nanofluids, explores the advantages brought by hybrid nanofluids, and examines recent research on their application in cooling systems, heat exchangers, and other thermal management solutions.

1. Introduction

The quest for efficient heat transfer materials has led to the development of nanofluids-suspensions of nanoparticles in conventional fluids-which offer superior thermal conductivity and heat transfer coefficients (Devi & Devi, 2016). Initially introduced by Choi and Eastman in 1995, the field of nanofluids has since evolved, encompassing various types of nanoparticles to improve thermal properties for applications in fields such as electronics, automotive cooling, and thermal energy storage. Hybrid nanofluids, which integrate two or more different nanoparticles into a single base fluid, have emerged as a promising advancement, providing synergistic effects that enhance performance beyond traditional nanofluid capabilities (Takabi & Shokouhmand, 2015).

2. Properties of Nanofluids

2.1 Thermal Conductivity

One of the key advantages of nanofluids is their enhanced thermal conductivity. Multiple studies have established that the addition of nanoparticles can drastically improve the thermal properties of the base fluid. For example, a study by Rashad *et al*. demonstrated that hybrid nanofluids like Cu-Al_2O_3/water exhibited significantly improved thermal conductivity

compared to their monomaterial counterparts (Rashad *et al*., 2018). This enhancement is largely attributed to mechanisms like Brownian motion, particle interaction, and the increased surface area-to-volume ratio of nanoparticles.

2.2 Heat Transfer Characteristics

The thermal performance of nanofluids extends beyond mere thermal conductivity; they also exhibit improved heat transfer coefficients in various flow configurations. For instance, Devi and Devi analyzed the boundary layer flow over a stretching sheet, revealing that the hybrid nanofluid demonstrated superior heat transfer characteristics in comparison to single nanofluids (Devi & Devi, 2016). The study highlighted how factors such as particle size, concentration, and flow conditions interact to affect the convective heat transfer mechanism.

2.3 Rheological Properties

Nanofluids can alter the viscosity of base fluids, which is critical for the understanding of their flow behavior in thermal systems. Higher viscosity can lead to decreased flow rates in certain systems but may also result in enhanced heat transfer due to prolonged contact times between fluid and heat exchange surfaces (Shahsavar *et al.,* 2019). Studies investigating hybrid nanofluids present insights into the complex interplay between thermal performance and rheological properties (Shahsavar *et al*., 2019).

3. Applications of Nanofluids and Hybrid Nanofluids

3.1 Heat Exchangers

Nanofluids and hybrid nanofluids are increasingly used in heat exchangers to enhance thermal efficiency. The inclusion of nanoparticles in fluid mediums allows for the reduction of overall size and weight of heat exchanger systems, leading to more compact designs with improved performance (Chamkha *et al.,* 2017). Several numerical studies have shown a significant increase in Nusselt numbers, indicating enhanced convective heat transfer when hybrid nanofluids are utilized (Tulu & Ibrahim, 2021).

3.2 Solar Collectors

The performance of solar thermal systems has significantly improved with the use of hybrid nanofluids. Studies demonstrate that hybrid nanofluids in flat-plate solar collectors boost thermal efficiency relative to single nanofluids (Wahid *et al.,* 2022). The improved heat-transfer properties also assist in better heat retention and temperature management in solar applications.

3.3 Electronic Cooling

In electronic applications, efficient heat removal is critical for device longevity and performance. Hybrid nanofluids are becoming a preferred option due to their higher thermal conductivities and heat capacity, which are vital in managing elevated temperatures associated with modern electronics (Shahsavar *et al.,* 2019). For instance, comparative studies indicate marked improvements in cooling efficiencies within microchannels when utilizing hybrid nanofluids (Shahsavar *et al.,* 2019).

4. Recent Advances and Numerical Modeling

The understanding of nanofluids has advanced significantly with computational fluid dynamics (CFD) simulations that model their behavior under various conditions. Studies by Takabi and Salehi explored laminar natural convection using hybrid nanofluids in geometries such as sinusoidal corrugated enclosures, providing valuable insights into thermal distribution and fluid dynamics (Takabi & Salehi, 2014). Similarly, Tulu and Ibrahim discussed the effects of variable viscosity and second-order slip flow on natural convection, further highlighting the nuanced behaviors of hybrid nanofluids in real-world applications (Tulu & Ibrahim, 2021).

5. Conclusion

Nanofluids and hybrid nanofluids represent a significant advancement in thermal management fluids, offering improved thermal properties that facilitate their application in critical fields such as heat exchangers and electronic cooling systems. Ongoing research continues to unveil the complexities of their thermophysical properties, rheological behavior, and modeling challenges. The future of hybrid nanofluids, driven by technological advancements and increased understanding of their behavior, holds promise for improved energy efficiency and performance in various thermal applications.

References

1. Ali, A. and Makinde, O. (2015). Modelling the Effect of Variable Viscosity on Unsteady Couette Flow of Nanofluids with Convective Cooling. Journal of Applied Fluid Mechanics, 8(4), 793-802. https://doi.org/10.18869/acadpub.jafm.67.223.22967

2. Basha, H., Sivaraj, R., Animasaun, I., & Makinde, O. (2018). Influence of Non-Uniform Heat Source/Sink on Unsteady Chemically Reacting Nanofluid Flow over a Cone and Plate. Defect and Diffusion Forum, 389, 50-59. https://doi.org/10.4028/www.scientific.net/ddf.389.50

3. Bondareva, N., Sheremet, M., Öztop, H., & Abu-Hamdeh, N. (2018). Transient natural convection in a partially open trapezoidal cavity filled with a water-based nanofluid under the effects of Brownian diffusion and thermophoresis. International Journal of Numerical Methods for Heat & Fluid Flow, 28(3), 606-623. https://doi.org/10.1108/hff-04-2017-0170

4. Buongiorno, J., Venerus, D., Prabhat, N., McKrell, T., Townsend, J., Christianson, R., … & Zhou, S. (2009). A benchmark study on the thermal conductivity of nanofluids. Journal of Applied Physics, 106(9). https://doi.org/10.1063/1.3245330

5. Chamkha, A., Мирошниченко, И., & Sheremet, M. (2017). Numerical Analysis of Unsteady Conjugate Natural Convection of Hybrid Water-Based Nanofluid in a Semicircular Cavity. Journal of Thermal Science and Engineering Applications, 9(4). https://doi.org/10.1115/1.4036203

6. Corcione, M. and Quintino, A. (2022). Double-Diffusive Effects on the Onset of Rayleigh-Benard Convection of Water-Based Nanofluids. Applied Sciences, 12(17), 8485. https://doi.org/10.3390/app12178485

7. Devi, S. and Devi, S. (2016). Numerical investigation of three-dimensional hybrid Cu-Al2O3/water nanofluid flow over a stretching sheet with effecting Lorentz force subject to Newtonian heating. Canadian Journal of Physics, 94(5), 490-496. https://doi.org/10.1139/cjp-2015-0799

8. Kuznetsov, A. and Nield, D. (2009). Thermal Instability in a Porous Medium Layer Saturated by a Nanofluid: Brinkman Model. Transport in Porous Media, 81(3), 409-422. https://doi.org/10.1007/s11242-009-9413-2

9. Makinde, O. and Animasaun, I. (2016). Thermophoresis and Brownian motion effects on MHD bioconvection of nanofluid with nonlinear thermal radiation and quartic chemical reaction past an upper horizontal surface of a paraboloid of revolution. Journal of Molecular Liquids, 221, 733-743. https://doi.org/10.1016/j.molliq.2016.06.047

10. Makinde, O. and Aziz, A. (2011). Boundary layer flow of a nanofluid past a stretching sheet with a convective boundary condition. International Journal of Thermal Sciences, 50(7), 1326-1332. https://doi.org/10.1016/j.ijthermalsci.2011.02.019

11. Mansur, S. and Ishak, A. (2014). The Magnetohydrodynamic Boundary Layer Flow of a Nanofluid past a Stretching/Shrinking Sheet with Slip Boundary Conditions. Journal of Applied Mathematics, 2014, 1-7.

https://doi.org/10.1155/2014/907152

12. Nield, D. and Kuznetsov, A. (2009). The Cheng-Minkowycz problem for natural convective boundary-layer flow in a porous medium saturated by a nanofluid. International Journal of Heat and Mass Transfer, 52(25-26), 5792-5795. https://doi.org/10.1016/j.ijheatmasstransfer.2009.07.024

13. Rashad, A., Chamkha, A., Ismael, M., & Salah, T. (2018). Magnetohydrodynamics Natural Convection in a Triangular Cavity Filled With a Cu-Al2O3/Water Hybrid Nanofluid With Localized Heating From Below and Internal Heat Generation. Asme Journal of Heat and Mass Transfer, 140(7). https://doi.org/10.1115/1.4039213

14. Ruo, A., Yan, W., & Chang, M. (2021). The onset of natural convection in a horizontal nanofluid layer heated from below. Heat Transfer, 50(8), 7764-7783. https://doi.org/10.1002/htj.22252

15. Sabu, A., Ali, F., Reddy, C., Areekara, S., & Mathew, A. (2023). Insight on the dynamics of hydromagnetic stagnation-point flow of magnetite-water nanofluid due to a rotating stretchable disk: A two-phase modified Buongiorno modeling and simulation. Zamm - Journal of Applied Mathematics and Mechanics / Zeitschrift Für Angewandte Mathematik Und Mechanik, 103(8). https://doi.org/10.1002/zamm.202100520

16. Shahsavar, A., Godini, A., Talebizadehsardari, P., Toghraie, D., & Salehipour, H. (2019). Impact of variable fluid properties on forced convection of Fe3O4/CNT/water hybrid nanofluid in a double-pipe mini-channel heat exchanger. Journal of Thermal Analysis and Calorimetry, 137(3), 1031-1043. https://doi.org/10.1007/s10973-018-07997-6

17. Shahsavar, A., Talebizadehsardari, P., & Toghraie, D. (2019). Free convection heat transfer and entropy generation analysis of water-Fe3O4/CNT hybrid nanofluid in a concentric annulus. International Journal of Numerical Methods for Heat & Fluid Flow, 29(3), 915-934. https://doi.org/10.1108/hff-08-2018-0424

18. Srinivasacharya, D. and Barman, D. (2020). Linear stability of convection in a vertical channel filled with nanofluid saturated porous medium. Heat Transfer, 50(4), 3220-3239. https://doi.org/10.1002/htj.22025

19. Takabi, B. and Salehi, S. (2014). Augmentation of the Heat Transfer Performance of a Sinusoidal Corrugated Enclosure by Employing Hybrid Nanofluid. Advances in Mechanical Engineering, 6, 147059. https://doi.org/10.1155/2014/147059

20. Takabi, B. and Shokouhmand, H. (2015). Effects of Al2O3-Cu/water hybrid nanofluid on heat transfer and flow characteristics in turbulent regime. International Journal of Modern Physics C, 26(04), 1550047. https://doi.org/10.1142/s0129183115500473

21. Tulu, A. and Ibrahim, W. (2021). Effects of Second-Order Slip Flow and Variable Viscosity on Natural Convection Flow of CNTs−Fe. Mathematical Problems in Engineering, 2021, 1-18. https://doi.org/10.1155/2021/8407194

22. Wahid, N., Arifin, N., Khashi'ie, N., Pop, I., Bachok, N., & Hafidzuddin, M. (2022). Hybrid Nanofluid Radiative Mixed Convection Stagnation Point Flow Past a Vertical Flat Plate with Dufour and Soret Effects. Mathematics, 10(16), 2966. https://doi.org/10.3390/math10162966

Chapter - 11
Mathematical Modelling of Casson Fluid flow due to an Annular region under the Influence of Energy Transfer

Authors

Nayanmoni Rajkonwar
Department of Mathematics, Tingkhong College,
Dibrugarh, Assam, India

Pritishma Konwar
Department of Mathematics, Tingkhong College,
Dibrugarh, Assam, India

Chapter - 11

Mathematical Modelling of Casson Fluid flow due to an Annular region under the Influence of Energy Transfer

Nayanmoni Rajkonwar and Pritishma Konwar

Abstract

The purpose of this study is to investigate the nature of dual solutions and their stability of the magnetized Casson fluid flow through an annular gap with the effects of heat transfer phenomenon. An uniform magnetic field is applied in the normal direction of the fluid flow. The suitable similarity transformation and the MATLAB routine bvp4c solver scheme are employed to solve the governing equations. The stability analysis is executed to characterize the stable and physically tractable solutions. The outcomes of the non-dimensional factors on velocity, temperature distributions are exhibited graphically. Also, the skin friction coefficient and Nusselt number are scrutinized in tabular form. From the discussion, we have come out that the Casson fluid parameter and the Hartmann number accelerate the velocity of the fluid in different cases of present geometries. The Eckert number is used as temperature enhancing parameter. From the results, we have found that dual solutions exist up to certain region of the similarity variable and the first solution is stable and physically tractable over the second solution.

Index Terms: Dual Solutions, MHD, Casson fluid, Heat transfer, Stability Analysis, Annular region.

Introduction

The significance of the non-Newtonian fluids (non-linear relationship between the shear stress and the rate of deformation) due to their appropriate applications in the engineering sciences, industrial processes, medical sciences etc., are advanced than the Newtonian fluid in the recent times. The Casson fluid is a special kind of non-Newtonian fluid which need an yield stress to express their constitutive equations and it behaves like an elastic solid. This type of fluid flow has multifarious realistic applications such as food processing, bio-engineering operations, fuel cell, fiber technology and nuclear reactors etc. Jelly, Tomato sauce, Honey and human blood etc are

some real life examples of the Casson fluid. Again, the impact of magnetic field on the fluid flow has been widely recognized by engineers and scientists because of the imperative applications such as MHD pump and MHD horizontal multistage pump etc. Fluid motion over stretching/shrinking surfaces with the heat transfer phenomena have many implications in several industrial processes. Also, the fluid flow through this present geometry has occurred in many practical technology-driven applications such as in the assembly of oil and gas, electrochemical cells, fluid viscometers and hydraulic equipment etc.

Crane [1] was the first author who has investigated the nature of fluid flow due to the stretching/shrinking surface. After that, a huge amount of research works of different fluids flow due to this type of geometries are available in different research areas from the several decades. In the recent times, many authors (Tamoor *et al.* [2], Debnath *et al.* [3], Dey and Hazarika [4] and Mahdy and Ahmed [5]) have investigated the impact of MHD on boundary layer flows of different fluids. Nagaraju and Garvandha [6] have inspected the thermally stratified viscous fluid flow with the influence of magnetic field through a circular pipe.

Nomenclature:

β Casson fluid parameter

Pr Prandtl number

α curvature parameter

μ_B plastic dynamic viscosity

(u_0, l) characteristic velocity (m s^{-1}) and length (m)

(r_1, r_2) radii of inner and outer cylinders (m)

ρ density of the fluid (Kg m^{-3})

ψ stream function

$f'(\eta)$ dimensionless velocity

(T_0, T_1) surface temperature of the inner and outer cylinders (K)

$\theta(\eta)$ dimensionless temperature

η similarity variable

τ dimensionless time variable

C_f skin friction coefficient

μ dynamic viscosity (Kg m^{-1} s^{-1})

C_p specific heat at constant pressure (J Kg^{-1} K^{-1})

Ec Eckert number

T temperature of the fluid (K)

σ electrical conductivity
t time (s)
Ha Hartmann number
k thermal conductivity (W m^{-1} K^{-1})
υ kinematic viscosity (m^2 s)
ω unknown eigen value
Re_x local Reynolds number
(u,v) velocity along (x,r) directions (m s^{-1})
Nu_x local Nusselt number
u_w velocity at surface (m s^{-1})
B_0 magnetic field strength (Ns C^{-1} m^{-1})
P_y yield stress

Krishna *et al.* [7] have put their ideas about the influence of chemically stratified MHD flow over stretching sheet. Okedayo *et al.* [8] have examined the MHD flow with the effects of the heat transfer by accounting cylindrical pipe which is filled with porous medium. Eldesoky *et al.* [9] have investigated the effects of magnetic field and thermal transmission of fluid flow by assisting catheterized wavy tube. Recently, Gireesha and Sindhu [10] have investigated the significance of MHD boundary layer flow through annular microchannel with porous medium. Barman *et al.*[11] have examined the fluid flow through the annular gap between the concentric cylinders and offered many practical applications related to this present model. Again, Eldesoky *et al.* [12] have investigated the interface between compressibility and particulate suspension on peristaltically constrained flow due to planner channel. In the recent time, many researchers such as Shafee *et al.* [13], Ahmed *et al.* [14] and Ahmed *et al.* [15] have examined the flow behaviours within a tube and channel walls of different fluids like hybrid nanofluid and micropolar fluid etc. Sadaf and Abdelsalam [16] have investigated the characteristic of hybrid nanofluid with different flow parameters by considering wavy non-unoform annular region.

Due to the lack of information about the smoothness of the surface, length of the geometries, shrinking and moving surfaces, some irregular behaviours of fluid flow are observed which are occurred with the change of time. To control this type of instability of the flow, many researchers have spent their time with this type of problems and got two solutions, one is dependent on time and another one is independent on time. Markin [17] was the first author who has investigated the dual solutions and their stability. After that, many

researchers (Weidmann *et al.*[18], Zaib *et al*. [19], Adnan *et al.*[20] and Ishak *et al.*[21] etc) have investigated the stability analysis on the dual solutions of the Newtonian and non-Newtonian (Casson fluid and nanofluid etc) fluids with heat transfer due to the different surfaces and put their importance of these fluid model in the various scientific fields. In the recent times, Dey and Borah [22,23] have investigated the dual solutions of viscous fluid flow over exponentially shrinking cylinder and their nature of flow. Mishra *et al.*[24] have investigated the hydromagnetic flow and their stability on the dual solutions over stretching/shrinking surface.

This present work is all inspired by the above literatures and its immense relevance in different physical fields. We have studied the MHD Casson fluid flow through an annular gap between the concentric cylinders by assisting the MATLAB routine bvp4c solver scheme. Due to the contracting surfaces of the outer/inner cylinders of this model, the existence of dual solutions and their stability analysis are investigated together with heat transfer phenomena. The results are discussed pictorially and the stable/unstable flow are analysed by using the concept of the normal mode method. Based on our knowledge, we have confirmed that the dual (steady and unsteady) solutions and their stability analysis of this fluid model through the annular region of the concentric cylinders is not established till now. From the literature review, we have seen that lots of studies have focused on various aspects of the topic or subject area, none of them deal with this particular research idea. So, we are unable to make comparison our work with existing literatures.

Mathematical Formulation:

We have considered the hydromagnetic two-dimensional steady and incompressible Casson fluid flow with heat transfer through an annulus. During the entrance part of the annular region, the flow is behaving like a boundary layer flow until it reaches to fully developed flow (where flow properties are independent of the direction of x). So, we mainly concentrate on the boundary layer region. The geometry of this present problem is shown in Fig.1. Here, we have considered the following three cases:

i) The inner cylinder of radius r_1 of this annulus characterized with the shrinking velocity $u_w = \frac{u_0 x}{l}$ such that the constant $u_0 < 0$ signifies shrink at the surface of the inner cylinder and T_0 the prescribed temperature at the surface,

ii) The outer cylinder of radius r_2 characterised with the shrinking velocity $u_w = \frac{u_0 x}{l}$ with T_1 the surface temperature of the outer cylinder

iii) Both the cylinder are shrank at the respective surface.

The relationship of their radii and wall temperatures are given by $r_2 > r_1 \,\&\, T_0 > T_1$. An uniform magnetic field B_0 is applied in the transverse direction of the flow.

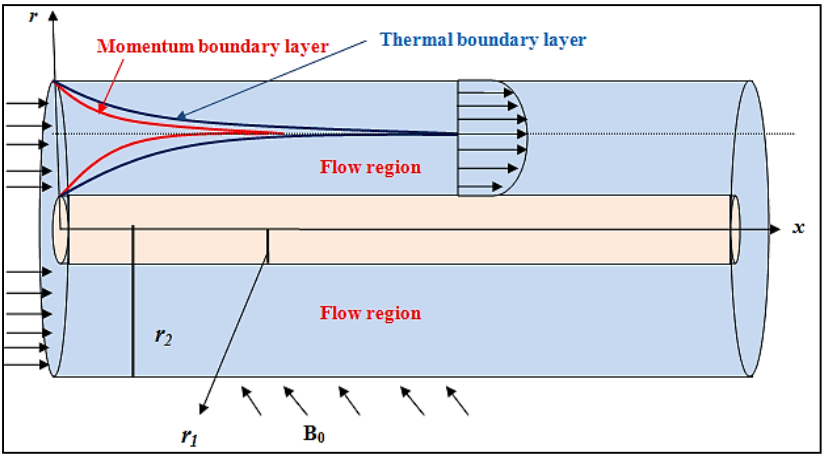

Fig 1: Flow Diagram

Following the theory of boundary layer approximations, the governing equations of this present problem are:

$$\frac{\partial (ru)}{\partial x} + \frac{\partial (rv)}{\partial r} = 0, \tag{1}$$

$$u\frac{\partial u}{\partial x} + v\frac{\partial u}{\partial r} = \upsilon\left(1+\frac{1}{\beta}\right)\left(\frac{\partial^2 u}{\partial r^2} + \frac{1}{r}\frac{\partial u}{\partial r}\right) - \frac{\sigma {B_0}^2}{\rho}u, \tag{2}$$

$$u\frac{\partial T}{\partial x} + v\frac{\partial T}{\partial r} = \frac{k}{\rho C_p}\left(\frac{\partial^2 T}{\partial r^2} + \frac{1}{r}\frac{\partial T}{\partial r}\right) + \frac{\mu_\beta}{\rho C_p}(1+\frac{1}{\beta})\left(\frac{\partial u}{\partial r}\right)^2 + \frac{\sigma {B_0}^2}{\rho C_p}u^2, \tag{3}$$

where, $u \,\&\, v$ are the velocity components along the flow direction and radial direction respectively. $\beta = \frac{\mu_\beta \sqrt{2\pi_c}}{P_y}$ is responsible for the Casson fluid

such that its value $\beta \to \infty$ represent the Newtonian fluid. $\upsilon, \rho, \sigma, C_p, k \& T$ are the kinetic viscosity, density of the fluid, electrical conductivity, specific heat at constant pressure, thermal conductivity and temperature of the fluid respectively.

The significant boundary conditions for the above cases are:

1) For the case of shrinking inner cylinder

$$\begin{aligned} &r = r_1 : u = u_w = -\frac{u_0 x}{l}, v = 0, T = T_0; \\ &r = r_2 : u = 0, T = T_1. \end{aligned} \tag{4}$$

2) For the case of shrinking outer cylinder

$$\begin{aligned} &r = r_1 : u = 0, v = 0, T = T_0; \\ &r = r_2 : u = u_w = -\frac{u_0 x}{l}, T = T_1. \end{aligned} \tag{5}$$

3) Both the cylinders are shrinking

$$\begin{aligned} &r = r_1 : u = u_w = -\frac{u_0 x}{l}, v = 0, T = T_0; \\ &r = r_2 : u = u_w = -\frac{u_0 x}{l}, T = T_1. \end{aligned} \tag{6}$$

The following similarity transformations [which must satisfy the continuity equation (1)] are adopted to alter the related non-linear governing equations into a new set of solvable systems.

$$\eta = \sqrt{\frac{u_0}{\upsilon l}}\left(\frac{r^2 - r_1^2}{2r_1}\right), \psi = \sqrt{\frac{\upsilon u_0}{l}} r_1 x f(\eta), \theta(\eta) = \frac{T - T_1}{T_0 - T_1}. \tag{7}$$

Implementing the equation (7) into the equations [(2) & (3)], we have achieved the following set of equations:

$$\left(1 + \frac{1}{\beta}\right)\left[(1 + 2\alpha\eta) f''' + 2\alpha f''\right] + f f'' - f'^2 - Ha^2 f' = 0, \tag{8}$$

$$(1 + 2\alpha\eta)\theta'' + 2\alpha\theta' + \Pr f\theta' + \Pr Ec(1 + 2\alpha\eta)\left[1 + \frac{1}{\beta}\right] f''^2 + \Pr EcHa^2 f'^2 = 0. \tag{9}$$

The relevant boundary conditions become:

$$\eta = 0 : f(\eta) = 0,\ f'(\eta) = -1, \theta(\eta) = 1;\quad \eta = m : f'(\eta) = 0, \theta(\eta) = 0. \tag{10}$$

$$\eta = 0 : f(\eta) = 0,\ f'(\eta) = 0, \theta(\eta) = 1;\quad \eta = m : f'(\eta) = -1, \theta(\eta) = 0. \tag{11}$$

$$\eta = 0 : f(\eta) = 0,\ f'(\eta) = -1, \theta(\eta) = 1;\quad \eta = m : f'(\eta) = -1, \theta(\eta) = 0. \tag{12}$$

The boundary conditions [(10)-(12)] represent all the considering cases of this problem. $\alpha = \sqrt{\frac{\upsilon l}{u_0 r_1^2}} = \sqrt{\frac{\upsilon l}{u_0 r_2^2}}, Ha^2 = \frac{\sigma B_0^2 l}{\rho u_0}, \Pr = \frac{\mu C_P}{k}$ & $Ec = \frac{u_w^2}{C_P T_\infty}$ are the curvature of the cylinders, the Hartmann number, the Prandtl number and the Eckert number respectively.

The following physical quantities of interest observed in this problem are skin friction coefficient and the Nusselt number that are very important in different physical fields like engineering sciences and geo-physics etc. The quantities are defined as the following way:

$$C_f = \frac{2\mu\left(1+\frac{1}{\beta}\right)}{\rho u_w^2}\left(\frac{\partial u}{\partial r}\right)_{r=R} \text{ \& } Nu_x = -\frac{Kx}{K(T-T_\infty)}\left(\frac{\partial T}{\partial r}\right)_{r=R}. \tag{13}$$

Using the similarity transformation (7) in (13), we have got the following expression for these quantities:

$$\frac{1}{2} C_f \,\mathrm{Re}_x^{\frac{1}{2}} = \left(1+\frac{1}{\beta}\right) f''(0) \text{ \& } Nu_x \,\mathrm{Re}_x^{-\frac{1}{2}} = -\alpha\left(1+\frac{1}{\beta}\right)\theta'(0), \tag{14}$$

where, $\mathrm{Re}_x = \frac{U_0 x^2}{\upsilon l}$ is the local Reynolds number.

Flow Stability

The flow stability is carried out to distinguish the stable and physically achievable solution. Many researchers (Markin [17] and Weidmann *et al.*[18] etc) have examined the flow stability and put their conclusions that the upper branch (first) solution is stable and physically realizable. To differentiate flow stability of this fluid model, the unsteady form of equations (2) and (3) are

considered by adding $\frac{\partial u}{\partial t}$ & $\frac{\partial T}{\partial t}$ in equations (2) and (3) respectively. The following similarity transformations are utilized to revolutionize the unsteady governing equations into a set of solvable system.

$$\eta = \sqrt{\frac{u_0}{\upsilon l}}\left(\frac{r^2 - r_1^2}{2r_1}\right), \psi = \sqrt{\frac{\upsilon u_0}{l}} r_1 x f(\eta,\tau), \theta(\eta,\tau) = \frac{T - T_1}{T_0 - T_1}, \tau = \frac{u_0 t}{l}. \quad (15)$$

Substituting equation (15) into the time dependent flow governing equations, the we have got the subsequent set of equations.

$$\left(1+\frac{1}{\beta}\right)\left[(1+2\alpha\eta)\frac{\partial^3 f}{\partial \eta^3} + 2\alpha\frac{\partial^2 f}{\partial \eta^2}\right] + f(\eta,\tau)\frac{\partial^2 f}{\partial \eta^2} - \left(\frac{\partial f}{\partial \eta}\right)^2 - Ha^2\frac{\partial f}{\partial \eta} - \frac{\partial^2 f}{\partial \eta \partial \tau} = 0, \quad (16)$$

$$(1+2\alpha\eta)\frac{\partial^2 \theta}{\partial \eta^2} + 2\alpha\frac{\partial \theta}{\partial \eta} + \Pr f(\eta,\tau)\frac{\partial \theta}{\partial \eta} + \Pr Ec(1+2\alpha\eta)\left[1+\frac{1}{\beta}\right]\left(\frac{\partial^2 f}{\partial \eta^2}\right)^2 + \Pr EcHa^2\left(\frac{\partial f}{\partial \eta}\right)^2 - \Pr\frac{\partial \theta}{\partial \tau} = 0.$$

(17)

The associated boundary conditions for this problem are:

$$\begin{aligned} &\eta = 0: f(\eta,\tau) = 0, \frac{\partial f}{\partial \tau}(\eta,\tau) = -1, \theta(\eta,\tau) = 1; \\ &\eta = m: \frac{\partial f}{\partial \tau}(\eta,\tau) = 0, \theta(\eta,\tau) = 0. \end{aligned} \quad (18)$$

$$\begin{aligned} &\eta = 0: f(\eta,\tau) = 0, \frac{\partial f}{\partial \tau}(\eta,\tau) = 0, \theta(\eta,\tau) = 1; \\ &\eta = m: \frac{\partial f}{\partial \tau}(\eta,\tau) = -1, \theta(\eta,\tau) = 0. \end{aligned} \quad (19)$$

$$\begin{aligned} &\eta = 0: f(\eta,\tau) = 0, \frac{\partial f}{\partial \tau}(\eta,\tau) = -1, \theta(\eta,\tau) = 1; \\ &\eta = m: \frac{\partial f}{\partial \tau}(\eta,\tau) = -1, \theta(\eta,\tau) = 0. \end{aligned} \quad (20)$$

For the check of flow stability, the following perturb equations which are taken from Normal Mode Method are considered:

$$\begin{aligned} f(\eta,\tau) &= f_0(\eta) + e^{-\omega\tau}F(\eta,\tau), \\ \theta(\eta,\tau) &= \theta_0(\eta) + e^{-\omega\tau}G(\eta,\tau). \end{aligned} \quad (21)$$

where, ω is the unknown eigen value parameter. $f_0(\eta)$ & $\theta_0(\eta)$ are steady

flow solutions and $F(\eta,\tau)\&G(\eta,\tau)$ small relative to the steady flow solutions which are determined by setting $\tau=0$ i.e., the small related solutions taken in the forms $F_0(\eta)\&G_0(\eta).$ Hence $F(\eta,\tau)=F_0(\eta)\&G(\eta,\tau)=G_0(\eta)$ in equations (16) and (17) reflects the initial decay or growth of the solution of equation (21). In this respect, we have to solve the following linearized eigen value problems which are obtained by Substituting (21) into equations (16) and (17) and used the case $\tau=0.$

$$\left(1+\frac{1}{\beta}\right)\left[(1+2\alpha\eta)F_0'''+2\alpha F_0''\right]+\left(f_0F_0''+F_0f_0''\right)-2f_0'F_0'-Ha^2F_0'+\omega F_0'=0, \tag{22}$$

$$(1+2\alpha\eta)G_0''+2\alpha G_0'+\Pr\left(f_0G_0'+F_0\theta_0'\right)+2\Pr EC(1+2\alpha\eta)\left[1+\frac{1}{\beta}\right]f_0''F_0''+2\Pr EcHa^2f_0'F_0'-\Pr\omega G_0=0. \tag{23}$$

The boundary conditions became:

$$\begin{aligned}&\eta=0: F_0(\eta)=0, F_0'(\eta)=0, G_0(\eta)=0;\\ &\eta=m: F_0'(\eta)=0, G_0(\eta)=0.\end{aligned} \tag{24}$$

This eigen-value problem gives an infinite set of eigen-values $\omega_1<\omega_2<...,.$ The stability of the steady flow solution is based on the least eigen value $\omega_1.$ If the least eigen- value $\omega_1<0$ then an initial escalation of complexity on the flow is observed and the flow becomes unstable in nature. On the other hand, the positive smallest eigen-value recognizes an initial lie down of disturbances on the flow and it provides stable and achievable flow solution. Following Harish *et al.* [25] and Junoh *et al.* [26], the boundary condition $F_0(0)=0$ is reduced to $F_0''(0)=1$ for calculating the eigen-values $(\omega).$

Methodology

Following Sastry [27] and Dey and Chutia [28], the "MATLAB routine bvp4c solver technique" is executed to solve the equations [(8), (9), (22) and (23)] with the relevant boundary conditions for all the cases of this present investigation. It gives the solutions by taking finite difference codes. It needs three basic functions such as (i) initial guess solutions, (ii) system of first order equations and (iii) boundary conditions of the problems. Here, we have introduced the following new variables which switch the resultant equations into its system of first order equations:

$$f=y_1, f'=y_2, f''=y_3, \theta=y_4, \theta'=y_5; F_0=y_6, F_0'=y_7, F_0''=y_8, G_0=y_9, G_0'=y_{10}$$

Then we have achieved the following new system:

$$y_1' = y_2, y_2' = y_3, y_3' = \left(\frac{({y_2}^2 + Ha^2 y_2 - y_1 y_2)}{\left(1+\frac{1}{\beta}\right)(1+2\alpha\eta)} - \frac{2\alpha y_3}{(1+2\alpha\eta)} \right); y_4' = y_5,$$

$$y_5' = \frac{-2\alpha y_5 - \Pr y_1 y_5 - \Pr Ec(1+2\alpha\eta)(1+1/\beta){y_3}^2 - \Pr EcHa{y_2}^2}{(1+2\alpha\eta)}$$

$$y_6' = y_7, y_7' = y_8, y_8' = \frac{2y_2 y_7 + Ha^2 y_7 - \omega y_7 - y_1 y_8 - y_6 y_3}{\left(1+\frac{1}{\beta}\right)(1+2\alpha\eta)} - \frac{2\alpha y_8}{(1+2\alpha\eta)};$$

$$y_9' = y_{10}, y_{10}' = \frac{\Pr \omega y_9 - 2\Pr EcHa y_1 y_7 - 2y_3 y_8 \Pr Ec(1+2\alpha\eta)\left(1+\frac{1}{\beta}\right) - \Pr(y_1 y_{10} + y_6 y_5) - 2\alpha y_{10}}{(1+2\alpha\eta)}$$

and the boundary conditions for all the cases are attached into their format.

Discussion of the Results

In this study, we have focused on the existence of dual solutions during fluid flow through the annular gap (in the boundary layer region formed in the entrance region) of the concentric cylinders and these exist up to a certain region of dimensionless similarity variable η. The flow behaviour and the heat transfer phenomena of the Casson fluid motion are discussed graphically for the different flow parameters. Here, the solid lines represent the first solutions, independent of time and the dash lines denote the second solutions, dependent on time. The flow over the shrinking surface helps to form dual solutions. We have discussed the results of this problem in the following cases:

Case-I: When the outer cylinder is stationary with the shrinking inner cylinder of the concentric cylinders

The impact of the Casson fluid parameter (β) on the fluid motion is shown in Fig. 2. The increasing values of β reduce the viscous force of the fluid which helps to enhance the speed of the fluid during time-independent solution. But, an opposite nature is observed during time dependent solution. Physically, it can be interpreted that at a particular instant of time, the Casson fluid parameter accelerate the fluid motion but with the variation of time, fluid motion experiences retardation with the enhancement of Casson fluid parameter. Also, the temperature of the fluid is reducing with improving values of β [see Fig. 3] during steady case. But, it has the ability to enhance

the temperature of the fluid during time dependent case. The curvature parameter helps to accelerate the fluid motion in both the cases (figure 4). From Fig. 5, it is perceived that the curvature parameter helps to reduce the temperature of the fluid motion in both the cases. It is also perceived that the thickness of the thermal boundary layer of the first solution is thicker as compared to the second solution. Physically it can be interpreted that the fluid flow in 2nd case reaches its thermal equilibrium stage sooner than first case. Impacts of Hartmann number (Ha) on velocity and temperature profiles are depicted by Fig. 6 and Fig. 7. Speed of fluid motion diminishes with Ha. The reason behind this phenomenon is that developing values of Ha enhances the resistance of the fluid over the surface and hence the velocity of the fluid enhances. From Fig. 7, it is observed that the Hartmann number (Ha) helps to cool down the fluid motion during both time dependent and independent cases. Thus, the Hartmann number plays an important role to control the thermal transmission of the fluid between the annular region of the cylinders. But, the Eckert number plays a role to enhance the temperature of the fluid during both time-dependent (second solution) and time-independent (first solution) cases [see Fig. 8]. The Eckert number (Ec) is the relation between flow kinetic energy and thermal enthalpy. The kinetic energy enhances for developing values of Ec. Again, it is well known fact that temperature is defined as average kinetic energy, so increasing values of Ec helps to make system warm.

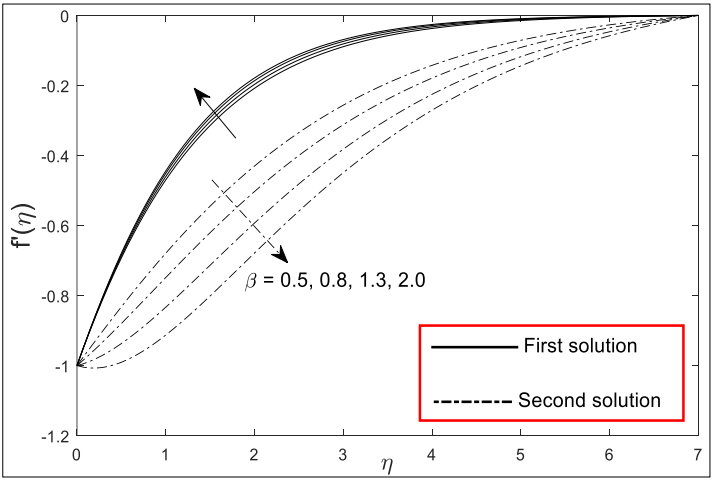

Fig. 2 Velocity distribution for incremental values of Casson fluid parameter (β) when $\Pr = 0.71, \alpha = 1, Ha = 0.5, Ec = 0.01$ and inner cylinder is shrinking.

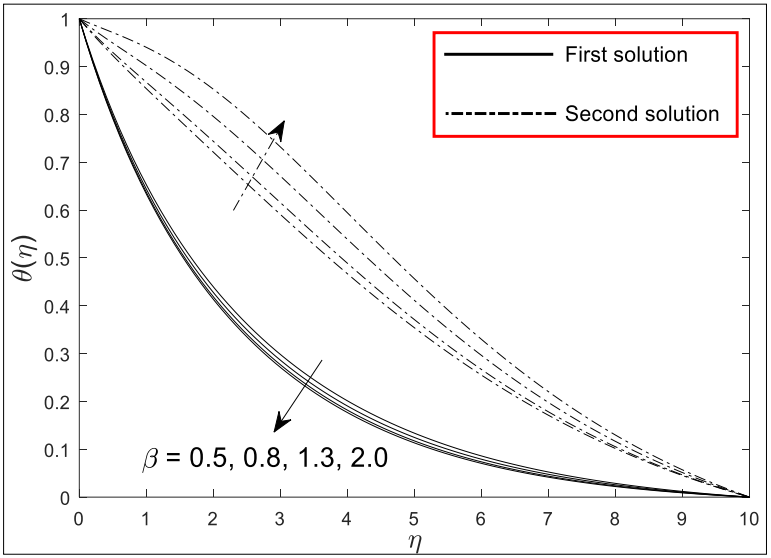

Fig. 3 Temperature distribution for incremental values of Casson fluid parameter (β) when $\Pr = 1.7, \alpha = 1, Ha = 0.4, Ec = 0.01$ and inner cylinder is shrinking.

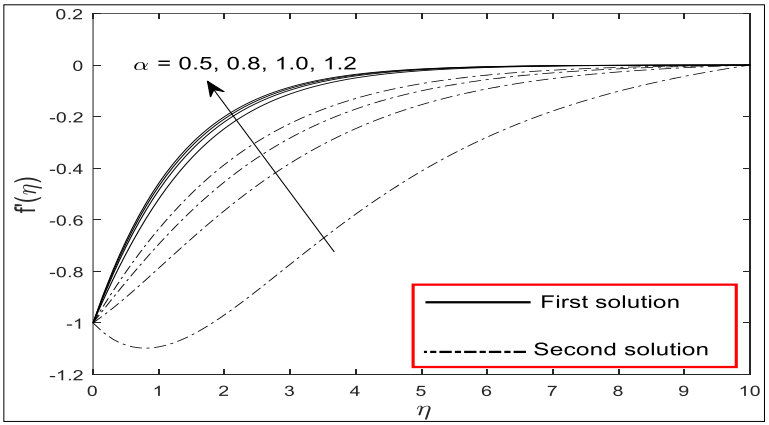

Fig. 4 Velocity distribution for incremental values of curvature parameter (α) when $\Pr = 0.71, Ha = 0.4, \beta = 1, Ec = 0.01$ and inner cylinder is shrinking.

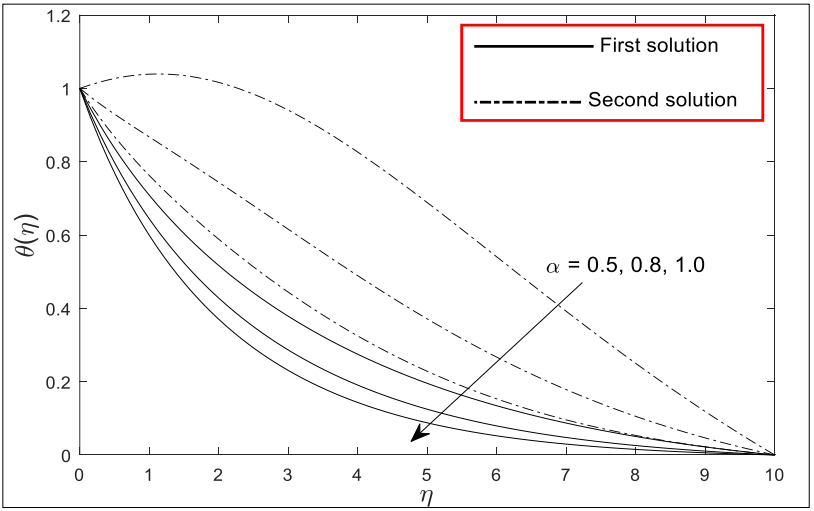

Fig. 5 Temperature distribution for incremental values of curvature parameter (α) when $\Pr = 0.71, \beta = 1, Ec = 0.01, Ha = 0.5$ and inner cylinder is shrinking.

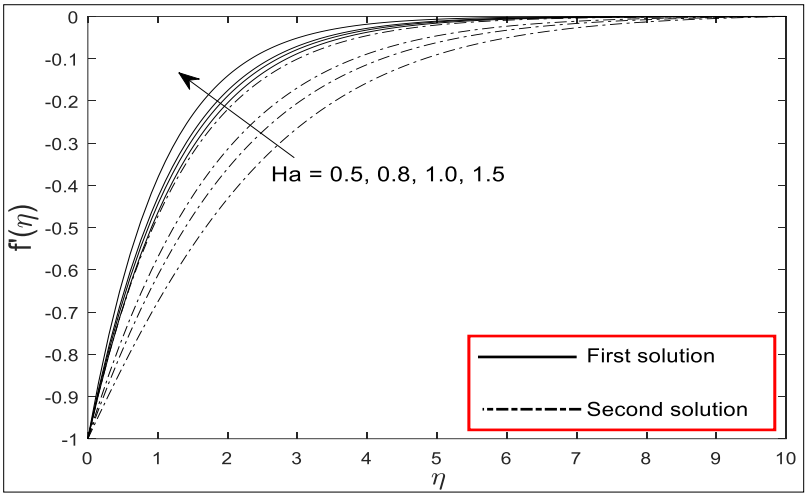

Fig. 6 Velocity distribution for incremental values of Hartmann number (Ha) when $\Pr = 0.71, \alpha = 1, \beta = 0.5, Ec = 0.01$ and inner cylinder is shrinking.

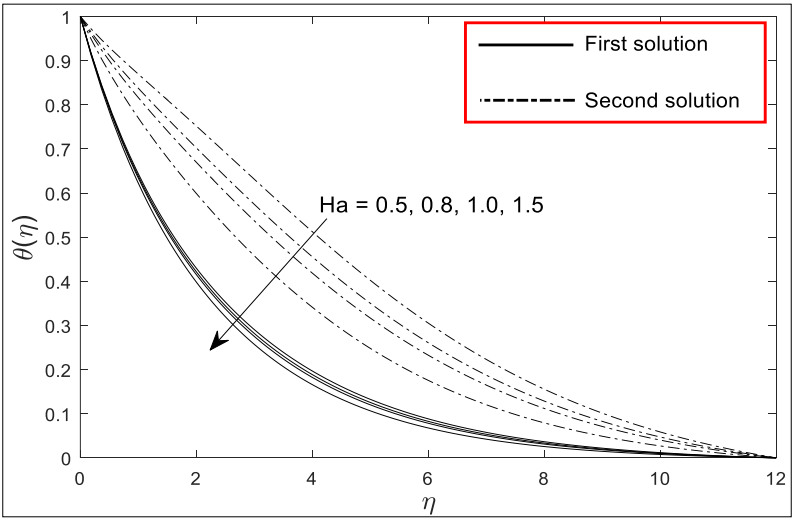

Fig. 7 Temperature distribution for incremental values of Hartmann number (Ha) when $\Pr = 1.7, \alpha = 1, \beta = 0.4, Ec = 0.01$ and inner cylinder is shrinking.

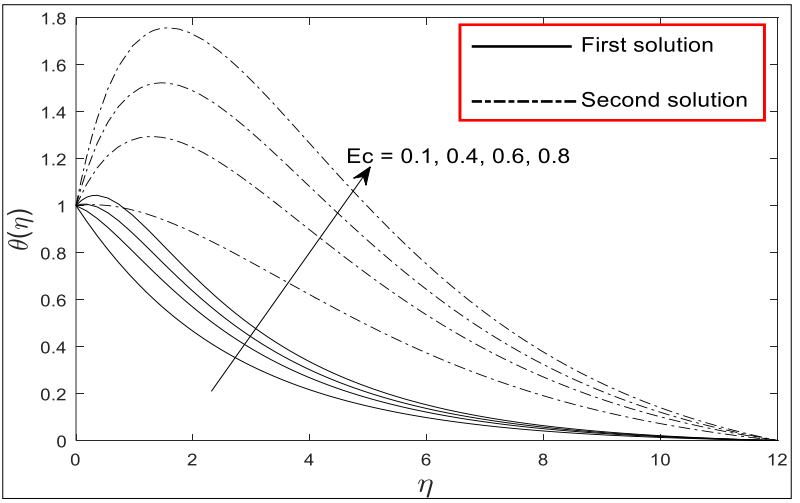

Fig 8: Temperature distribution for incremental values of the Eckert number (Ec) when $\Pr = 1.7, \alpha = 1, \beta = 0.4, Ha = 0.4$ and inner cylinder is shrinking.

All the figures in the above cases visualize the dual solutions of this problem and assure the boundary conditions asymptotically. Again, it is observed that the first solutions appear near the surface of the annular gap and hence it can be achievable practically than the second solutions. The stable and unstable flow solutions are observed in this flow model. To characterise

the instability of the dual solutions, a table of smallest eigen values for various values of β is included for the three cases. If the smallest eigen values are happened to be positive then an initial decay of disturbances on the flow is observed and hence the flow become stable. Again, if the least eigen value is found to be negative then the flow will be unstable because it intensifies the initial disturbances on the flow. From the table-1, it is seen that the smallest eigen values for the first solutions are positive for all the cases and hence the first solutions are stable. But, in case of second solution for all the cases, the smallest eigen values are negative and hence an unstable flow is observed during time-dependent case.

Table 1: Numerical values smallest eigen-value (ω) for various values of Casson fluid parameter when $\Pr = 1.2, Ha = 0.2, \alpha = 1.6, Ec = 0.3$.

	β	Eigen-Value (ω)	
		First Solution	**Second Solution**
First Case (inner cylinder is shrank)	1.0	0.8808	-0.4104
	1.2	0.8731	-0.4132
	1.4	0.8676	-0.4155

The physical quantities of interest such as shear stress and rate of heat transfer at the surface are tabulated numerically in Table-2 and Table-3 for all three cases. From the Table-2, it is noticed that the skin friction coefficient of the first solution for the first case enhances but in case of time-dependent solution, it experiences reduction for different values of the Casson fluid parameter. On the other hand, both the solutions of the skin friction coefficient enhance in all the cases for incremental values of β.

Table 2: Numerical values of skin friction coefficient for various values of the Casson fluid (β) and curvature (α) parameters when $\Pr = 0.71, Ec = 0.01, Ha = 0.5.$

β	α	**Case-I**	
		Skin friction coefficient	
		First solution	Second solution
0.5	1.0	0.7182	0.3524
0.8		0.7285	0.2350
1.0		0.7330	0.1736
1.0	0.5	0.5976	-0.1599
	0.8	0.6796	0.2161
	1.0	0.7182	0.3524

Table 3: Numerical values of Nusselt number for various values of the Casson fluid (β) and curvature (α) parameters when $\Pr = 0.71, Ec = 0.01, Ha = 0.5.$

β	α	Case-I	
		Nusselt number	
		First solution	Second solution
0.5	1.0	0.4766	0.1700
0.8		0.4812	0.1520
1.0		0.4833	0.1420
1.0	0.5	0.1619	-0.5790
	0.8	0.3782	-0.0583
	1.0	0.4766	-0.1700

Conclusions

The overall conclusions of this investigation are highlighted in the following points:

a) From the stability analysis, it is observed that the dual solutions are occurred up to a certain region of the flow direction and the first solutions is stable in manner and physically attainable.

b) All the flow parameters for the first case facilitate to enhance the motion of the fluid, but the Casson fluid parameter controls the speed of the fluid during the time dependent situation. In the case of temperature field of the fluid, all the parameters control the temperature of the fluid, but the Casson fluid parameter has an opposite influence on the time dependent temperature field of the fluid.

c) For the second case, the Casson fluid and curvature parameters have the tendency to speed up the fluid, but the curvature parameter plays an important rule because it helps to manage the motion of the fluid.

d) The same flow characteristics are seen for the different flow parameters in the third case with the second case.

e) Enhancing values of the Eckert number rise the temperature of the fluid during all the cases.

Reference

1. L.J. Crane, Flow past a stretching plate, Zeitschrift für Angew. Math. und Phys. ZAMP 21(4): 645-7(1970).

2. M. Tamoor, M. Waqas, M.I. Khan, A. Alsaedi, T. Hayat, Magnetohydrodynamic flow of Casson fluid over a stretching cylinder, Results Phys 7: 498-502 (2017).

3. K. Debnath, D. Dey, R. Borah, Thermophoresis and Diffusion Thermo Effects on Shear Thickenning and Shear Thining Cases of Fluid Motion Past a Permeable Surface, J. Mech. Cont. & Mat. Sci 5: 68-81(2020).

4. D. Dey, M. Hazarika, Entropy Generation of Hydro-Magnetic Stagnation Point Flow of Micropolar Fluid With Energy Transfer Under the Effect of Uniform Suction / Injection, Lat. Am. Appl. Res 50(3): 209-14 (2020).

5. A. Mahdy, S.E. Ahmed, Unsteady MHD Convective Flow of Non-Newtonian Casson Fluid in the Stagnation Region of an Impulsively Rotating Sphere, J. Aerosp. Eng 30(5): 04017036 (2017).

6. G. Nagaraju, M. Garvandha, Magnetohydrodynamic viscous fluid flow and heat transfer in a circular pipe under an externally applied constant suction, Heliyon 5(2): 01281 (2019).

7. Y.H. Krishna, G.V.R Reddy, O.D. Makinde, Chemical reaction effect on MHD flow of casson fluid with porous stretching sheet, Defect Diffus. Forum 389: 100-9 (2018).

8. T.G. Okedayo, E. Enenche, B.I. Obi, A Computational Analysis Of Magneto-Hydrodynamic (MHD) Flow And Heat Transfer In A Cylindrical Pipe Filled With Porous Media 4(7): 89-96 (2017).

9. I.M. Eldesoky, S.I. Abdelsalam, W.A. El-Askary, A.M. El-Refaey, M.M. Ahmed, Joint Effect of Magnetic Field and Heat Transfer on Particulate Fluid Suspension in a Catheterized Wavy Tube. Bionanoscience 9(3): 723-39 (2019). https://doi.org/10.1007/s12668-019-00651-x

10. B.J. Gireesha, S. Sindhu, MHD natural convection flow of Casson fluid in an annular microchannel containing porous medium with heat generation/absorption, Nonlinear Eng 9(1): 223-32 (2020).

11. K, Barman, S. Mothupally, A. Sonejee, P.L. Mills, Fluid Motion Between Rotating Concentric Cylinders Using COMSOL, Multiphysics ™ 2-8 (2015).

12. I.M. Eldesoky, S.I. Abdelsalam, R.M. Abumandour, M.H. Kamel, K. Vafai, Interaction between compressibility and particulate suspension on peristaltically driven flow in planar channel, Appl. Math. Mech 38(1):137-54 (2017). DOI: 10.1007/s10483-017-2156-6

13. A. Shafee, M. Sheikholeslami, M. Jafaryar, H. Babazadeh, Hybrid nanoparticle swirl flow due to presence of turbulator within a tube, J. Therm. Anal. Calorim no. 0123456789 (2020). https://doi.org/10.1007/s10973-020-09570-6

14. S.E. Ahmed, A.K. Hussein, H.A. Mohammed, S. Sivasankaran, Boundary layer flow and heat transfer due to permeable stretching tube in the presence of heat source/sink utilizing nanofluids, Appl. Math. Comput 238: 149-62 (2014). http://dx.doi.org/10.1016/j.amc.2014.03.106

15. S. Ahmad, M. Ashraf, K. Ali, Simulation of thermal radiation in a micropolar fluid flow through a porous medium between channel walls, J. Therm. Anal. Calorim no. 0123456789 (2020). https://doi.org/10.1007/s10973-020-09542-w

16. H. Sadaf, S.I. Abdelsalam, Adverse effects of a hybrid nanofluid in a wavy non-uniform annulus with convective boundary conditions.RSC Adv 10(26): 15035-43 (2020). DOI: 10.1039/d0ra01134g

17. J.H. Merkin, On dual solutions occurring in mixed convection in a porous medium. J. Eng. Math 20(1): 171-9 (1986).

18. P.D. Weidmann, A.I.IS. Awaludin, Stability Analysis of Stagnation-Point Flow over a Stretching/Shrinking Sheet, in AIP ADVANCES 045308 (2016).

19. A. Zaib, K. Bhattacharyya, M.S. Uddin, S. Shafie, Dual Solutions of Non-Newtonian Casson Fluid Flow and Heat Transfer over an Exponentially Permeable Shrinking Sheet with Viscous Dissipation, Model. Simul. Eng. (2016). DOI:10.1155/2016/6968371

20. N.S.M. Adnan, N.M. Arifin, N. Bachok, F.M. Ali, Stability analysis of MHD flow and heat transfer passing a permeable exponentially shrinking sheet with partial slip and thermal radiation, CFD Lett 11 (12): 34-42 (2019).

21. A. Ishak, Dual solutions in mixed convection boundary layer flow : A stability analysis, Int. J. Math. , Comput. Phys. Quantum Eng 8(9): 1131-4 (2014).

22. D. Dey, R. Borah, Dual Solutions of Boundary Layer Flow with Heat and Mass Transfers over an Exponentially Shrinking Cylinder: Stability Analysis, Lat. Am. Appl. Res 50(4): 247-53 (2020).

23. D. Dey, R. Borah, Stability Analysis on Dual Solutions of Second- grade Fluid flow with Heat and Mass Transfers over a Stretching sheet, Int. J.

Thermofluid Sci. Technol 8(2): no. 080203 (2021) .https://doi.org/10.36963/IJTST.2021080203

24. G.S. Mishra, M.R. Hussain, O.D. Makinde, S.M. Seth, Stability analysis and dual multiple solutions of a hydromagnetic dissipative flow over a stretching / shrinking sheet. Bulg. Chem. Commun 52(2): 259-71 (2020).
25. S.D. Harris, ID.B. ngham, I. Pop, Mixed convection boundary-layer flow near the stagnation point on a vertical surface in a porous medium: Brinkman model with slip, Transp. Porous Media, 77(2): 267-85 (2009).
26. M.M. Junoh, F.M. Ali, N.M. Arifin, N. Bachok, A Stability Analysis of Stagnation-Point Flow of Heat and Mass Transfer over a Shrinking Sheet with Radiation and Slip Effects, Int. J. of Adv. in Sci., Eng. and Technol 6(1):28-32 (2018).
27. D.R.V.S.R.K. Sastry, Melting and radiation effects on mixed convection boundary layer viscous flow over a vertical plate in presence of homogeneous higher order chemical reaction, *Front. Heat Mass Transf* 11(3) (2018). DOI: 10.5098/hmt.11.3
28. D. Dey, B. Chutia, Dusty nanofluid flow with bioconvection past a vertical stretching surface. J. King Saud Univ. - Eng. Sci. (2020). DOI:10.1016/j.jksues.2020.11.001

Chapter - 12
q- Bessel Operator On $[0,\infty)$ and Continuous Wavelet Transforms

Authors

Bhadra Devi Cheleng
Department of Mathematics, Tingkhong College,
Dibrugarh, Assam, India

Rajiv Singh
Department of Mathematics, Tingkhong College,
Dibrugarh, Assam, India

Dipankar Borah
Department of Mathematics, Tingkhong College,
Dibrugarh, Assam, India

Ariyan Dhadumia
Department of Mathematics, Tingkhong College,
Dibrugarh, Assam, India

Chapter - 12

q- Bessel Operator On $[0,\infty)$ And Continuous Wavelet Transforms

Bhadra Devi Cheleng, Rajiv Singh, Dipankar Borah and Ariyan Dhadumia

Abstract

In this paper, we investigate a differential operator defined on the half-line and study harmonic analysis tools associated with this operator. Using these tools, we introduce and analyze the definitions and properties of the continuous wavelet transform related to the q-Bessel operator. Furthermore, we examine the generalized q-Bessel Fourier transform and establish the associated convolution product on the half-line.

Keywords: Generalized wavelets, q-Bessel Fourier transform, generalized continuous wavelet transform, q-Bessel operator.

Introduction

Wavelet theory is based on a family of functions generated from a single function, known as the *mother wavelet*, through translation and dilation operators. This construction leads naturally to the definition of the continuous wavelet transform, which has found wide applications in harmonic analysis and differential equations.

In this work, we introduce and study a q-Bessel operator (see [1, 2]) and develop a corresponding wavelet framework. The q-Bessel operator is associated with the normalized q-Bessel function through a specific eigenvalue problem.

Unlike elementary functions such as trigonometric or exponential functions, Bessel wavelets are closely connected to special functions. The concept of q-analysis was first introduced by Jackson in the early twentieth century and has since played an important role in various branches of mathematical analysis.

The paper is organized as follows. In Section 2, we briefly review the fundamentals of the q-Bessel Fourier transform, including essential definitions, notation, and basic properties of the translation operator and

convolution product. Section 3 is devoted to harmonic analysis associated with the generalized q-Bessel operator, where we define the generalized q-Bessel transform and study its main properties along with the corresponding convolution structure.

Background and Preliminaries

Here we state some facts about q-Bessel operator with respect to harmonic analysis.

Define the space $L_{q,p,\nu}$, here p is finite and greater than or equal to one, is the sets of all real functions on $\mathbb{R}_q^+$ such that

$$\|f_1\|_{q,p,\nu} = \left[\int_0^\infty |f_1(y)|^p \, x^{2|\nu|+1} d_q y\right]^{\frac{1}{p}} < \infty$$

$$\|f_1\|_{q,\infty} = \sup_{y \in \mathbb{R}_q^+} |f_1(y)| < \infty.$$

And $\mathbb{R}_q^+ = \{q^n : n \in \mathbb{Z}\}$

The q-Bessel Fourier transform $F_{q,\nu}$ for a function $f_1 \in L_{q,1,\nu}$ as in [3] is given by

$$F_{q,\nu}(f_1)(y) = c_{q,\nu}\left(\int_0^\infty f_1(t) j_\nu(yt, q^2) t^{2\nu+1} d_q t\right), \forall\, y \in \mathbb{R}_q^+ \qquad (1)$$

Where

$$c_{q,\nu} = \frac{1}{1-q} \frac{\left(q^{2\nu+2}; q^2\right)_\infty}{\left(q^2, q^2\right)_\infty}, \qquad (2)$$

and j_ν with index ν is given in [2]

Proposition 1

i) If f_1 and $F_{q,\nu}$ belongs to $L_{q,1,\nu}(\mathbb{R}_q^+)$ then $f_1(y) = c_{q,\nu}\left(\int_0^\infty F_{q,\nu}(f_1)(\lambda) j_\nu(\lambda y, q^2) \lambda^{\{2\alpha+1\}} d_q \lambda\right) \forall\, y \in \mathbb{R}_q^+.$ (3)

ii) The inverse q-Bessel Fourier transform is defined as

$$F_{q,\nu}^{-1}(f_2)(y) = \int_0^\infty f_2(\lambda) j_\nu\left(\lambda y, q^2\right) \lambda^{2\alpha+1} d_q \lambda. \qquad (4)$$

The translation operator of q-Bessel $\tau_{q,x}^{v}, v > -1$ are defined as

$$\tau_{q,x}^{v}(f_1)(y) = \int_0^{\infty} f_1(z) D_{q,v}(x,y,z) z^{2v+1} d_q z, \quad such \quad that \quad x, y > 0 \tag{5}$$

Where,

$$D_{q,v}(x,y,z) = c_{q,v}^2 \left(\int_0^{\infty} j_v\left(x.s, q^2\right) j_v\left(y.s, q^2\right) j_v\left(z.s, q^2\right) s^{2v+1} d_q s \right) \tag{6}$$

The convolution product of q-Bessel for two functions f_1, f_2 is defined as

$$f_1 *_q f_2(x) = c_{q,v} \left(\int_0^{\infty} \tau_{q,x}^{v} f_1(y) f_2(y) y^{2v+1} d_q y \right), \quad x \geq 0. \tag{7}$$

Proposition 2

i) For f_1 *on* $L_{q,1,v}$, we have $\left\| \tau_{q,x}^{v} f_1 \right\|_{q,1,v} \leq \| f_1 \|_{q,1,v}$

ii) For f_1, f_2 *on* $L_{q,1,v}$, we have $f_1 *_q f_2$ *belongs to* $L_{q,1,v}$, then

$$F_{q,v}\left(f_1 *_q f_2\right) = F_{q,v}(f_1) F_{q,v}(f_2) \tag{8}$$

Definition 1: If an even function $f_2 \in L_{q,2,\alpha}(\mathbb{R}_q^+)$ holds the admissibility condition, then it is called a q-Bessel wavelet.

$$0 < C_{\alpha, f_2} = \int_0^{\infty} \left| F_{q,\alpha}(f_2)(\lambda) \right|^2 \frac{d\lambda}{\lambda} < \infty. \tag{9}$$

Definition 2: Let $f_2 \in L_{q,2,\alpha}(\mathbb{R}_q^+)$ be a q-Bessel wavelet. For a function $f_1 \in L_{q,1,\alpha}(\mathbb{R}_q^+)$ the continuous q-Bessel wavelet transform is defined as

$$W_{q,g}^{\alpha}(f_1)(a,b) = \int_0^{\infty} f_1(x) \overline{f_{2(a,b)}^{\alpha}(x)} x^{2\alpha+1} d_q x, \ \forall a, b \in \mathbb{R}_q^+. \tag{10}$$

Where

$f_{2(a,b)}^{\alpha}(x) = \sqrt{a} T_{q,b}^{a}(f_{2a}); \ \forall a, b \in \mathbb{R}_q^+, f_{2a}(x) = \frac{1}{a^{2\alpha+1}} f_2\left(\frac{x}{a}\right)$

Theorem 1: Let $f_2 \in L_{q,2,\alpha}(\mathbb{R}_q^+)$ be a Bessel wavelet of order α. Then

i) For all $f_1 \in L_{q,1,\alpha}(\mathbb{R}_q^+)$ the Plancherel formula we have

$$\int_0^\infty \left| f_1(x) \right|^2 x^{2\alpha+1} d_q x = \frac{1}{C_{\alpha,g}} \left(\int_0^\infty \int_0^\infty \left| W_{q,g}^{\alpha} (f_1)(a,b) \right|^2 b^{2\alpha+1} d_q b \frac{d_q a}{a^2} \right) . \quad (11)$$

ii) For such $F_{q,\alpha}(f) \in L_{q,1,\alpha}(\mathbb{R}_q^+)$, we have

$$f_1(x) = \frac{c_{q,\alpha}}{C_{\alpha,f_2}} \int_0^\infty \left(\int_0^\infty W_{q,f_2}^{\alpha}(f_1)(a,b) \overline{f_{2(a,b)}^{\alpha}(x)} b^{2\alpha+1} d_q b \right) \frac{da}{a^2}, \forall\, x \in \mathbb{R}_q^+ \quad (12)$$

Harmonic Analysis Associated With Λ

Let $\nu > -\frac{1}{2}$, $n \in \mathbb{N} \cup \{0\}$ and the map M in [4] is defined as

$$M\left(f_1(x) \right) = x^{2n} f_1(x) \quad (13)$$

And let $L_{q,p,\nu,n}$, $1 \le p \le \infty$ be the measurable functions f on the half line such that

$$\left\| f_1 \right\|_{q,p,\nu} = \left\| M^{-1} f_1 \right\|_{q,p,\nu+2n} < \infty \quad \forall x \in \mathbb{R}_q^+ \quad (14)$$

Proposition 3

i) The map M is a isomorphism from $L_{q,p,\nu}$ onto $L_{q,p,\alpha,n}$

$$\varphi_{\nu,n}\left(\lambda y, q^2 \right) = y^{2n} j_{\nu+2n}\left(\lambda y, q^2 \right) \quad (15)$$

where $j_{\nu+2n}$ is normalized q-Bessel function.

ii) $\varphi_{\alpha,n}$ satisfies the differential equation.

$$\Lambda_{q,\nu,n} \varphi_{\nu,n}\left(\lambda y, q^2 \right) = -\lambda^2 \varphi_{\nu,n}\left(\lambda y, q^2 \right) \quad (16)$$

Definition 3: The generalized q-Bessel transform for a function $f_1 \in L_{q,1,\nu}$ is defined as

$$B_{q,\nu}\left(f_1 \right)(y) = c_{q,\nu} \left(\int_0^\infty f_1(y) \varphi_{\nu,n}\left(\lambda y, q^2 \right) y^{2\nu+1} d_q y \right). \quad (17)$$

Where $c_{q,\nu}$ is given by (2)

Proposition 4

i) $\forall f_1 \in L_{q,1,v}$, $B_{q,v}\left(f_1\right)(\lambda) = F_{q,v+2n} \circ M^{-1} f_1(\lambda)$

Proof

i) $\forall f_1 \in L_{q,1,v}$,

$$
\begin{aligned}
B\left(f_1\right)(\lambda) &= c_{q,v}\left(\int_0^{\infty} f_1(y)\,\varphi_{v,n}\left(\lambda y, q^2\right) y^{2v+1} d_q y\right), \\
&= c_{q,v}\left(\int_0^{\infty} f_1(y)\, x^{2n}\, j_{v+2n}\left(\lambda y, q^2\right) y^{2v+1} d_q x\right), \\
&= c_{q,v}\left(\int_0^{\infty} M^{-1} f_1(y)\, j_v\left(\lambda y, q^2\right) y^{2v+4n+1} d_q x\right), \\
&= F_{q,v} \circ M^{-1} f_1(\lambda).
\end{aligned}
\tag{18}
$$

Theorem 2

i) For every $f_1 \; belongs \; L_{q,1,v} \; \text{int}er\,\text{sec}tion \; L_{q,2,v}$ the Plancherel formula we have

$$\int_0^{\infty} \left| f_1(y) \right|^2 y^{2v+1} dy = \int_0^{\infty} \left| B_{q,v}\left(f_1\right)(\lambda) \right|^2 d\mu_{q,v+2n}(\lambda).$$

ii) The inverse transform is given as

$$B_{q,v}\left(f_2\right)(t) = \int_0^{\infty} f(\lambda)\,\varphi_{v,n}\left(\lambda y, q^2\right) d\mu_{v+2n}(\lambda).$$

Proof

i) For every $f_1 \; belongs \; L_{q,1,v} \; \text{int}er\,\text{sec}tion \; L_{q,2,v}$ we have

$$\int_0^\infty \left|B_{q,v}\left(f_1\right)(\lambda)\right|^2 d\mu_{q,v}(\lambda) = \int_0^\infty \left|F_{q,v}\left(M^{-1}f_1\right)(\lambda)\right|^2 d\mu_{q,v+2n}(\lambda),$$

$$= \int_0^\infty \left|M^{-1}f_1(y)\right|^2 y^{2v+4n+1}, \tag{19}$$

$$= \int_0^\infty \left|f_1(y)\right|^2 y^{2v+1}dy$$

which gives i). The ii) proof is standard.

Generalized convolution product

Definition 4: Define the generalized q-Bessel translation operator $T_{q,y}$ associated with $\Lambda_{q,v}$ are defined by

$$T_{q,x}f_1(t) = (yt)^{2n} M \circ \tau_{q,y}^v \circ M^{-1} \tag{20}$$

Where $t \geq 0$ and $\tau_{q,y}^v$ is given by (4).

Definition 5. The generalized q-convolution product of two functions f_1 and f_2 on $L_{q,1,v}$ is given by

$$f_1 \#_{q,v} f_2(y) = c_{q,v}\left(\int_0^\infty T_{q,y}f_1(t)\, f_2(t) t^{2v+1} d_q t\right), \tag{21}$$

where $c_{q,v}$ is given by (2).

Remarks 1

i) Notice by equation (19) that

$$f_1 \#_{q,v} f_2 = M\left[\left(M^{-1}f_1\right)\#_{q,v}\left(M^{-1}f_2\right)\right] \tag{22}$$

Proposition 5

i) For $f_1, f_2 \in L_{q,1,v}$ we have $B_{q,v}\left(f_1 \#_{q,v} f_2\right) = B_{q,v}\left(f_1\right)B_{q,v}\left(f_2\right)$.

ii) For $f_1, f_2 \in L_{q,1,v}$ $\left\|f_1 \#_{q,v} f_2\right\| \leq \left\|f_1\right\|_{q,1,v}\left\|f_2\right\|_{q,1,v}$.

iii) $f_1 \in L_{q,2,v}$, we have $B_{q,v}\left(T_{q,y}f_1\right)(\lambda) = \varphi_v\left(\lambda y, q^2\right)B_{q,v}\left(f_1\right)(\lambda)$.

Proof

i) For $f_1, f_2 \in L_{q,1,v}$ we have

$$\begin{aligned} B_{q,v}\left(f_1 \#_{q,v} f_2\right) &= B_{q,v}\left(M\left[\left(M^{-1}f_1\right)\#_{q,v}\left(M^{-1}f_2\right)\right]\right)(\lambda), \\ &= F_{q,v} \circ M^{-1}\left(M\left[\left(M^{-1}f_1\right)\#_{q,v}\left(M^{-1}f_2\right)\right]\right)(\lambda), \\ &= F_{q,v}\left(M^{-1}f_1\right)(\lambda) \times F_{q,v}\left(M^{-1}f_1\right)(\lambda), \\ &= B_{q,v}\left(f_1\right) B_{q,v}\left(f_2\right). \end{aligned} \tag{23}$$

ii) For $f_1, f_2 \in L_{q,1,v}$,

$$\begin{aligned} \left\| f_1 \#_{q,v} f_2 \right\| &= \left\| M^{-1}(f_1 \#_{q,v} f_2) \right\|_{q,1,v+2n}, \\ &= \left\| M^{-1} f_1 \right\|_{q,1,v+2n} \left\| M^{-1} f_2 \right\|_{q,1,v+2n}, \\ &\le \left\| f_1 \right\|_{q,1,v} \left\| f_2 \right\|_{q,1,v}. \end{aligned} \tag{24}$$

iii) For $f_1 \in L_{q,2,v}$,

$$\begin{aligned} B_{q,v}\left(T_{q,y} f_1\right)(\lambda) &= B_{q,v}\left(y^{2n} M \circ \tau_{q,y}^{v} \circ M^{-1} f_1\right)(\lambda), \\ &= y^{2n} F_{q,v}\left(\tau_{q,y}^{v} \circ M^{-1} f_1\right)(\lambda), \\ &= y^{2n} j_{v+2n}\left(\lambda y, q^2\right) F_{q,v}\left(M^{-1} f_1\right)(\lambda), \\ &= \varphi_v\left(\lambda y, q^2\right) B_{q,v}\left(f_1\right)(\lambda). \end{aligned} \tag{25}$$

Conclusion

In this article, by considering this particular differential operator on $[0,\infty)$ the q-Bessel operator is generalized. And then investigated the classical analysis on the continuous wavelet transform corresponding to the operator. As the concept wavelet has many uses in finding solutions of different differential equations, the idea of this paper can be extend to other classical wavelets.

References

1. Imen Rezgui, A.Ben Mabrouk, Some Generalized q-Bessel Type wavelet and associated transforms, Analysis in Theory and Application, 2017

2. Lazhar Dhaouadi and Manel Hleili, Generalized q-Bessel operator, Bulletin of Mathematical analysis and application, 2017
3. L.Dhaouadi and Hedi Elmonser, q-Bessel Fourier transform and Variation Diminishing Kernel.
4. Ahmed Abbouelaz, Rodouan Daher and EL Mehdi Loualid, Harmonic analysis associated with the generalized q-Bessel operator, International Journal of Analysis and Applications, 2016.